TITLE:

An analysis of the mechanism of chip formation in orthogonal cutting(Dissertation_全文)

AUTHOR(S):

Hitomi, Katsundo

CITATION:

Hitomi, Katsundo. An analysis of the mechanism of chip formation in orthogonal cutting. 京都大学, 1962, 工学博士

ISSUE DATE:

1962-03-23

URL:

https://doi.org/10.14989/74975

RIGHT:

京都大学学術情報リポジトリ
KURENAI 紅
Kyoto University Research Information Repository

AN ANALYSIS OF THE MECHANISM OF CHIP FORMATION IN ORTHOGONAL CUTTING

Katsundo Hitomi

(1 9 6 1)

AN ANALYSIS OF THE MECHANISM OF CHIP FORMATION IN ORTHOGONAL CUTTING

Katsundo Hitomi

(1 9 6 1)

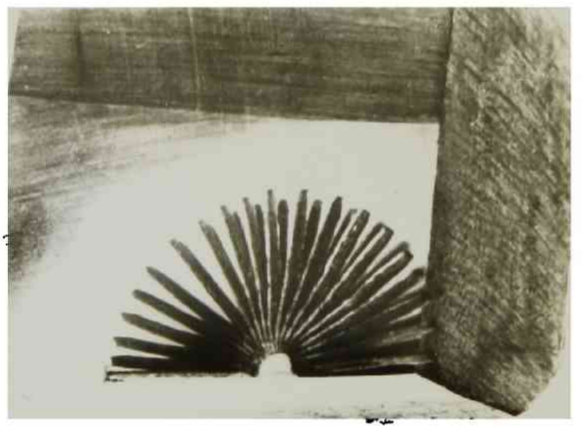

ART IN METAL CUTTING

....A FAN-SHAPED CHIP PRODUCED DURING THE CONDUCT OF EXPERIMENTS FOR THIS INVESTIGATION

WORK MATERIAL, BRASS(Cu: 75.0%, Zn: 25.0%); TOOL MATERIAL, HIGH SPEED STEEL SKH 2(18-4-1)

AN ANALYSIS OF THE MECHANISM OF CHIP FORMATION IN ORTHOGONAL CUTTING

KATSUNDO HITOMI

Department of Precision Engineering
Kyoto University
Kyoto, Japan

(August, 1961)

ABSTRACT

Instead of the conventional theory of the mechanism of orthogon cutting based on a process of shear confined to a single shear plane the concept of the flow region, the transitional deformation zone which exists between the rigid region of the work and the plastic re gion of the steady chip, was developed.

The mechanism of chip formation in orthogonal cutting was analyzed. Theoretical equations for boundary lines of the flow region and for strain in the chip were deduced in the case of simple contin ous chip formation, and confirmed in cutting tests with lead.

The concept of the flow region was also applied to discontinuou chip formation, and equations expressing angles of the starting boun ary line and the ending boundary line(i.e., fracture line) of the fl region were deduced theoretically, and determined to be in agreement with the experimental results for carbon steel.

The grid deformation for the cutting mechanism based upon the flow region concept was analyzed.

The direction in which metal structure arranges in the chip due to the primary plastic flow in the flow region was investigated in a wide range of experiments on carbon steel, and the effects of cuttin conditions on the size of the flow region were discussed. In relati to this, the secondary plastic flow in the chip on the tool-chip interface was also investigated.

The concept of the flow region was applied to partly explain th phenomenon of chip curl in orthogonal cutting, and the effects on cu ting conditions on chip curl were investigated with lead and carbon steel.

CONTENTS

I. INTRODUCTION

Recently theoretical studies on metal cutting have been well developed. Especially regarding the most fundamental analysis of the mechanics of orthogonal cutting producing a continuous or discontinuous chip, various theories have been presented, e.g., by Piispanen(1, 2)*, Ernst and Merchant(3, 4), Lee and Shaffer(5), Hill(6), and others, assuming perfectly plastic property, strain-hardening property or inhomogenuity of the work material. In most analyses, however, it has also been assumed for the sake of simplicity that the chip formation is a process of shear (without fracture for continuous chip formation and with fracture for discontinuous chip formation) confined to a single plane, which is usually called the shear plane, extending from the tip of a cutting tool to the sharp intersection of the free surfaces of the work and the chip as shown in Fig. 1.

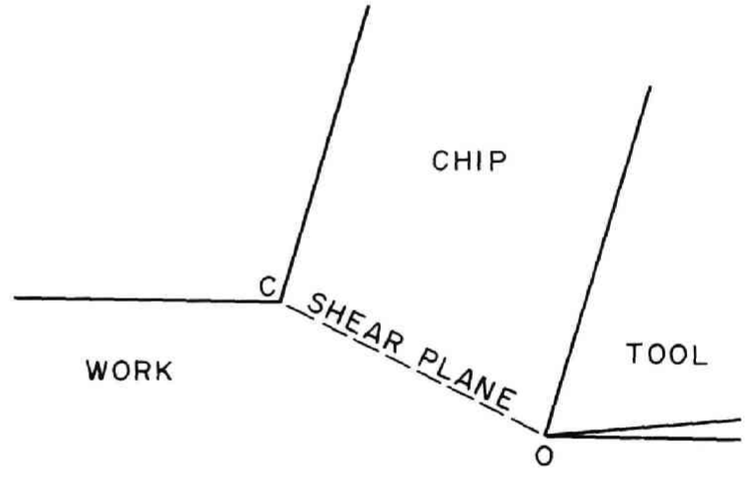

Fig. 1 Cutting process with a single shear plane

However, analysis of the cutting mechanism based on simple shear along a single shear plane contains the following conflicts:

(a) A moving metal particle must attain an infinite amount of acceleration when it passes across the shear plane, changing its position from the work region to the chip region.

---

* Numbers in parentheses designate References at end of paper.

(b) An infinite stress gradient exists on the shear plane.

(c) The rate of strain is extremely large compared with that in static material tests.

(d) Extremely large strain is produced abruptly on the shear plane, and the relationship between stress and strain in cutting tests does not agree with that in static material tests.

In order to eliminate these conflicts in the conventional cutting theory based on the shear process along a single plane, in this paper the cutting mechanism based on the shear process taken over a large transitional deformation zone will be introduced, and a new concept of the cutting mechanism will be discussed, analyzing the mechanics of orthogonal cutting.

In the case of the simple continuous chip formation the location and the size of the transitional deformation zone were analyzed theoretically, assuming the work material as a perfectly plastic solid. The strain which is produced in the transitional deformation zone and the strain in the chip were deduced theoretically. These theoretical equations were applied to cutting tests on lead, and the regional cutting process was discussed.

The grid deformation for the cutting mechanism based upon a new concept was analyzed, and an equation for direction of arrangement of metal structure was deduced.

This concept of metal-flow process over the transitional deformation zone was also applied to the discontinuous chip formation, and the location of fracture line was analyzed, considering the strain-hardening property of the work material. The equations obtained by this analysis were ascertained to be in agreement with experimental results of cutting tests on carbon steel.

The existence of this transitional deformation zone was also verified by a wide range of experiments on carbon steel regarding direc-

tion in which metal structure arranges in the chip due to the primary plastic flow in the transitional deformation zone, and the relation between the size of this transitional deformation zone and the cutting conditions was discussed. In addition to this, the secondary plastic flow process in the chip along the tool-chip interface was investigated.

The present new concept was applied to partly explain the phenomenon of chip curl in orthogonal cutting, and a wide range of experiments was conducted on lead and carbon steel, investigating the relationship between chip curl and cutting conditions.

II. THE CONCEPT OF THE FLOW REGION*

In order to eliminate several conflicts in the conventional cutting theory based on the shear process along a single plane, which were pointed out in the previous section, a new concept of the regional cutting mechanism will be introduced in this section.

In this new concept, a fairly large transitional zone of plastic deformation AOB is taken into consideration between the rigid region of the work and the plastic region of the steady chip, as shown

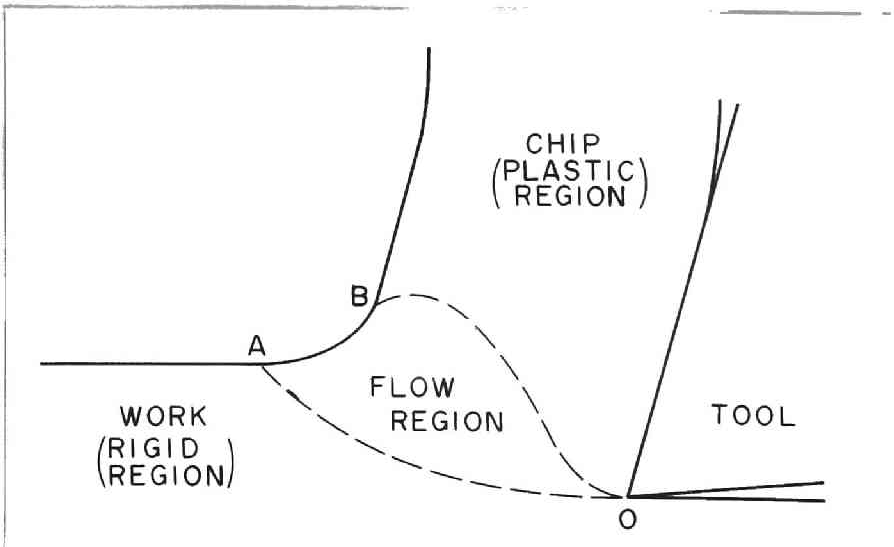

Fig. 2 Cutting process with a flow region (a transitional deformation zone between the work and the chip)

* For a detailed discussion on this section, see Reference(7).

in Fig. 2. Through this deformation zone, the velocity of a moving metal particle, the shearing stress, and the plastic strain change gradually and continuously. The free surface of the work and the chip in this case has no sharp intersection as in the conventional theory based on a single shear plane, but is a smooth curve from the free surface of the work to the back side of the steady chip. This deformation zone will be called the "flow region" in this paper.

A similar deformation zone has been considered quite recently by several investigators. Nakayama(8) observed the deformation zone in the cutting process by taking microphotographs during cutting. Kececioglu(9, 10) discussed the size of the deformation band, investigated the deformation aspect of metal structure with a wide range of experiments, and analyzed the shear-strain rate and its effect on shear-flow stress. Christopherson, Oxley, and Palmer(11) observed that deformation in metal cutting occurs continuously in a triangular plastic zone instead of along a concentrated single shear plane by taking photographs of the cutting process. They analyzed the mechanics of orthogonal cutting for work-hardening material.

The flow region, which is discussed in this paper, is different from the preflow region, which, according to Finnie and Shaw(12), is located in the vicinity of the free surface of the work ahead of the shear plane. With the preflow region they tried to explain the differences between calculated values of shear angle from theoretically derived equations and observed values and between stress-strain relationships in static material tests and cutting tests. In this case plastic flow is confined within the vicinity of the free surface of the work, and shear process is assumed to occur on a single shear plane. In the concept of the flow region, however, plastic deformation is not limited only near the free surface, but takes place over a large area from the tip of the cutting tool to the free surface of

the work and the chip. This is a main difference between the two concepts, and actually the preflow region is contained in the flow region.

The concept of the flow region can also be applied to the analysis of discontinuous chip formation. This also removes the conventional conflict that the fracture occurs abruptly on a particular single shear plane and is associated with extremely large shearing strain. In Fig. 3, the plastic deformation begins to occur at the starting boundary line OA of the flow region. As the cut progresses, the plastic strain increases gradually, and the shearing stress increases due to strain-hardening. Finally, the stress reaches the shearing breaking limit, fracture occurs at the ending boundary line OB, and a fragment of discontinuous chip is produced. When fracture occurs, the shearing stress at the ending boundary line of the flow region decreases below the breaking limit, and a new fragment of chip begins to form. The behavior of the cutting process is almost the same as continuous chip formation except that fracture occurs when the shearing stress or strain on the ending boundary line of the flow region reaches the breaking limit as the cut proceeds. The continuous chip might be produced if the shearing stress or strain does not reach the breaking limit at the ending boundary line.

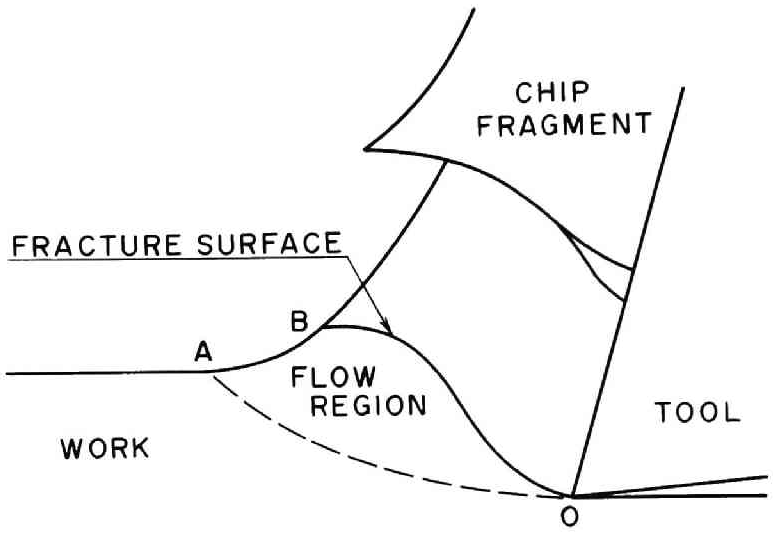

Fig. 3 Discontinuous chip formation accompanying a flow region

Thus both mechanisms of continuous and discontinuous chip forma-

tions in metal cutting can be explained logically by the concept of the flow region. The following sections deal with the analysis of the cutting mechanism from the standpoint of the concept of the flow region.

III. CUTTING PROCESSES IN ORTHOGONAL CUTTING*

a. Experimental Procedure

Preliminary cutting tests were conducted, cutting soft metals such as lead and Lipowitz alloy at relatively low cutting speed dry on a specially designed cutting test device, and the cutting processes were observed continuously through the microscope.

The orthogonal cutting test device is shown in Fig. 4. The work material is installed in the work holder ①. The view side of the work is supported with a hard glass plate in order to eliminate side flow of metal during cutting and permit the observation of the formation of the chip. The work holder ① is set on the tool holder ② which has an orthogonal cutting tool ③. The cutting is performed manually with the handle ④, and the cutting process is observed through a microscope

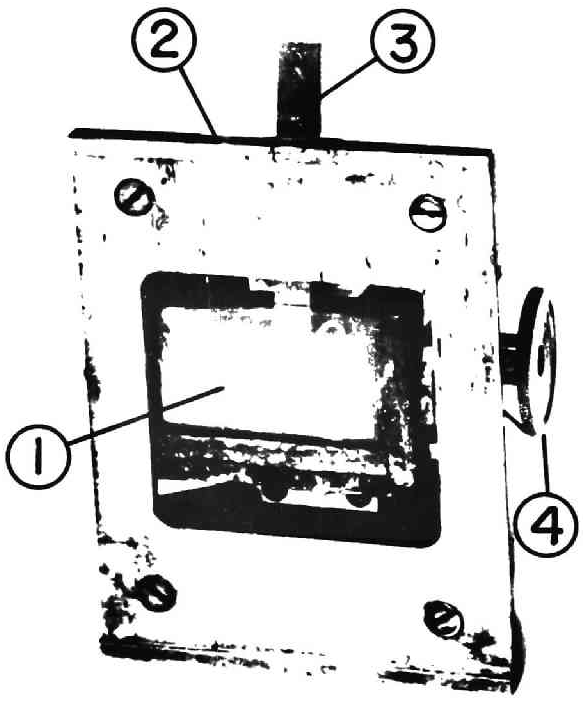

Fig. 4 Orthogonal cutting test device

* For a detailed statement on this section, see Reference(7).

and photographs are taken with a magnification of 25 to 200.

The weakness in this cutting device is that the cutting speed is low and not consistent; i.e., 0.01 to 0.03 ^{m}/min. On the other hand, however, the cutting can be stopped whenever it is necessary to observe the cutting process in detail or to take photomicrographs. In addition, the effect of cutting temperature on the cutting mechanism is eliminated.

Work materials tested were lead and Lipowitz alloy[Bi 50.0%, Pb 26.7%, Sn 13.3%, and Cd 10.0%]. The former material is ductile and the latter material is slightly brittle. Physical and mechanical properties of both metals are given in Table 1.

Table 1 Physical and mechanical properties of soft metals tested

DESCRIPTION	LEAD	LIPOWITZ ALLOY
MELTING POINT (°C)	327	65
DENSITY (g/cm^3)	11.4	7.9
TENSILE STRENGTH (kg/mm^2)	2	5
HARDNESS (VICKERS)	6	140

Tool material was carbon tool steel. Various shapes such as sharp-edged, flat-edged, round-nosed, and negative rake sharp-edged tools were used in the cutting tests.

b. Some Observations on the Cutting Process

Examples of the cutting process are illustrated in Figs. 5 and 6. Fig. 5 is for lead, and Fig. 6 is for Lipowitz alloy. Usually both work materials produced a continuous type of chip. It is evident from these photographs, examining the grid deformation near the cutting edge, that the shear process in metal cutting takes place over a large

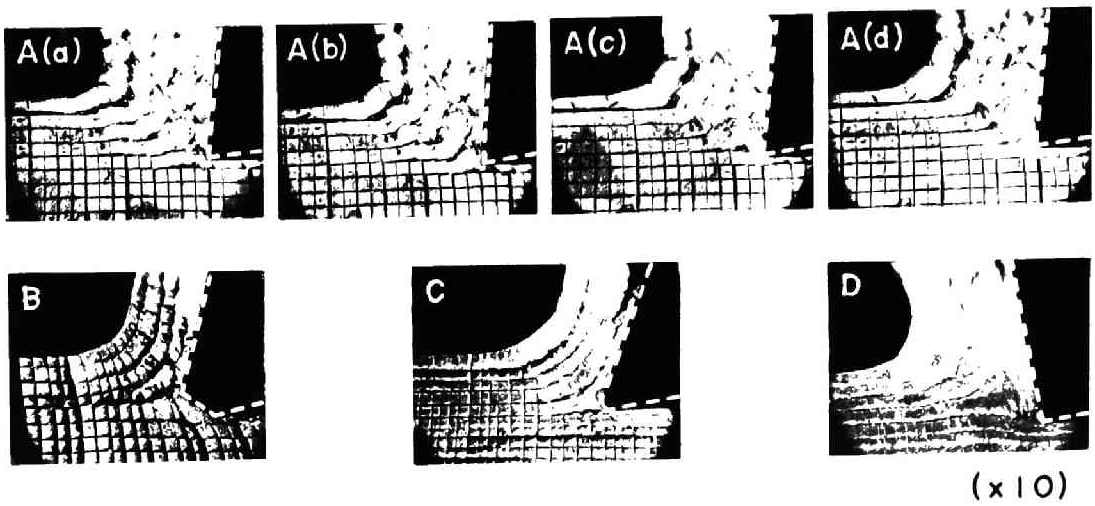

Fig. 5 Typical photographs of cutting process for lead (continuous chip formation) [Tool material, carbon tool steel; A: sharp-edged tool, (a), (b), (c), and (d): periodic change of the contour of the flow region, B: flat-edged tool, C: round-nosed tool, and D: negative rake sharp-edged tool; dry]

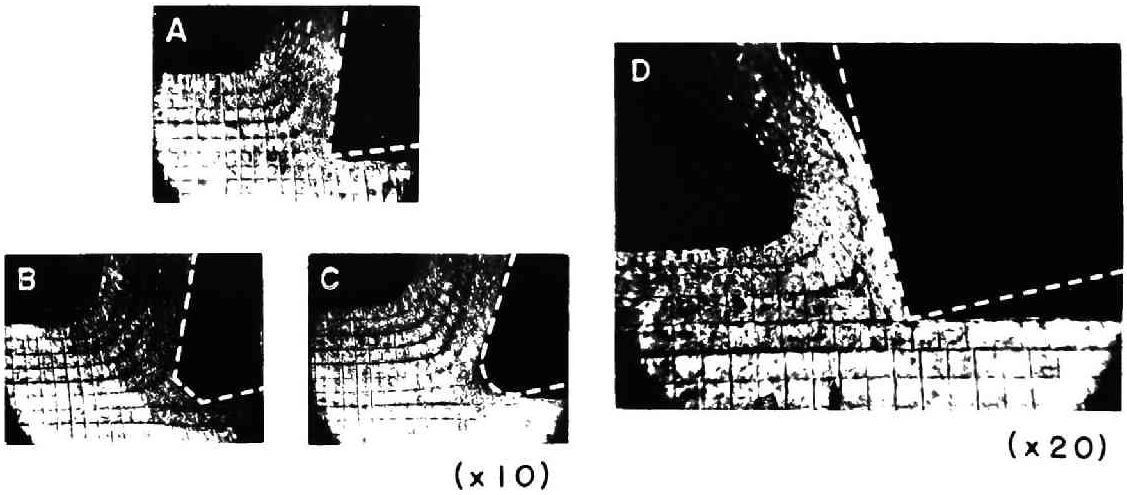

Fig. 6 Typical photographs of cutting process for Lipowitz alloy (continuous chip formation) [Tool material, carbon tool steel; A: sharp-edged tool, B: flat-edged tool, C: round-nosed tool, and D: negative rake sharp-edged tool; dry]

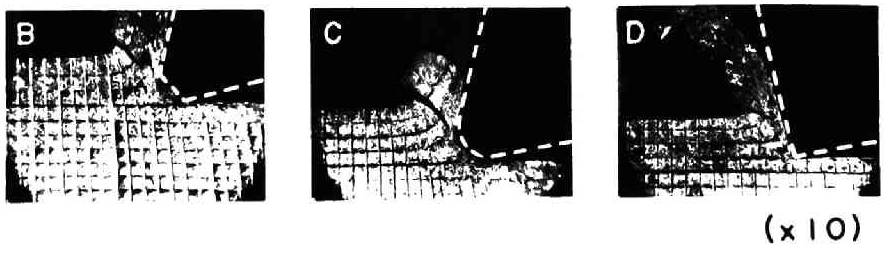

Fig. 7 Typical photographs of cutting process for Lipowitz alloy (discontinuous chip formation) [Tool material, carbon tool steel; B: flat-edged tool, C: round-nosed tool, and D: negative rake sharp-edged tool; dry]

area instead of along a single plane. In other words, a transitional deformation zone of plastic flow, i.e., the flow region, exists between the rigid region of the work and the plastic region of the steady chip. In some of the photographs, the cutting processes show a condition resembling the stream lines in the flow of water.

Since Lipowitz alloy is relatively brittle, a discontinuous type of chip was observed in several cases. Typical examples are shown in Fig. 7. This tendency to produce a discontinuous chip was quite pronounced for dull-edged and negative-rake tools at relatively high speeds. Some amount of deformation zone was always observed ahead of the fracture in the chip even at the instant the fracture occurred; that is, the flow region existed during cutting ---- not only during the formation of chip fragment but also at the very instant the fracture occurred. The cutting process accompanying a discontinuous chip is almost the same as the process accompanying a continuous chip except that fracture occurs periodically at the ending boundary line of

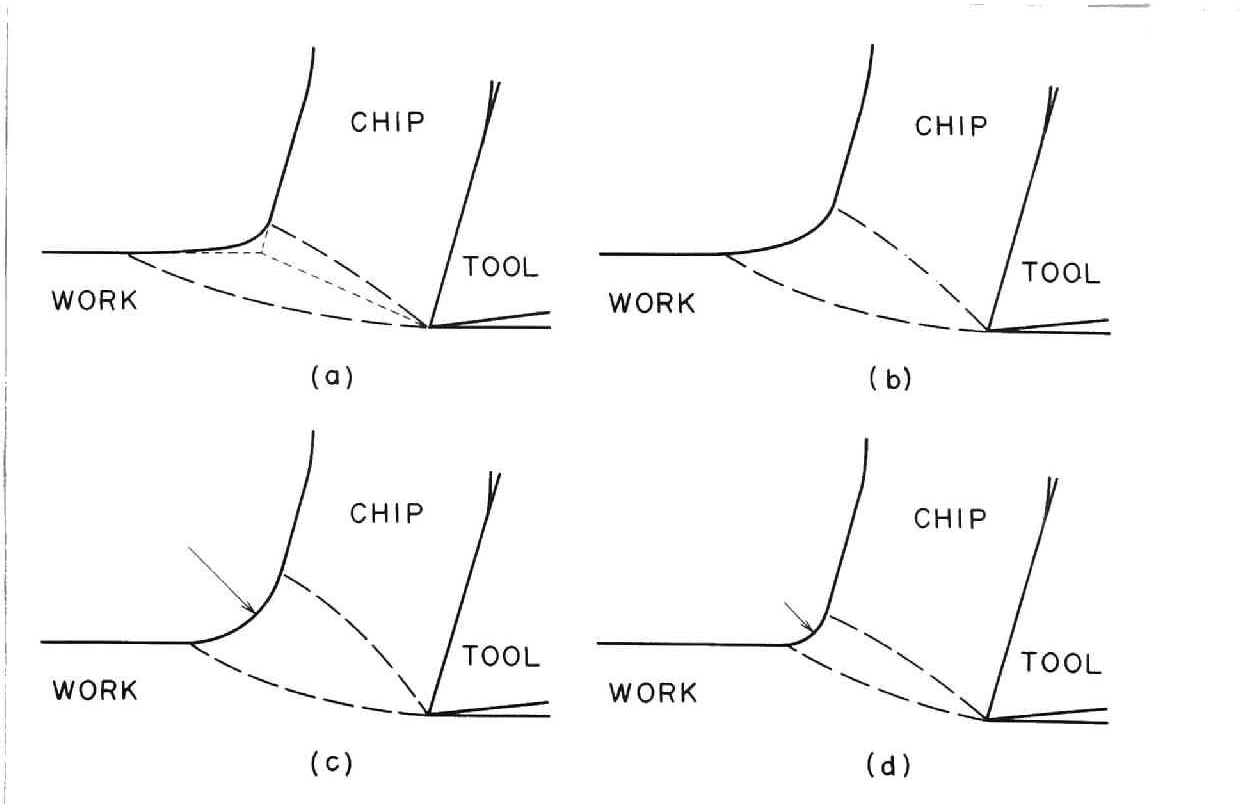

Fig. 8 Periodic change of the contour of the flow region

the flow region, as explained in the previous section.

Fracture line was always observed to be convex upward rather than straight. This shows that the ending boundary line, namely, the line which is the easiest to slip is not a straight line, but a upwardly convex curve.

It was sometimes observed that the shape of the flow region changed periodically during cutting. Fig. 8 shows a typical schematic model. The cutting model or the contour of the flow region changes from (a) to (b), to (c), to (d), and to (a) again. This process is repeated. In some cases, only (c) and (d) are repeated. A typical example is shown in Fig. 5[A(a), (b), (c), and (d)]. This periodic change of the shape of the flow region is considered to be caused by tool vibration.

The most important factor which affects the size of the flow region was found to be cutting speed. Increasing the cutting speed reduced the size of the flow region.

IV. ANALYSIS OF THE MECHANISM OF CONTINUOUS CHIP FORMATION BASED ON THE FLOW REGION CONCEPT*

In this section, the cutting mechanism producing a continuous chip without built-up edge will be analyzed according to the concept of the flow region.

a. Analysis of the Location and Size of the Flow Region

Assuming that the work material is a perfectly plastic solid and that the elastic strain is negligible in comparison with the plastic

---

* For a detailed discussion on this and the next sections, see Reference(13).

strain as is often considered in metal-cutting analysis, the shearing stress and strain relation (τ - γ diagram) is shown in Fig. 9. In this figure, τ_0 is the yield shearing stress, i.e., the shear-flow stress.

It might be also assumed for the sake of simplicity that the starting(work side) boundary line OA and the ending(chip side) boundary line OB of the flow region are straight lines as shown in

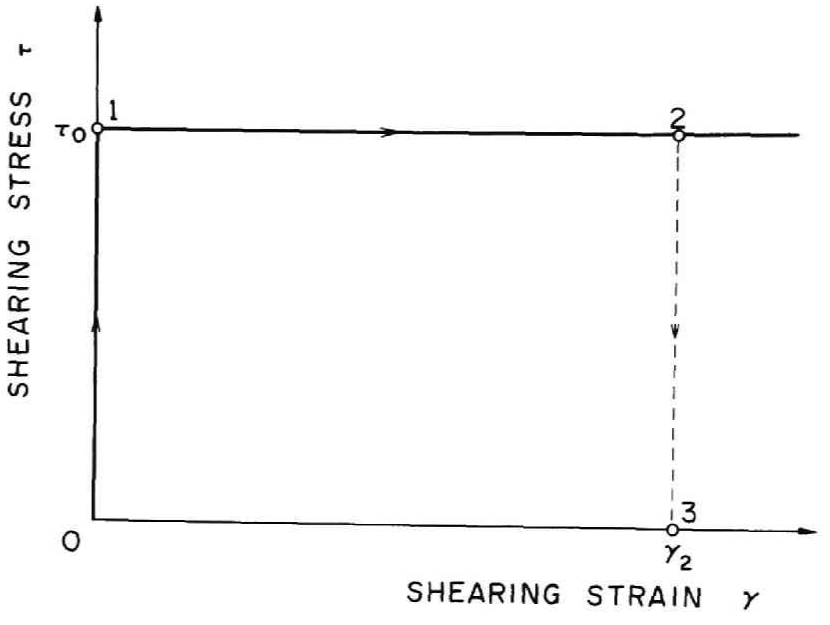

Fig. 9 Shearing stress-strain diagram for perfectly rigid-plastic material

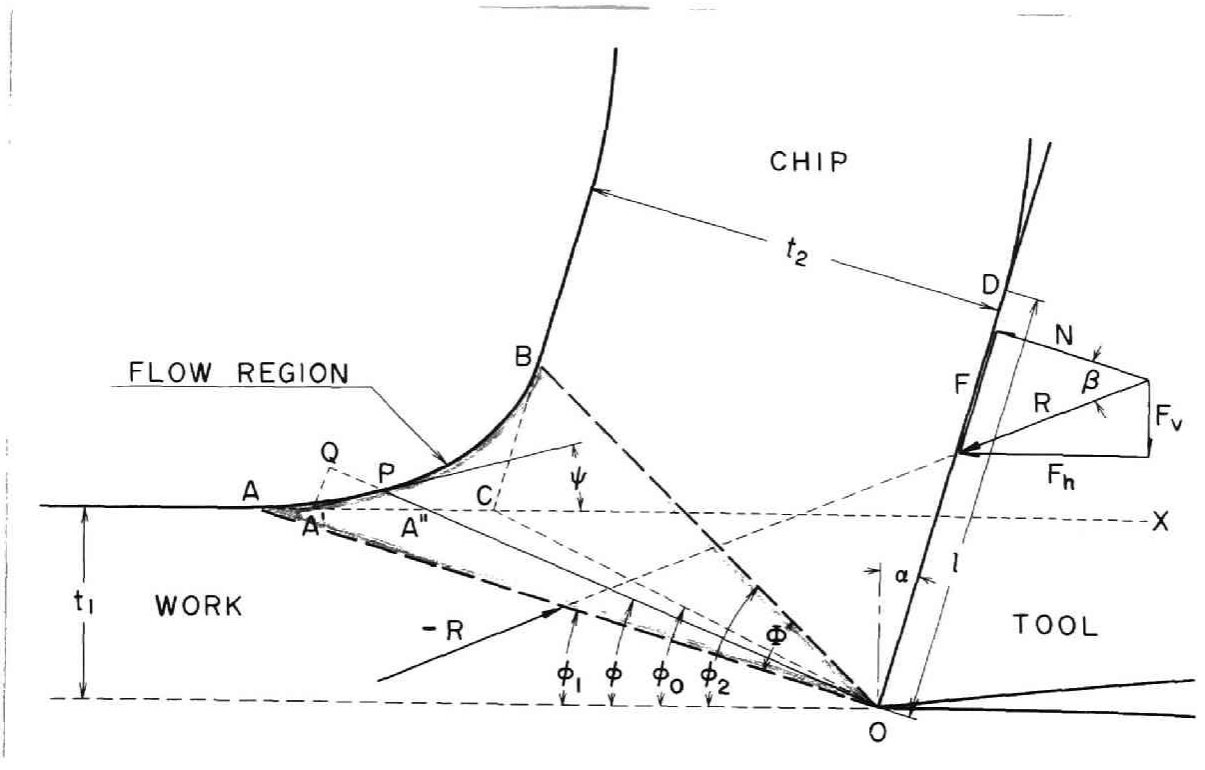

Fig. 10 Analysis of the mechanism of continuous chip formation based on the flow region concept

Fig. 10, though they are in reality slightly convex downward and upward, respectively. The transitional flow of metal transforming from the rigid region of the work to the plastic region of the steady chip occurs in the flow region AOB, and the stress in this area must be in the yield state. Hence, on both boundary lines,

$$\tau_{OA} = \tau_{OB} = \tau_0. \qquad [1]$$

When a cut with a width b and a depth t_1 is made by an orthogonal cutting tool with a rake angle α, thickness of chip and resultant cutting force are denoted by t_2 and R, respectively. Assuming that the shearing stresses on both boundary lines distribute uniformly, the following expressions are obtainable:

$$\tau_{OA} = \frac{R \sin\phi_1 \cos(\phi_1 - \alpha + \beta)}{b\ t_1} \qquad [2]$$

and

$$\tau_{OB} = \frac{R \cos(\phi_2 - \alpha) \cos(\phi_2 - \alpha + \beta)}{b\ t_2}, \qquad [3]$$

where β is the average friction angle on the tool-chip interface, and ϕ_1 and ϕ_2 are the inclination angles of the starting and ending boundary lines of the flow region, respectively.

According to recent reports by Finnie and Shaw(14) and Sata and Mizuno(15), the average tangential stress along the tool-chip interface OD is in the yield state; that is,

$$\tau_{OD} = \frac{R \sin\beta}{b\ l} = \tau_0, \qquad [4]$$

where l is the chip contact length on the tool face.

The inclination angles of the starting and ending boundary lines of the flow region ϕ_1 and ϕ_2 are expressed explicitly from Equations [1] to [4].

$$\phi_1 = \frac{K_1}{2} + \frac{\alpha}{2} - \frac{\beta}{2} \qquad [5]$$

$$\phi_2 = \frac{K_2}{2} + \alpha - \frac{\beta}{2} \qquad [6]$$

$$K_1 = \sin^{-1}\left\{\frac{2}{k_1}\sin\beta + \sin(\beta - \alpha)\right\} \qquad [7]$$

$$K_2 = \cos^{-1}\left(\frac{2}{k_2}\sin\beta - \cos\beta\right) \qquad [8]$$

$$k_1 = \frac{1}{t_1} \qquad [9]$$

$$k_2 = \frac{1}{t_2} \qquad [10]$$

The sector angle of the flow region is obtained as the difference between both angles; that is, from Equations [5] and [6]

$$\Phi = \phi_2 - \phi_1 = \frac{\alpha}{2} - \frac{K_1}{2} + \frac{K_2}{2}. \qquad [11]$$

Meyer and Archibald(16, 17) and Creveling, Jordan, and Thomsen (18) obtained

$$k_1 \approx 2 \quad \text{and} \quad k_2 \approx 1, \qquad [12]$$

respectively, as cutting test results on steel. Substituting Equation [12] into Equations [7] and [8],

$$K_1 = \sin^{-1}\left\{\sin\beta + \sin(\beta - \alpha)\right\} \qquad [7']$$

$$K_2 = \cos^{-1}(2\sin\beta - \cos\beta). \qquad [8']$$

It is well known that the average friction angle on the tool face β, which is seen in the above equations, can be calculated from the following expression:

$$\tan\beta = \frac{F}{N} = \frac{F_v + F_h\tan\alpha}{F_h - F_v\tan\alpha}, \qquad [13]$$

where F = tangential force on the tool-chip interface

N = normal force on the tool-chip interface

F_h = horizontal or principal cutting force

F_v = vertical or thrust cutting force.

Recently, the opinion has been presented by Finnie and Shaw(14) and Takeyama(19) that Coulomb's law of friction is not satisfied along the tool-chip interface in metal cutting, and, consequently, the friction angle on the tool-chip interface is meaningless. However, since no theory has been established on the process of chip flowing-out, the average friction angle β, which is a value always calculated as arc tangent of the ratio between tangential and normal forces acting on the tool-chip interface by Equation [13], is adopted in this paper.

b. The Plastic Shearing Strain in the Flow Region and the Strain in Chip

In order to obtain the plastic shearing strain in the flow region, let us determine the shearing strain on an arbitrary radial plane OP which extends from the tip of the cutting tool to the free surface in the flow region, denoting its inclination angle to the cutting direction by ϕ. If the metal did not undergo plastic deformation, a metal particle on the free surface of the uncut material would proceed toward X. In reality, however, it moves toward P as a result of plastic deformation, and has the motion component toward A'P-direction (this is the tangent to the free surface of the flow region at an arbitrary point P, and makes angle ψ with the machined surface). Hence, the shearing strain which metal receives until a metal particle reaches the radial plane OP is given by $\frac{A''P}{A'Q}$, where A' and A'' are intersections between the original horizontal free surface of the work X and the tangent at P and the radial plane OP, respectively, and Q is a point at which a perpendicular line from A' to a radial plane OP intersects it. The amount of shearing strain is expressed with angles ϕ and ψ as follows:

$$\gamma = \cot\phi - \cot(\phi + \psi). \qquad [14]$$

In a particular case, the shearing strains on the starting and ending boundary lines of the flow region are

$$\gamma_1 = 0 \qquad [15]$$

and

$$\gamma_2 = \cot \phi_2 + \tan(\phi_2 - \alpha), \qquad [16]$$

respectively. It follows from this that instead of an abrupt large shearing strain which occurs on a single shear plane in the conventional theory, the shearing strain is zero on the starting boundary line of the flow region, and increases gradually until it reaches maximum at the ending boundary line of the flow region. Then the metal flows out into the chip region in a state of permanent plastic strain γ_2, which is given by Equation [16]. The variation of the shearing strain is shown in Fig. 9 as 0, 1, 2, and 3 which correspond, respectively, to the work region, the starting boundary line, the ending boundary line, and the chip region.

V. CUTTING TESTS WITH LEAD

a. Experimental Procedure

Orthogonal cutting was performed dry in a shaper[Wakayama Iron Works Co.; stroke, 48 cm].

Work material used in the cutting test was lead[Pb 98.94%, Sn 1.03%, and Sb 0.03%; Brinell hardness number, 12 at 500 kg] with a width of 11.0 mm and a length of 100 mm.

Since lead is ductile and does not strain-harden at room temperature because of its low recrystallization temperature, it always produces a continuous type of chip without built-up edge. Hence, it is an appropriate material to demonstrate the theoretical analysis of the

cutting mechanism developed under the assumption of a perfectly plastic solid as described in the previous section.

Tool material used was high-speed steel SKH 2(18-4-1). The tools were sharp-edged with a clearance angle of 6 deg and various rake angles(-20 to 20 deg), and well finished by a diamond grinder and an oil stone before cutting.

Cutting speed was constant, namely, 5.2 m/min.

Tool forces, namely, horizontal and vertical cutting forces were recorded on oscillograph paper by a strain-gage type tool dynamometer(20), and chip thickness and chip contact length on tool face were measured after cutting.

b. Experimental Results

Fig. 11 shows the effect of rake angle on tool forces, chip contact length on tool face and chip thickness when cutting lead with a width of 11.0 mm and a depth of 0.10 mm at a cutting speed

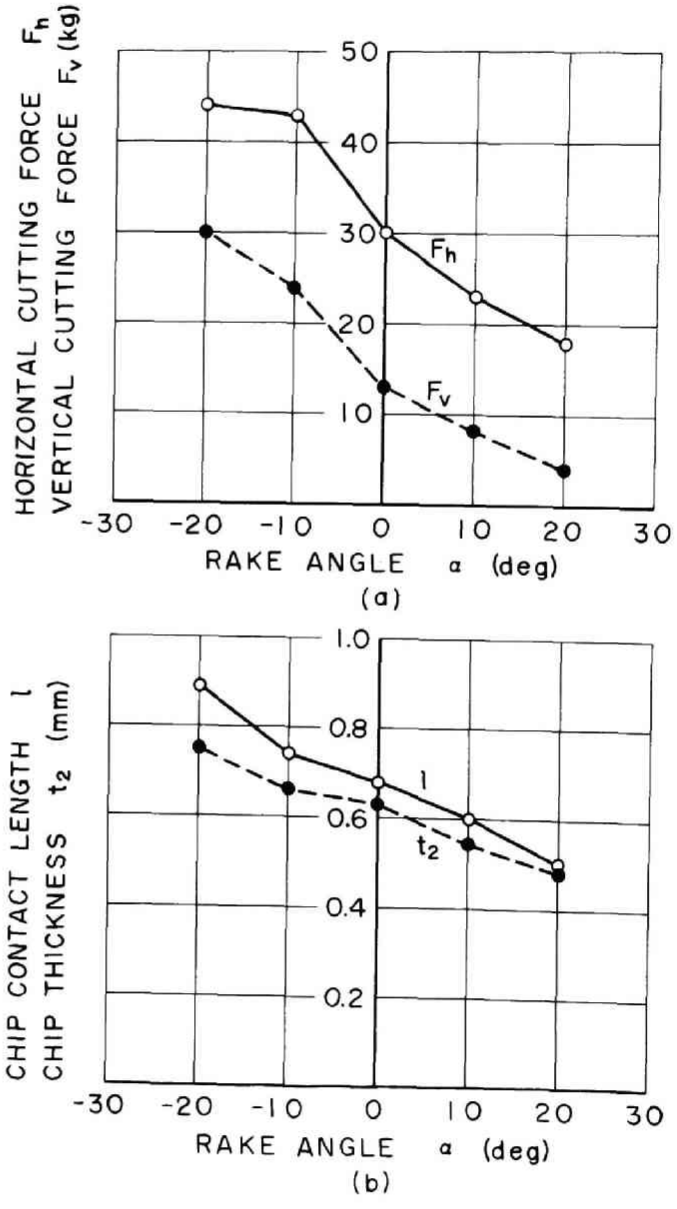

Fig. 11 Experimental results for lead in relation to rake angle; (a) Horizontal and vertical cutting forces; (b) Chip contact length on tool face and chip thickness [Tool material, high-speed steel SKH 2(18-4-1); clearance angle, 6 deg; width of cut, 11.0 mm; depth of cut, 0.10 mm; cutting speed, 5.2 m/min; dry]

of 5.2 m/min. Tool forces, chip contact length, and chip thickness decreased with an increase in rake angle.

Fig. 12 shows the effect of depth of cut when cutting the same material with a cutting tool of 0 deg rake angle at a cutting speed of 5.2 m/min. Tool forces, chip contact length, and chip thickness increased with an increase in depth of cut.

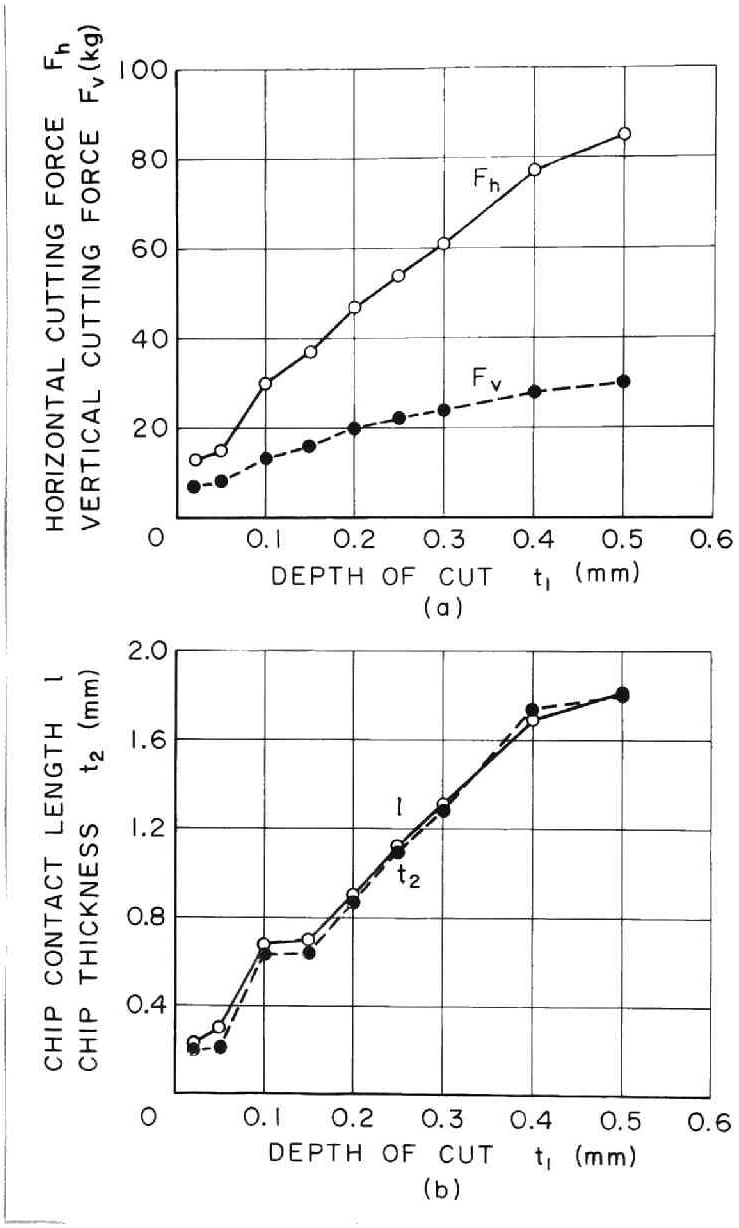

Fig. 12 Experimental results for lead in relation to depth of cut; (a) Horizontal and vertical cutting forces; (b) Chip contact length on tool face and chip thickness [Tool material, high-speed steel SKH 2(18-4-1); rake angle, 0 deg; clearance angle, 6 deg; width of cut, 11.0 mm; cutting speed, 5.2 m/min; dry]

c. Analysis of the Cutting Mechanism

The theoretical expressions deduced in Section IV will be applied to the experimental results shown in Figs. 11 and 12 in order to analyze the cutting mechanism based on the flow region concept.

Using the cutting data shown in Figs. 11 and 12, the ratio between chip contact length and depth of cut k_1, ratio between chip contact length and chip thickness k_2, mean friction angle on tool face β, inclination angles of the starting and ending boundary lines of the

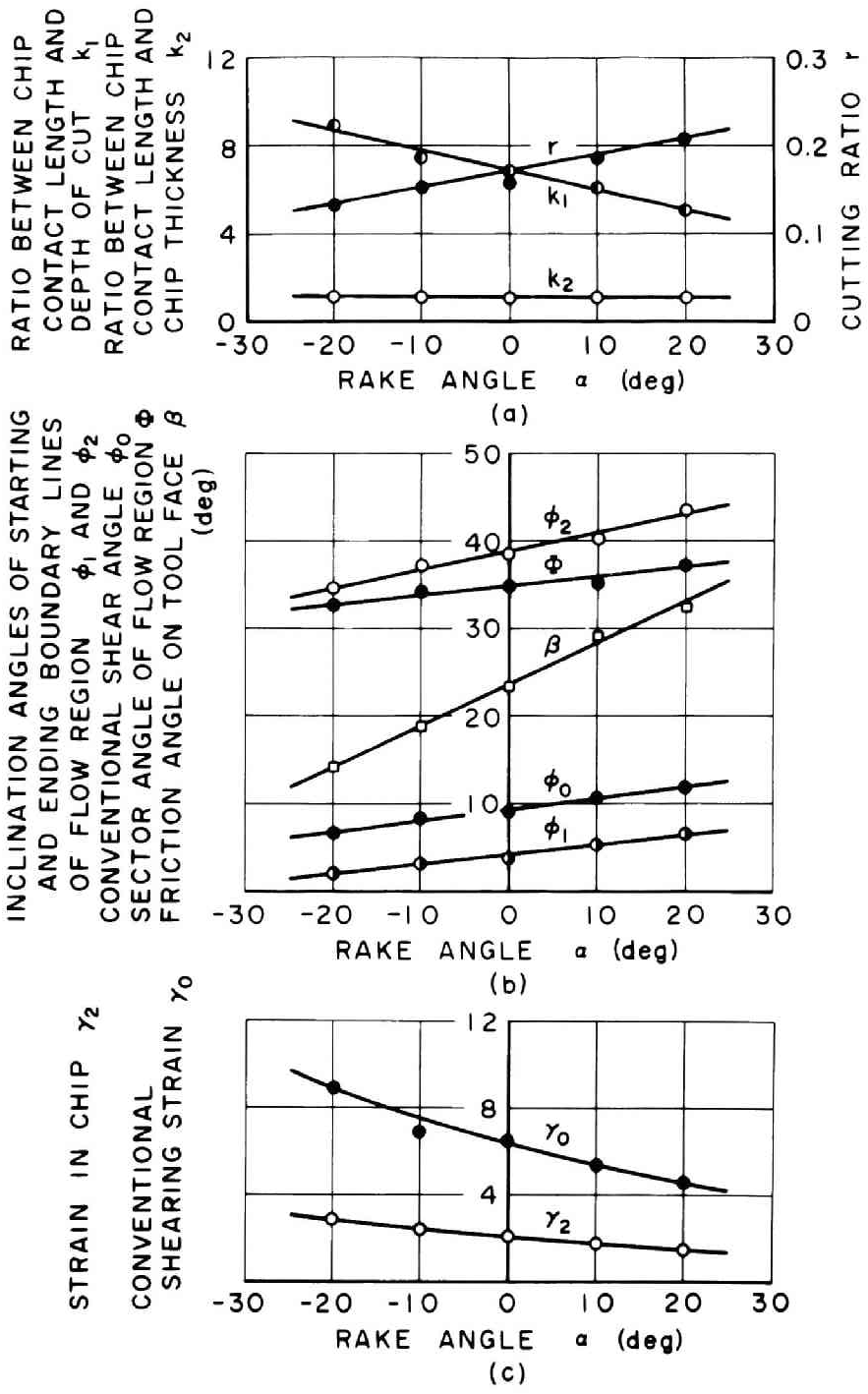

Fig. 13 Calculated values from cutting data shown in Fig. 11 in relation to rake angle; (a) Ratio between chip contact length and depth of cut, ratio between chip contact length and chip thickness, and cutting ratio; (b) Inclination angles of the starting and ending boundary lines of the flow region, sector angle of the flow region, conventional shear angle, and mean friction angle on tool face; (c) Strain in the chip and conventional shearing strain [Work material, lead; tool material, high-speed steel SKH 2(18-4-1); clearance angle, 6 deg; width of cut, 11.0 mm; depth of cut, 0.10 mm; cutting speed, 5.2 m/min; dry]

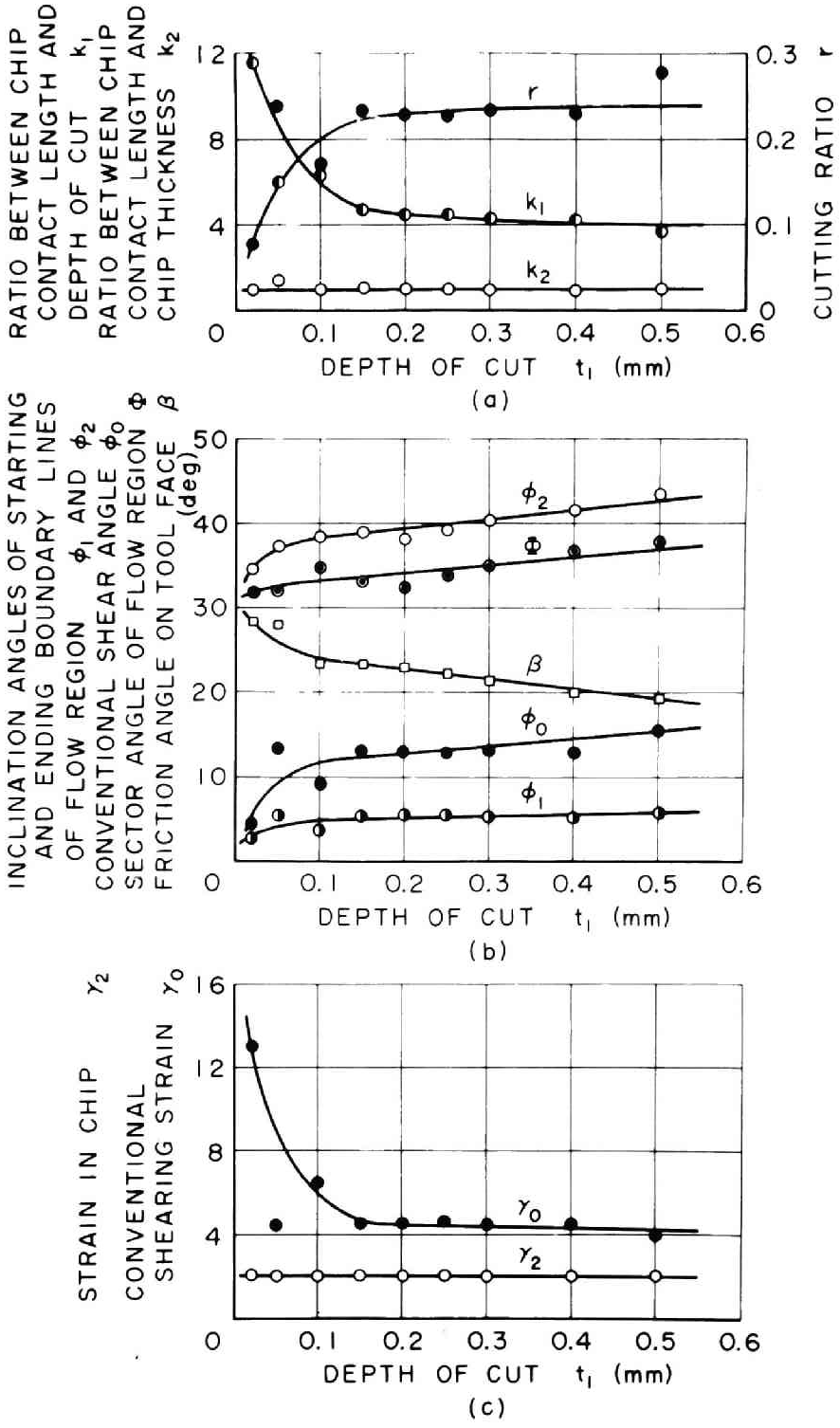

Fig. 14 Calculated values from cutting data shown in Fig. 12 in relation to depth of cut; (a) Ratio between chip contact length and depth of cut, ratio between chip contact length and chip thickness, and cutting ratio; (b) Inclination angles of the starting and ending boundary lines of the flow region, sector angle of the flow region, conventional shear angle, and mean friction angle on tool face; (c) Strain in the chip and conventional shearing strain [Work material, lead; tool material, high-speed steel SKH 2(18-4-1); rake angle, 0 deg; clearance angle, 6 deg; width of cut, 11.0 mm; cutting speed, 5.2 m/min; dry]

flow region ϕ_1 and ϕ_2, sector angle of the flow region Φ, and strain in the chip γ_2 were calculated from Equations [5] through [11], [13], and [16], and are shown in Figs. 13 and 14 in relation to rake angle and depth of cut, respectively. In these figures, the cutting ratio r, the conventional shear angle ϕ_0, and the conventional shearing strain γ_0, which are calculated from the following equations based on the cutting mechanism of a single shear plane, are also shown.

$$r = \frac{t_1}{t_2} \qquad [17]$$

$$\phi_0 = \tan^{-1} \frac{r \cos\alpha}{1 - r \sin\alpha} \qquad [18]$$

$$\gamma_0 = \cot \phi_0 + \tan(\phi_0 - \alpha) \qquad [19]$$

It is evident from Figs. 13(a) and 14(a) that with an increase in rake angle and with an increase in depth of cut, the cutting ratio r increases, the ratio between chip contact length and depth of cut k_1 decreases, and the ratio between chip contact length and chip thickness k_2 does not change. The value of k_1 is seen to vary over a wide range[4~12] much larger than the value[2] obtained by Meyer and Archibald(16, 17). However, the value of k_2 is almost constant and nearly equal to 1 [0.9~1.5], which is consistent with the experimental result on steel obtained by Creveling, Jordan, and Thomsen(18). This leads to the conclusion that the inclination angle of the ending boundary line of the flow region ϕ_2 may be calculated fairly accurately from Equation [8'], while that of the starting boundary line ϕ_1 cannot be determined by Equation [7'].

Referring to Figs. 13(b) and 14(b), the friction angle on tool face β increases with an increase in rake angle, and decreases with an increase in depth of cut. Inclination angles of the starting and ending boundary lines of the flow region ϕ_1 and ϕ_2, sector angle of

the flow region Φ, and the conventional shear angle ϕ_0 have a tendency to increase with an increase in rake angle and with an increase in depth of cut. The inclination angle of the starting boundary line ϕ_1 is smaller and that of the ending boundary line ϕ_2 is larger than

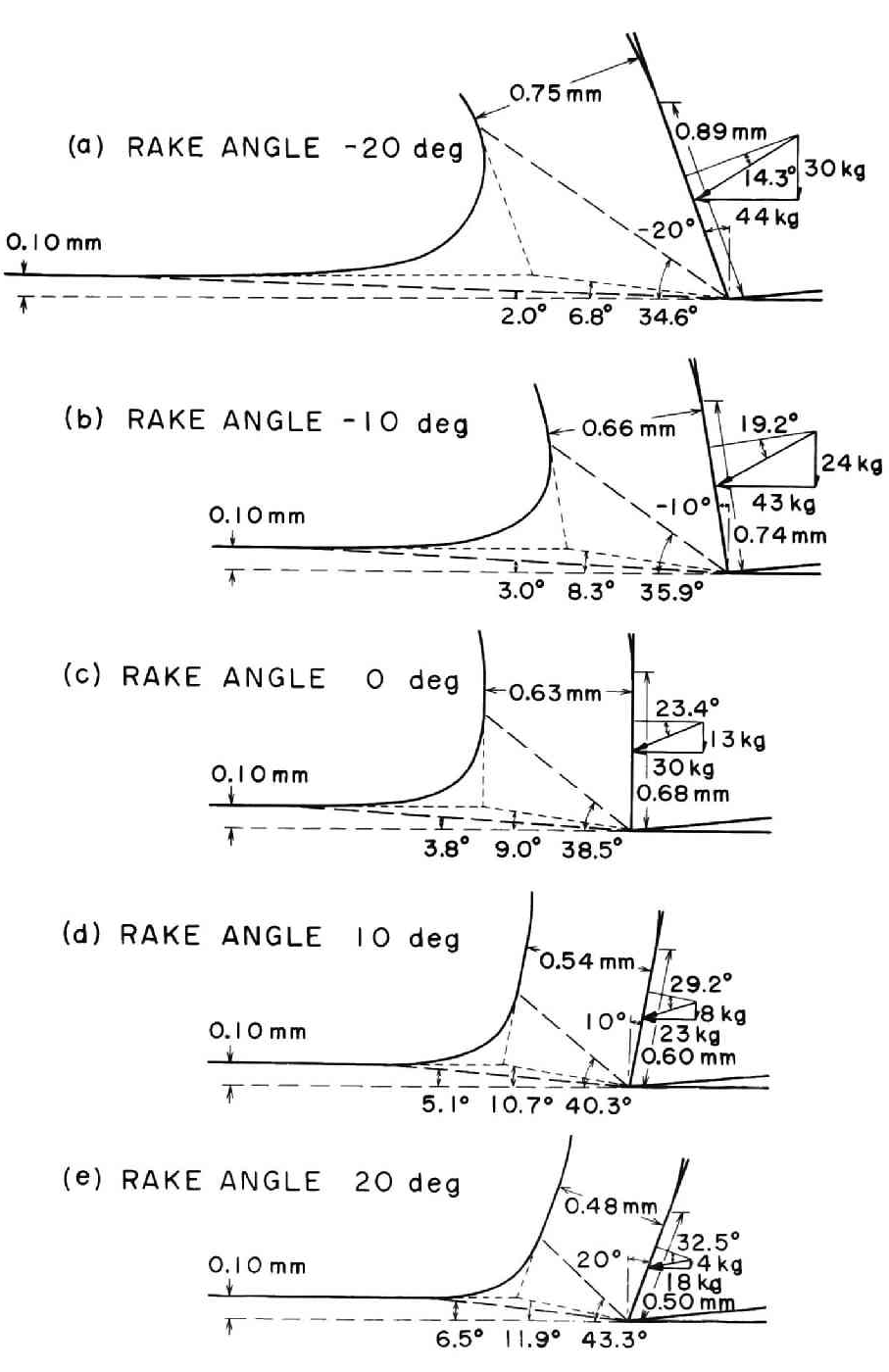

Fig. 15 Schematic cutting model for lead in relation to rake angle [Tool material, high-speed steel SKH 2(18-4-1); clearance angle, 6 deg; width of cut, 11.0 mm; depth of cut, 0.10 mm; cutting speed, 5.2 m/min; dry]

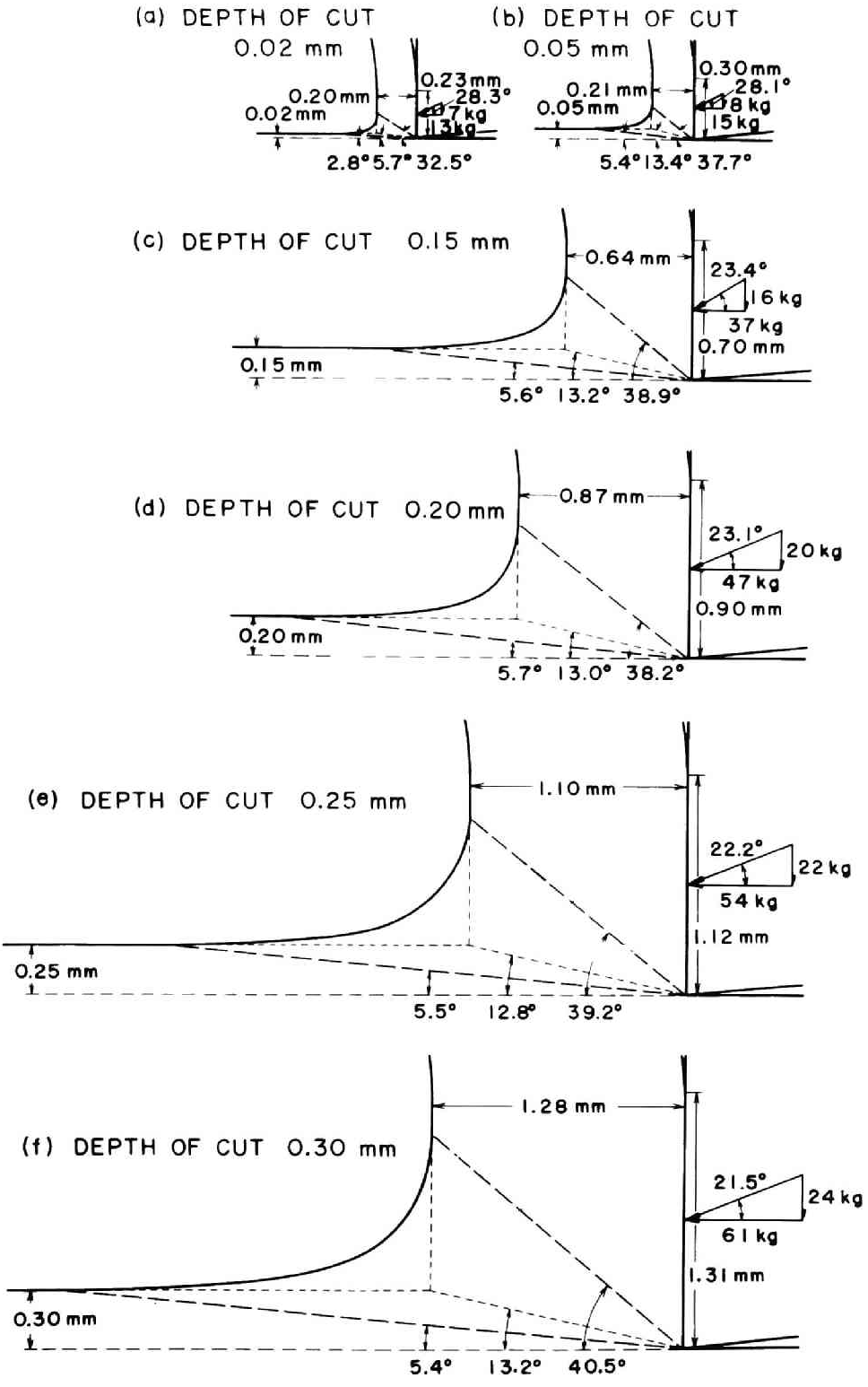

Fig. 16 Schematic cutting model for lead in relation to depth of cut [Tool material, high-speed steel SKH 2(18-4-1); rake angle, 0 deg; clearance angle, 6 deg; width of cut, 11.0 mm; cutting speed, 5.2 m/min; dry]

the conventional shear angle ϕ_0; in other words, the sector angle of the flow region Φ always has some positive value. This proves the rationality of the flow region concept. This is shown schematically in Figs. 15 and 16 in relation to rake angle and depth of cut, respectively. Referring to these figures, the transitional deformation zone between the work and the steady chip is significantly wide, and the plastic flow is observed to occur in a wide region rather than along a single plane. Moreover, while the calculated values of the conventional shear angle by theoretical equations which have been presented by many investigators are not in complete accord with the observed values or the calculated values from Equation [18], especially for negative rake angles, it is a noteworthy fact that the flow region concept shows quite rationally the machining state.

From Figs. 13(c) and 14(c), the strain in chip γ_2 and the conventional shearing strain γ_0 decrease with an increase in rake angle and with an increase in depth of cut. Comparing both strains, the strain in chip γ_2 based on the flow region concept is much smaller than the conventional shearing strain γ_0 based on the single slip plane concept. It appears from this result that the rate of strain is smaller for the cutting state based on the flow region concept than that for the cutting state based on the single slip plane concept. Thus the cutting model with a flow region seems to be more reasonable than the conventional cutting model with a single shear plane not only from the standpoint of smooth movement of a metal particle but from the viewpoint of strain and strain rate.

VI. GRID DEFORMATION IN CONTINUOUS CHIP FORMATION*

Grid deformation in the case of formation of a continuous chip without built-up edge was analyzed, considering the flow region between the rigid region of the work and the plastic region of the steady chip.

It is assumed for simplicity that the steady chip slides uniformly and continuously along the tool face, and that grid deformation under the machined surface is neglected. Let us consider a case in which the free surface of the flow region is a circular arc, as shown in Fig. 17. Denoting the intersection of the free surfaces of the work and the steady chip by C, AC = BC ≡ s. The grid which was a rectangle LL' perpendicular to the cutting direction before cut is deformed to parallelogram MM' after cut. Taking account of nonchange in density of metal during cutting which is plastic deformation, ϵ, the angle between a perpendicular line to the tool face and a grid line in the steady chip which was formerly perpendicular to the cutting direction, was derived as follows:

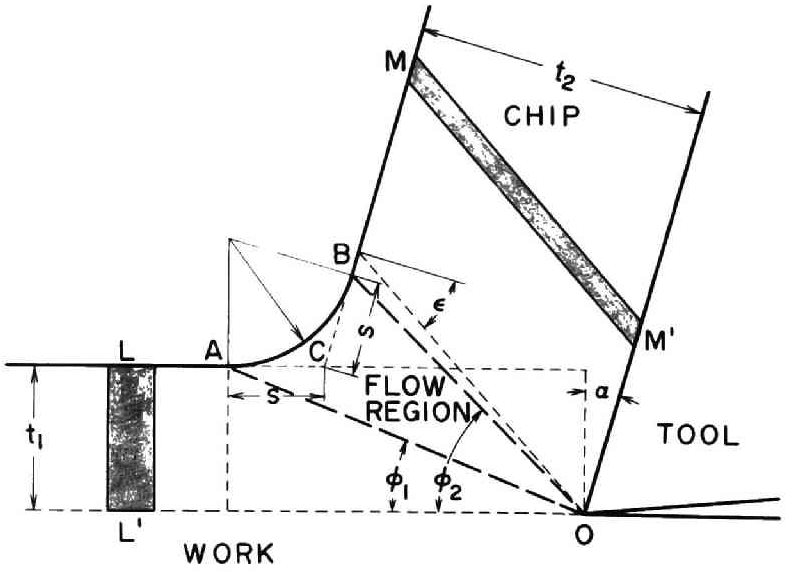

Fig. 17 Analysis of grid deformation in the process of orthogonal cutting accompanying a flow region

* For a detailed discussion on this subject, see Reference(7).

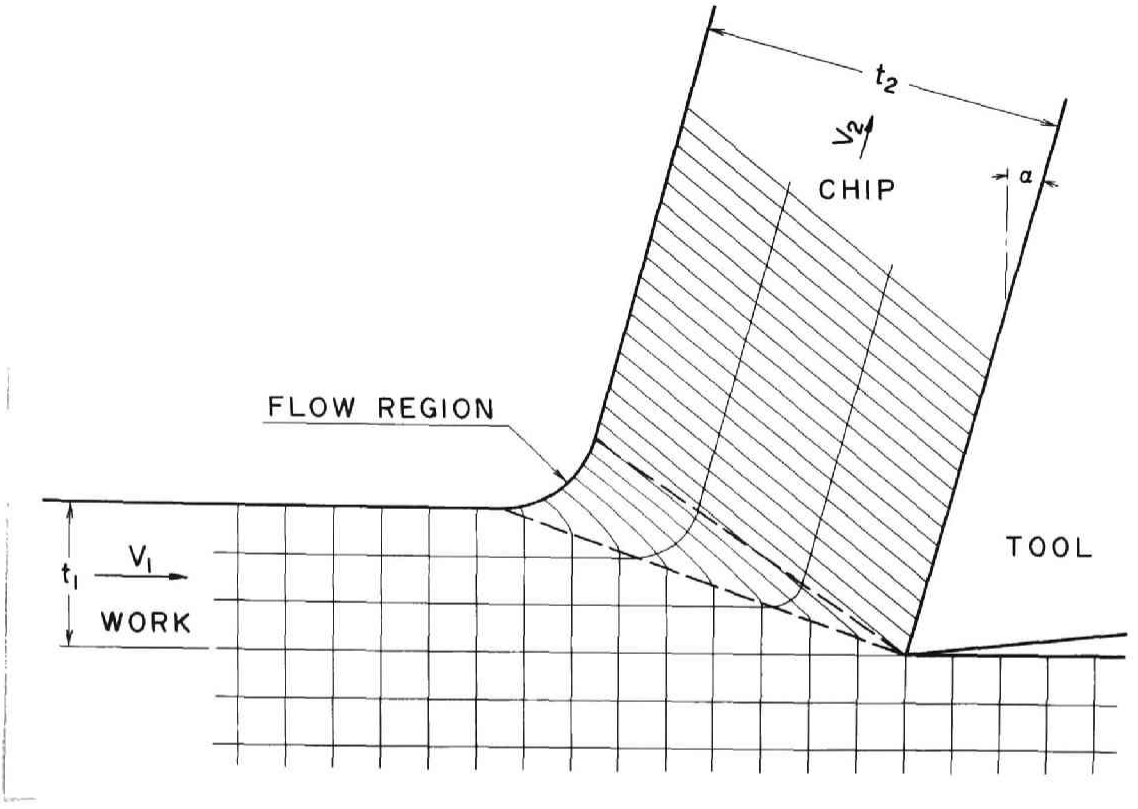

Fig. 18 Typical example of grid deformation in the process of orthogonal cutting accompanying a flow region

$$\tan\epsilon = \tan(\phi_2 - \alpha) + r^2\cot\phi_1 - f(r+1) - 2f^2\left[1 - (\frac{\pi}{4} - \frac{\alpha}{2})\cot(\frac{\pi}{4} - \frac{\alpha}{2})\right]\cot(\frac{\pi}{4} - \frac{\alpha}{2}), \qquad [20]$$

where f is a dimentionless quantity, that is, a ratio of the size of the flow region relative to chip thickness.

$$f = \frac{s}{t_2} \qquad [21]$$

Fig. 18 shows an example of grid deformation in cutting process accompanying a flow region. Smooth distortion of grid during cutting is observed.

In the conventional theory based upon the single shear plane concept, ϵ_0, the angle between a perpendicular line to the tool face and a grid line in the steady chip which was formerly perpendicular to the cutting direction, was derived by Shaffer(21) as follows:

$$\tan\epsilon_0 = \tan(\phi_0 - \alpha) + r^2\cot\phi_0. \qquad [22]$$

However, this is also derived as a special case of Equation [20], putting $\phi_1 = \phi_2 = \phi_0$ and s = 0. It is evident from this that Equation [20] is a general equation which includes the single shear plane concept as a special case.

VII. SOME OBSERVATIONS AND EXPLANATION OF DISCONTINUOUS CHIP FORMATION*

a. Experimental Procedure

The carbon steel was cut with an orthogonal cutting tool, using a specially designed sudden-stop cutting device which was set on a shaper[Wakayama Iron Works Co.; stroke, 48 cm].

The chemical composition and mechanical properties of the test material are given in Table 2.

Table 2 Chemical composition and mechanical properties of work material(carbon steel)

COMPOSITION (%)	
C	0.44
Mn	0.65
Si	0.33
Cu	0.17
Cr	0.10
S	0.024
P	0.017
Fe	BAL
HARDNESS	
ROCKWELL B SCALE	89
ULTIMATE STRENGTH (kg/mm^2)	64
PERCENTAGE ELONGATION (%)	25

Tool material was high-speed steel SKH 2 (18-4-1). The tool was sharp-edged, with a rake angle of 12 deg and a clearance angle of 6 deg, and well finished by a diamond grinder and an oil stone before cutting.

* For detail discussions on this and the following two sections, see Reference(22).

Cutting speed was kept constant, namely, 5.2 m/min, and depth of cut was varied.

A brief sketch of the specially designed sudden-stop cutting device is shown in Fig. 19. The instant the cutting tool ① cuts the work ② for some fixed cutting length, the trip block ③ touches the lever ④, which releases the clamp ⑤ that supports the work holder ⑥. Cutting stops and the work ② which is installed in the work holder ⑥ proceeds in the cutting direction together with the cutting tool ①. The cutting tool ① is set on the tool dynamometer ⑦(20), which is fixed on the ram ⑧ of a shaper, and the cutting resistance, i.e., horizontal and vertical components are recorded on oscillograph paper during cutting. The whole equipment except the cutting tool ①, the tool dynamometer ⑦, and the trip block ③ is

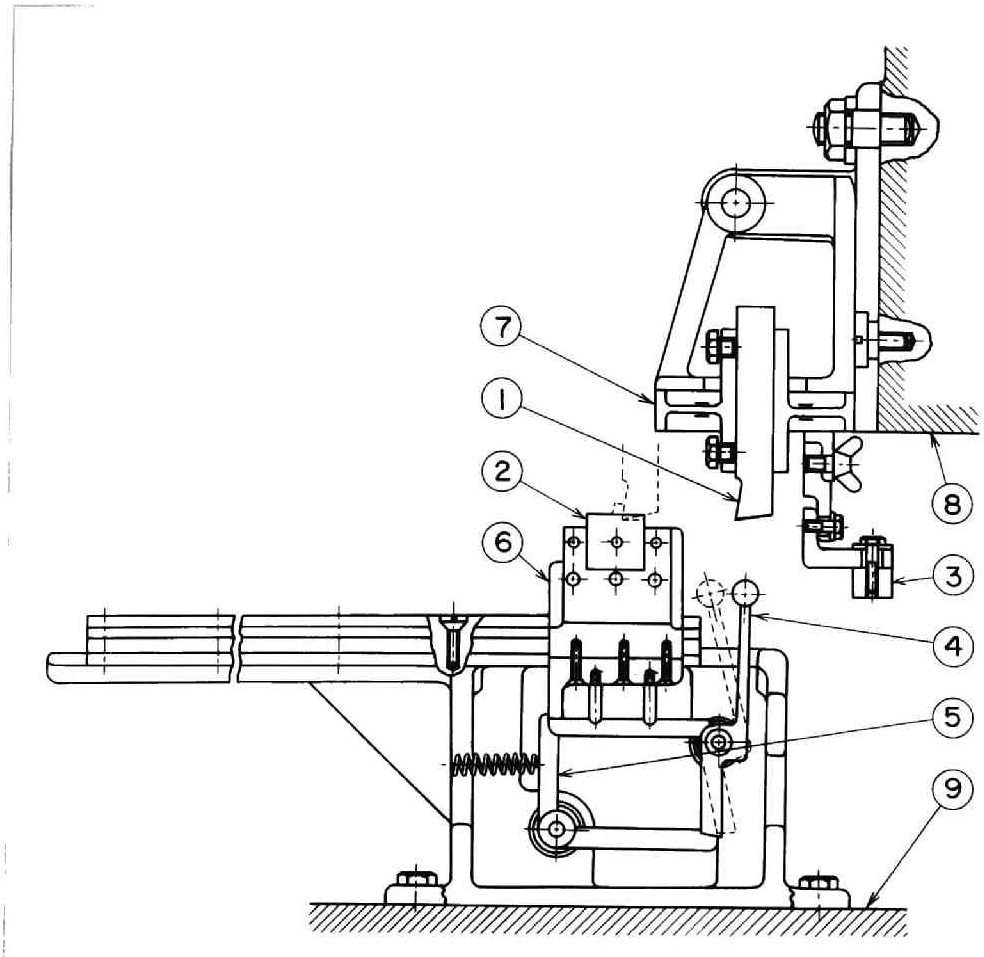

Fig. 19 Sketch of sudden-stop cutting device

set on the table ⑨ of the shaper. It was known from the experiment that the stopping time of cutting by this test equipment was about 0.0013 sec, which seems to be sufficiently short to be used for sudden-stop cutting tests.

The specimen which was obtained by sudden stop during cutting was mounted in a mold, polished, and etched in order to observe the mechanism of chip formation.

b. Examples and Discussion on Discontinuous Chip Formation

Cutting carbon steel with various depth of cut, a discontinuous type of chip was produced for depth of cut over 0.10 mm. A typical example of discontinuous chip formation is shown in Fig. 20. Fig. 21 shows a state at which a fragment of discontinuous chip is about to occur. A trace of the crack line is shown in a solid line marked OB. Plastic flow has already occurred ahead of this line, and so a flow region is recognized. The starting boundary line of the flow region, which is obtained by observing the deformation of the crystal lattice, is shown by the solid line OA. Thus, generally speaking, boundary lines of the flow region are not straight, but curved. This is explained as follows:

Since boundary lines of the flow region are slip lines, they intersect the free surfaces of the work or the chip at 45 deg. They also must cross the face of the cutting tool at its tip by at least 90 deg according to Hill's theorem on the maximum intensity of singularities in a material in yield state(23). Therefore, boundary lines of the flow region are obliged to be curved.

Referring to Figs. 20 and 21, the formation of discontinuous chip is explained as follows:

Fig. 22 shows schematic cutting model of processes of discontinu-

Fig. 20 Typical photograph of discontinuous chip formation [1] [Work material, 0.44% carbon steel; tool material, high-speed steel SKH 2(18-4-1); rake angle, 12 deg; clearance angle, 6 deg; width of cut, 1.45 mm; depth of cut, 0.40 mm; cutting speed, 5.2 m/min; dry]

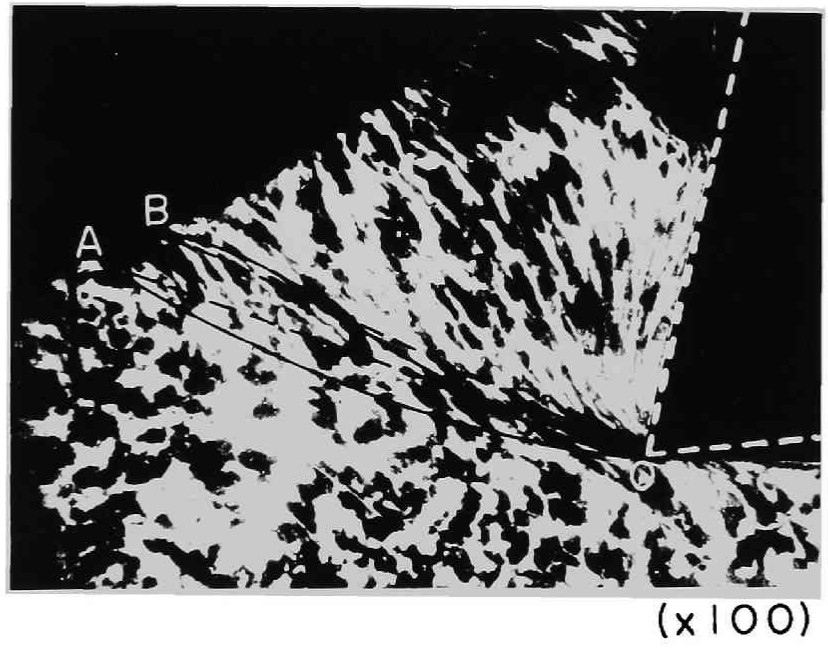

Fig. 21 Typical photograph of discontinuous chip formation [2] [Work material, 0.44% carbon steel; tool material, high-speed steel SKH 2(18-4-1); rake angle, 12 deg; clearance angle, 6 deg; width of cut, 1.45 mm; depth of cut, 0.26 mm; cutting speed, 5.2 m/min; dry]

ous chip formation. The state of the instant when fracture occurs on the ending boundary line of the flow region is shown in Fig. 22(a). Once fracture has occurred, a fragment of discontinuous chip flows out along the tool face without any restriction. The instant fracture occurs, the shearing stress decreases below the breaking limit, and a new chip is ready to be produced. This behavior and cutting process are almost the same as continuous chip formation except that fracture occurs when the shearing stress or strain on the ending boundary line reaches the breaking limit again as cutting proceeds. At the very initial stage the work, which has an inclined free surface at OB due to previous fracture as shown in Fig. 22(a), is not cut immediately, but a portion of the work near the cutting edge rises up to some degree so that some part OB' of the fracture

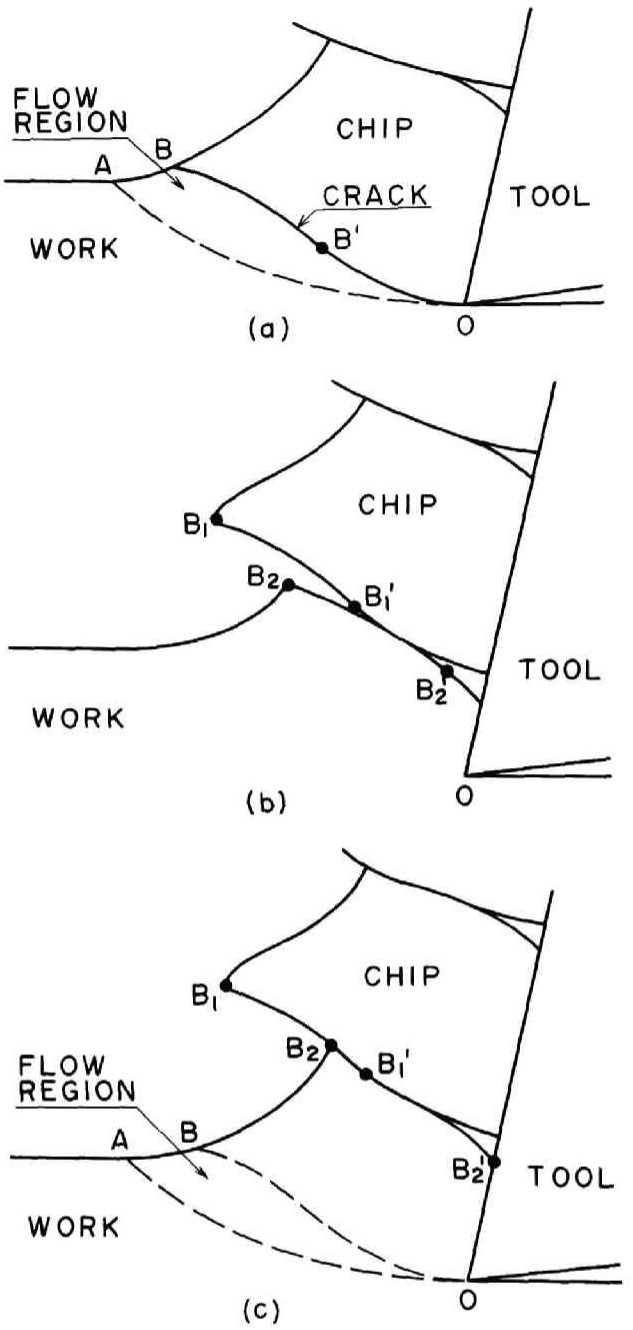

Fig. 22 Processes of discontinuous chip formation accompanying a flow region; (a) State of the instant when fracture occurs on the ending boundary line of the flow region; (b) and (c) Processes of plastic flow during formation of chip fragment

surface OB contacts the tool face and the remaining part BB' contacts the previous chip fragment as shown in Fig. 22(b) and (c). Then the metal starts to slide along the tool face as a regular chip, accompanying the flow region AOB. The shearing stress and strain are minimum at the starting boundary line OA and maximum at the ending boundary line OB. The cutting force is small at the initial stage, and, as cutting progresses, it increases. Whenever the shearing stress on the ending boundary line, which is maximum, increases enough to exceed the breaking limit, fracture occurs at the ending boundary line, and a new fragment of discontinuous chip is produced. The above process is repeated, and fragments of discontinuous chip are formed one by one.

VIII. APPLICATION OF THE FLOW REGION CONCEPT TO AN ANALYSIS OF DISCONTINUOUS CHIP FORMATION

The mechanism of discontinuous chip formation has been analyzed by Piispanen(2), Field and Merchant(24), Cook, Finnie, and Shaw(25), and Lee(26). These analyses, however, are based on the single shear plane concept. In this and the following sections, the flow region concept will be applied to an analysis of the mechanics of discontinuous chip formation, and an example of experimental results will be discussed.

It is evident from the experiments mentioned in Sections III and VII that the flow region exists in discontinuous chip formation and fracture occurs when the shearing stress or strain on the ending boundary line of the flow region exceeds the breaking limit.

As discussed in Fig. 21 in the previous section, both boundary lines of the flow region are curved. It is assumed, however, for the

sake of simplicity that the boundary lines of the flow region are straight lines extending from the tip of the cutting tool to the starting and ending points of the flow region on the free surface as shown with dashed lines in Fig. 21.

In the case of metal being cut with depth of cut t_1 by an orthogonal cutting tool of rake angle α as shown in Fig. 23, the inclination angle of the starting boundary line ϕ_1 and that of the ending boundary line(namely, a line at which fracture occurs) ϕ_2 of the flow region are deduced theoretically as follows.

Since the work material should strain-harden when fracture occurs such as in the discontinuous chip formation, the relationship between shearing stress and shearing strain or $\tau - \gamma$ diagram might be assumed as shown in Fig. 24; that is,

$$\tau = \tau_0 + k\gamma^m, \qquad [23]$$

where τ_0 is the yield shearing stress, and k and m are constants expressing the degree of strain-hardening of the material. Fig. 24 is associated with Fig. 23 as follows: A moving metal particle in the undeformed work corresponds to the position O, and when it reaches the starting boundary line of the flow region, it corresponds to the position L due to the yield of the metal in shear. When a metal particle passes through the flow region it changes its location from the position L to the position M continuously along the curve until it reaches the breaking point M. The breaking point M corresponds to the ending boundary line, i.e., the fracture line, at which fracture occurs periodically, and a discontinuous chip is produced. A metal particle in the chip region corresponds to the position N, and the shearing strain at this position is the strain in discontinuous chip(the equation for it will be deduced later).

Thus, the average shearing stress must reach its maximum value on the ending boundary line of the flow region. Denoting the distance

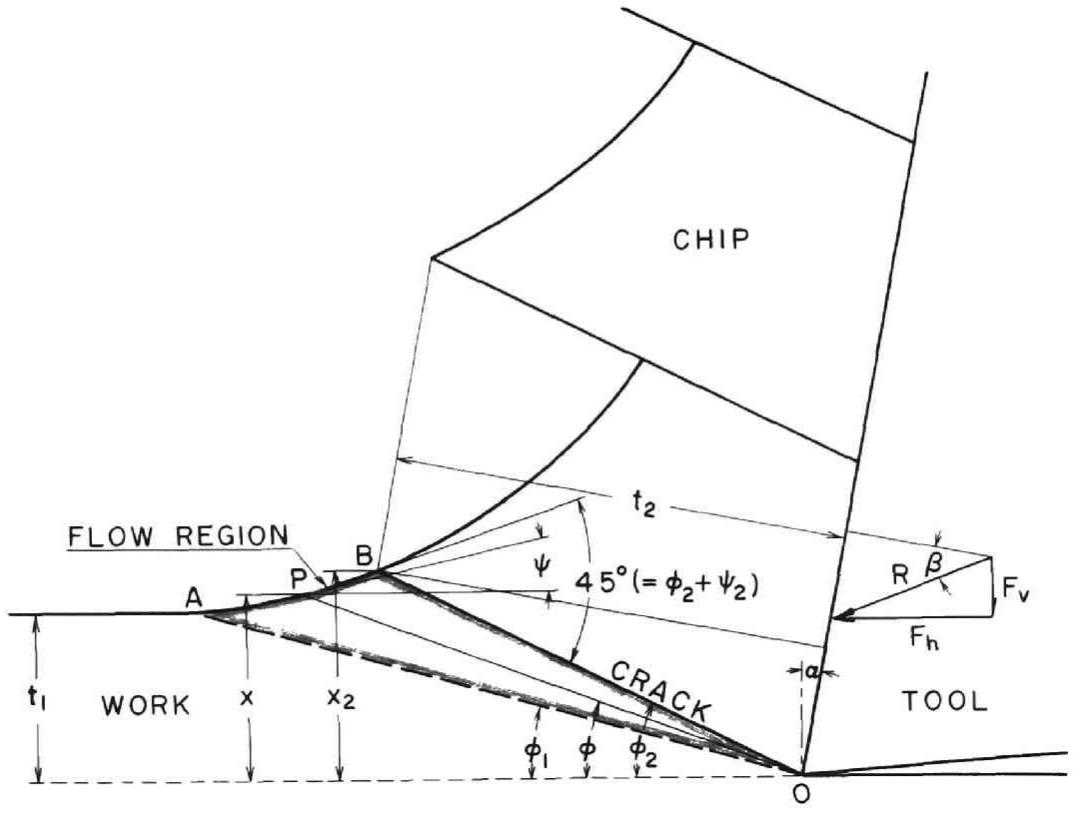

Fig. 23 Analysis of discontinuous chip formation based on the flow region concept

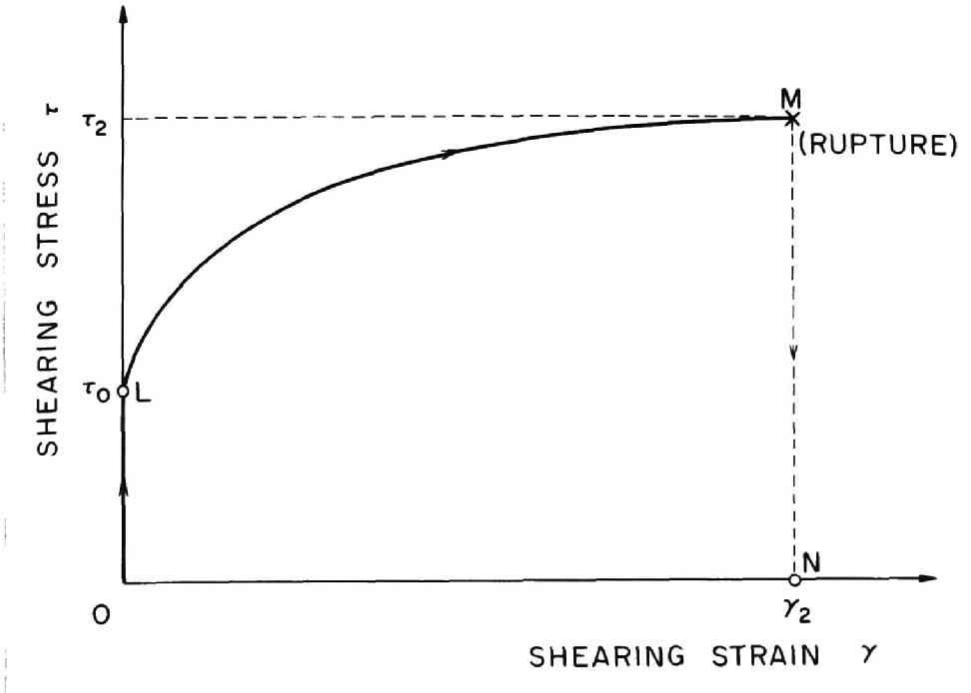

Fig. 24 Shearing stress-strain diagram for the strain-hardening rigid-plastic material

from an arbitrary point P on the free surface of the flow region to the horizontal line through the cutting edge by x, and the maximum cutting force with which fracture is about to occur by R for a width of cut b, and assuming that the shearing stress distributes uniformly on the radial plane in the flow region, the shearing stress on an arbitrary radial plane OP is expressed as

$$\tau = \frac{R \sin\phi \cos(\phi - \alpha + \beta)}{b\ x}. \qquad [24]$$

This reaches the maximum value when the inclination angle of an arbitrary radial plane ϕ becomes equal to the inclination angle of the ending boundary line ϕ_2; that is, from the condition that

$$\left(\frac{d\tau}{d\phi}\right)_{\phi=\phi_2} = 0, \qquad [25]$$

the following equation is obtained.

$$\left(\frac{dx}{x d\phi}\right)_{\phi=\phi_2} = \cot\phi_2 - \tan(\phi_2 - \alpha + \beta) \qquad [26]$$

On the other hand, geometrically

$$\frac{dx}{x d\phi} = \cot\phi - \cot(\phi + \psi). \qquad [27]$$

Hence, for $\phi = \phi_2$

$$\left(\frac{dx}{x d\phi}\right)_{\phi=\phi_2} = \cot\phi_2 - \cot(\phi_2 + \psi_2), \qquad [28]$$

where ψ_2 is the value of ψ at the ending boundary line. Since the ending boundary line of the flow region in the case of discontinuous chip formation is a slip line with fracture, it makes an angle of 45 deg with the free surface. Therefore,

$$\phi_2 + \psi_2 = \frac{\pi}{4}. \qquad [29]$$

From Equations [26], [28], and [29],

$$\phi_2 = \frac{\pi}{4} + \alpha - \beta. \qquad [30]$$

This is the equation showing the condition at which fracture occurs if a discontinuous chip is produced.

The inclination angle of the starting boundary line ϕ_1 in this case is obtained as follows: Since the shearing stress is τ_0, and x is equal to depth of cut t_1 and ϕ to ϕ_1 on the starting boundary line, from Equation [23],

$$\tau_0 = \frac{R \sin \phi_1 \cos(\phi_1 - \alpha + \beta)}{b\, t_1} . \qquad [31]$$

The shearing strain γ_2 and the shearing stress τ_2 on the ending boundary line are obtained by Equations [14]* and [24].

$$\gamma_2 = \cot \phi_2 - \cot(\phi_2 + \psi_2)$$

$$= \cot\left(\frac{\pi}{4} + \alpha - \beta\right) - 1 \quad \text{(from Equations [29] and [30])} \qquad [32]$$

$$\tau_2 = \frac{R \cos(\phi_2 - \alpha) \cos(\phi_2 - \alpha + \beta)}{b\, t_2}$$

$$= \frac{R \cos\left(\frac{\pi}{4} - \beta\right)}{\sqrt{2}\, b\, t_2}, \quad \text{(from Equation [30])} \qquad [33]$$

where t_2 is the theoretical maximum chip thickness. From Equation [23], the following relationship exists among τ_0, τ_2, and γ_2.

$$\tau_2 = \tau_0 + k \gamma_2^m \qquad [34]$$

Substituting Equations [31] to [33] into Equation [34], the required expression for the inclination angle of the flow region ϕ_1 can be obtained.

$$\phi_1 = \frac{K}{2} + \frac{\alpha}{2} - \frac{\beta}{2} \qquad [35]$$

---

* Regarding the shearing strain in the flow region in the case of discontinuous chip formation, it is expressed in Equation [14] as in the case of simple continuous chip formation discussed in Section IV-b.

$$K = \sin^{-1}\left[\sqrt{2}\, r \cos\left(\frac{\pi}{4} - \beta\right) - \frac{2bkt_1}{R}\left\{\cot\left(\frac{\pi}{4} + \alpha - \beta\right) - 1\right\}^m + \sin(\beta - \alpha)\right] \qquad [36]$$

Equations [35] and [30] are theoretical expressions for the starting and ending(fracture) lines of the flow region, respectively, in the case of discontinuous chip formation, and the breaking shearing strain, or the strain in discontinuous chip is expressed by Equation [32].

IX. CUTTING TESTS WITH CARBON STEEL FOR ANALYSIS OF DISCONTINUOUS CHIP FORMATION

The theoretical analysis of discontinuous chip formation discussed in the previous section was applied to cutting tests with carbon steel.

Orthogonal cutting was performed dry for carbon steel(see Table 2), using the specially designed sudden-stop cutting device set on a shaper as explained in Section VII-a.

The cutting conditions were:

Rake angle	α = 12.0 deg
Width of cut	b = 1.45 mm
Depth of cut	t_1 = 0.26 mm
Cutting speed	V_1 = 5.2 m/min.

The discontinuous type of chip obtained is shown in Fig. 21, and this is the state at which fracture is about to occur. The following quantities were measured.

Thickness of chip	t_2 = 0.68 mm
Horizontal cutting force	F_h = 101 kg
Vertical cutting force	F_v = 34 kg
Inclination angle of the starting boundary line of the flow region	ϕ_1 = 19.0 deg

Inclination angle of the ending boundary line
of the flow region $\phi_2 = 27.0$ deg

The mean friction angle on the tool-chip interface is calculated from Equation [13].

$$\beta = \tan^{-1} \frac{34 + 101\tan 12.0^\circ}{101 - 34\tan 12.0^\circ} = 30.6^\circ$$

From Equation [30] the theoretical value for the inclination angle of the ending boundary line(i.e., fracture line) is calculated.

$$\phi_2 = 45^\circ + 12.0^\circ - 30.6^\circ = 26.4^\circ$$

This is seen to be in agreement with the observed value(27.0 deg).

The inclination angle of the starting boundary line ϕ_1 can be calculated from Equations [35] and [36], but constants k and m in Equation [36] are unknown in the present stage. The shearing stress-strain diagram obtained by the conventional static material tests can not be used in this case because of the large strain rate and the heat generated in metal cutting. Therefore, it is necessary to determine the shearing stress-strain diagram for metal cutting, using the observed values in cutting tests.

Substituting the observed values into Equation [31], the shearing stress on the starting boundary line is obtained.

$$\tau_0 = \frac{\sqrt{101^2+34^2}\,\sin 19.0^\circ \cos(19.0^\circ - 12.0^\circ + 30.6^\circ)}{0.145 \times 0.026}$$

$$= 7.29 \times 10^3 \text{ kg/cm}^2$$

The shearing stress(i.e., breaking stress) and the shearing strain on the ending boundary line(i.e., fracture line) are calculated from Equations [32] and [33].

$$\tau_2 = \frac{\sqrt{101^2+34^2}\,\cos(27.0^\circ - 12.0^\circ)\,\cos(27.0^\circ - 12.0^\circ + 30.6^\circ)}{0.145 \times 0.068}$$

$$= 7.30 \times 10^3 \text{ kg/cm}^2$$

$$\gamma_2 = \cot 27.0^\circ - 1 = 0.96$$

Using thus obtained values($\tau = \tau_0 = 7.29 \times 10^3$ kg/cm^2 for $\gamma = 0$ and $\tau = \tau_2 = 7.30 \times 10^3$ kg/cm^2 for $\gamma = \gamma_2 = 0.96$), the shearing stress-strain diagram for carbon steel in the cutting test can be drawn as shown in a solid line in Fig. 25, where the yield point and the breaking point are connected with an approximately straight line. In this figure, the stress-strain diagram for the same material in static material test is drawn in a dashed line, which was obtained from the experimental result of the relationship between twisting moment and specific twisting angle by Ludwik's method(27). Comparing both diagrams, the yield shearing stress is larger, the degree of strain-hardening or the slope of the diagram in the plastic region is smaller, and the ductility is less in the case of cutting test than in the case of static material test. These are reasonable because of the large strain rate and the heat generated in metal cutting. Equations of these two diagrams are expressed as follows:

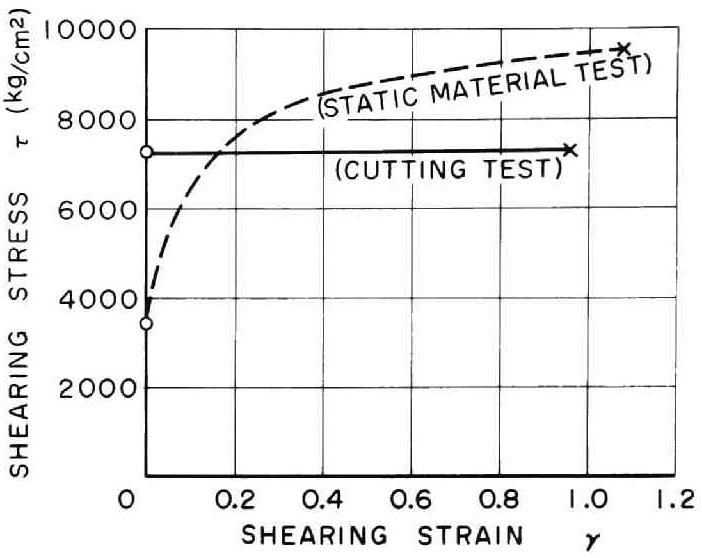

Fig. 25 Comparison of the shearing stress-strain diagrams for carbon steel in cutting test and static material test [o: yield point; x: breaking point]

$$\tau = 3420 + 6160\,\gamma^{0.235} \qquad \text{for static material test,}$$

$$\tau = 7290 + 10\,\gamma \qquad \text{for cutting test,}$$

where τ is in kg/cm^2.

Using constant values k and m in metal cutting, that is, k = 10 and m = 1, the inclination angle of the starting boundary line of the flow region is calculated from Equations [35] and [36].

$$K = \sin^{-1}\left[\sqrt{2} \times \frac{0.026}{0.068} \cos(45.0^\circ - 30.6^\circ) - \frac{2 \times 0.145 \times 10 \times 0.026}{\sqrt{101^2+34^2}}\left\{\cot(45.0^\circ + 12.0^\circ - 30.6^\circ) - 1\right\} + \sin(30.6^\circ - 12.0^\circ)\right]$$

$$= 57.4^\circ$$

$$\phi_1 = \frac{57.4^\circ}{2} + \frac{12.0^\circ}{2} - \frac{30.6^\circ}{2} = 19.4^\circ$$

This shows remarkable agreement with the observed value(19.0 deg).

X. PLASTIC FLOW IN THE CHIP*

Plastic flow in the chip or the secondary plastic flow is an important phenomenon in chip formation as well as the primary plastic flow in the flow region. Analysis of metal cutting is complicated when plastic flow in the chip is taken into consideration. A study by Albrecht(29) is the only one on this topic.

In this and the next sections, plastic flow in the chip will be investigated with a wide range of cutting tests on carbon steel, and the relationship between the primary and secondary plastic flows will be discussed in order to indirectly verify the existence of the flow region and to investigate the effect of cutting conditions on the size of the flow region.

a. Processes of Plastic Flow of Metal in Orthogonal Cutting

The metal structure is arranged in a fixed direction owing to the primary plastic flow in the flow region; that is, as shown in Fig. 26,

---

* For a detailed discussion on this and the next sections, see Reference(28).

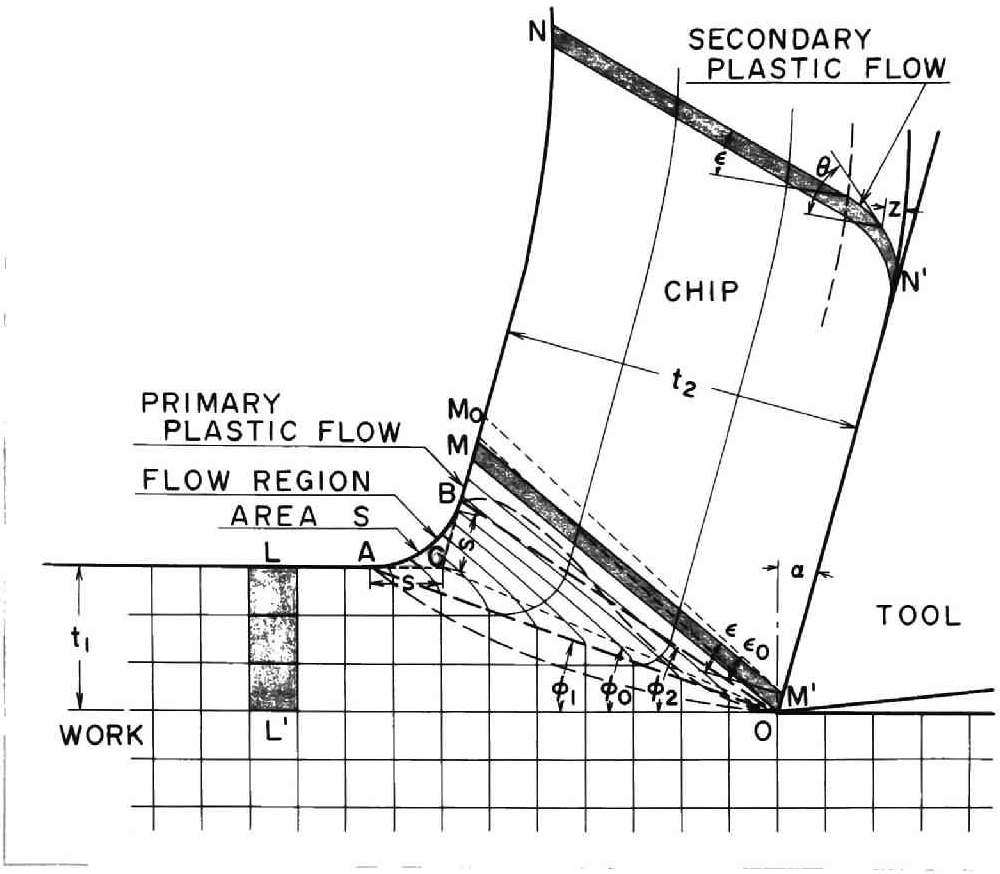

Fig. 26 Processes of the primary and secondary plastic flows of metal in orthogonal cutting

the rectangular portion LL', which was perpendicular to the cutting direction before cutting, is prolonged and arranged as the parallelogramic portion MM' after it has passed through the flow region AOB. The strain due to the primary plastic flow and the direction in which the metal structure is arranged after the primary plastic flow are expressed as Equations [16] and [20], respectively.

Various theories have been presented in regard to whether the process of flowing-out of chip on the tool face is merely a friction process or a shearing process. At present, it is considered that this process is a shearing process in which the yield shearing stress acts on the tool-chip interface, because welding occurs between the chip and the tool face due to the heat generated in cutting.

The secondary plastic flow occurs at the separating side of the chip due to this additional shearing process on the tool-chip inter-

face. Hence the metal structure changes its shape from MM' to NN' as shown in Fig. 26. The shearing strain which the metal receives due to this secondary plastic flow is expressed as follows:

$$\gamma_{sf} = \tan\theta - \tan\epsilon, \qquad [37]$$

where ϵ is the angle between the perpendicular line to the tool face and the straight grid line in the chip which was formerly perpendicular to the uncut surface and is given by Equation [20], and θ is the angle between the perpendicular line to the tool face and the tangent to the curved grid line which is caused by the secondary plastic flow.

b. Experimental Procedure

Orthogonal cutting was performed dry by feeding an orthogonal cutting tool into a tubular specimen in the longitudinal direction on a lathe[Niigata Iron Works Co., type 45SD; swing, 500 mm; center distance, 1100 mm; power, 15 HP].

The work material tested was a seamless tubular specimen of carbon steel[0.43% C; hardness, Rockwell B 92] with outer diameter of 138.0 mm and inner diameter of 132.0 mm so that the width of cut was 3.0 mm.

Tool materials were high-speed steel SKH 2(18-4-1) and steel cutting grade carbide S1(WC-Co-TiC). Tools were sharp-edged with a clearance angle of 6 deg and various rake angles(-40 to 40 deg).

Cutting speed and depth of cut were changed over a wide range.

Chips obtained in cutting tests were mounted, polished, and etched. The longitudinal section of the chip was observed through a microscope and photographed.

c. Flow Line in the Chip

A typical example of the plastic flow in a chip observed in the

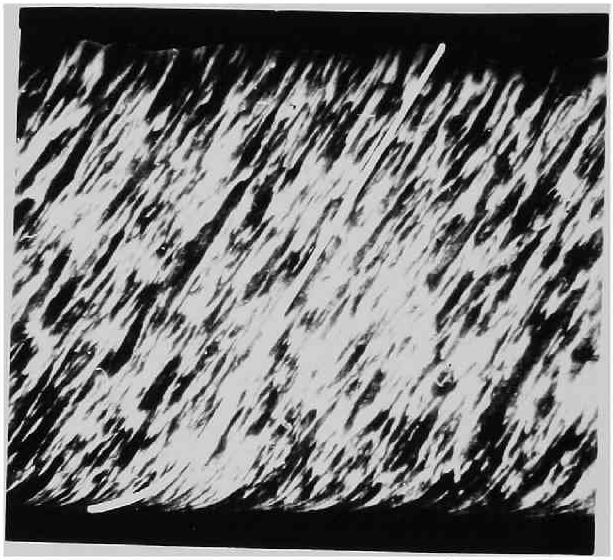

Fig. 27 Typical photograph of the secondary plastic flow in a chip [Work material, 0.43% carbon steel; tool material, carbide S1(WC-TiC-Co); rake angle, 20 deg; clearance angle, 6 deg; width of cut, 3.0 mm; depth of cut, 0.24 mm; cutting speed, 70 m/min; dry]

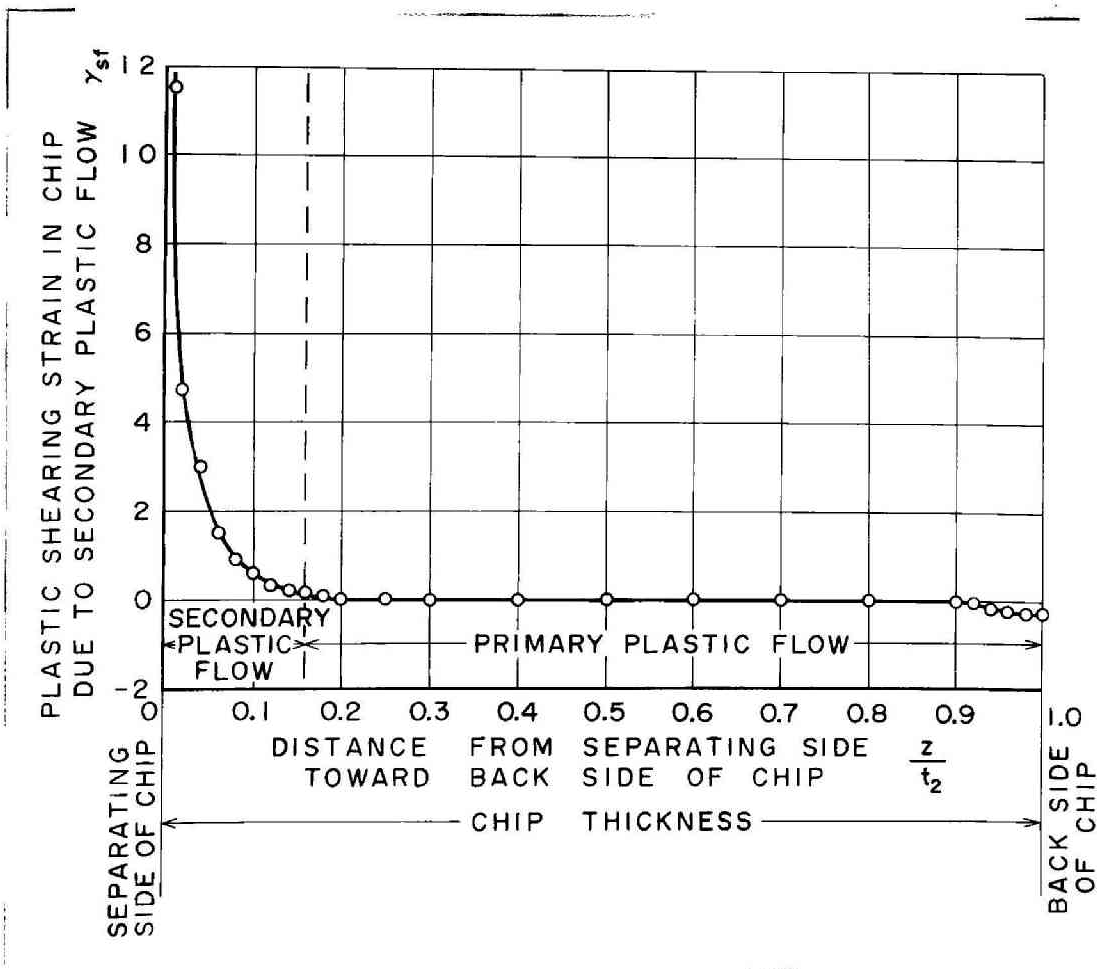

Fig. 28 Plastic shearing strain in the chip due to the secondary plastic flow [Work material, 0.43% carbon steel; tool material, carbide S1(WC-TiC-Co); rake angle, 20 deg; clearance angle, 6 deg; width of cut, 3.0 mm; depth of cut, 0.24 mm; cutting speed, 70 m/min; dry]

experiments is shown in Fig. 27. A trace of the direction of the plastic flow of metal structure or the flow line in the chip is shown in a white line. The portion in which the white line is straight is a layer due to the primary plastic flow in the flow region, and the portion near the tool face in which the white line is curved is considered to be a layer due to the additional secondary plastic flow on the tool-chip interface. The strain in the layer of the secondary plastic flow was calculated from Equation [37] and is shown in Fig. 28. Extremely large shearing strain is associated with in the vicinity of

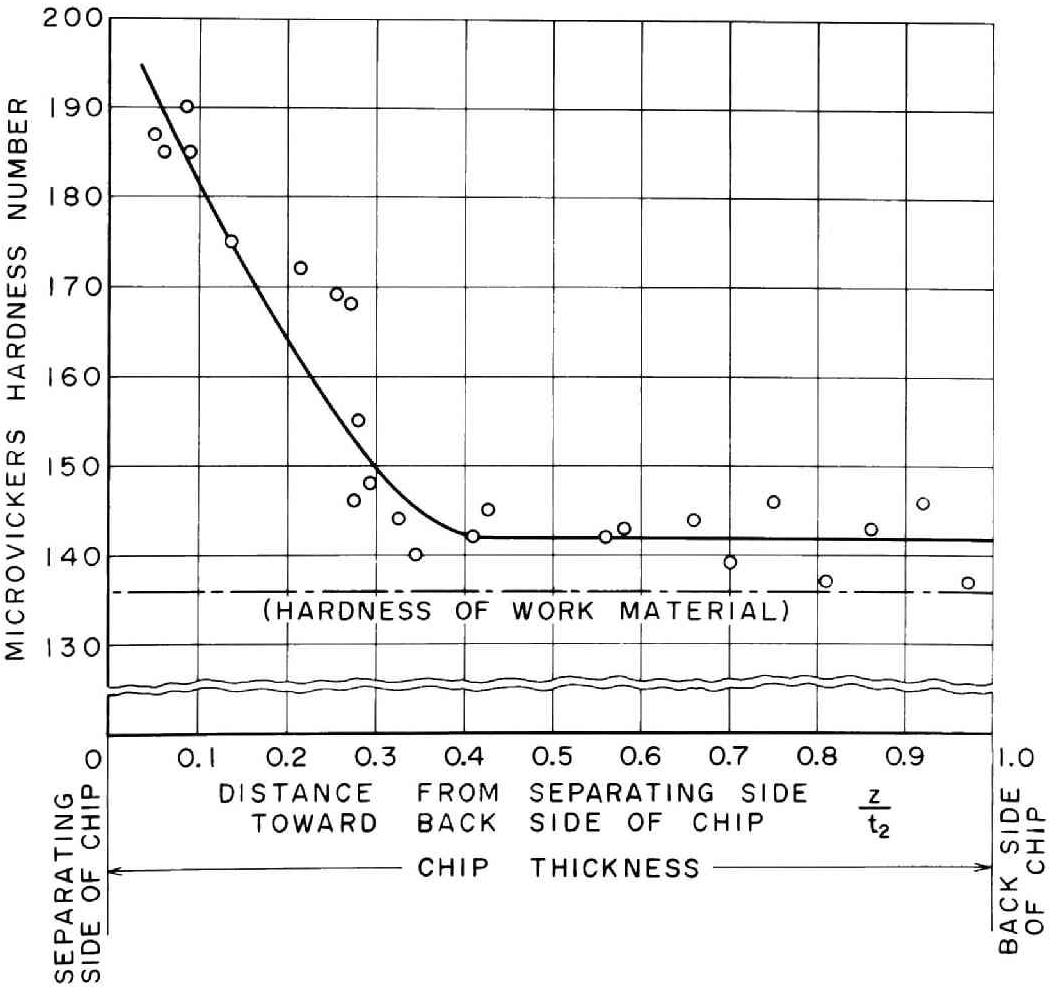

Fig. 29 Hardness distribution in a chip (Hardness, Vickers microhardness number; load, 50 g; loading time, 30 sec) [Work material, 0.43% carbon steel(Vickers microhardness number, 136); tool material, carbide S1(WC-TiC-Co); rake angle, 20 deg; clearance angle, 6 deg; width of cut, 3.0 mm; depth of cut, 0.24 mm; cutting speed, 70 m/min; dry]

the tool face.

The formation of the chip in metal cutting is associated with a large strain-hardening due to plastic flow. The amount of strain-hardening in the chip is greater at the separating side probably as a result of the additional secondary plastic flow on the tool-chip interface. Fig. 29 shows an example of hardness distribution in a chip which was measured with a Vickers microhardness tester[load, 50 g; loading time, about 30 sec]. The measured value of Vickers microhardness is the average value of both pearlite and ferrite structures. The average hardness of the uncut material was 136. It is evident from this hardness distribution in the chip that the amount of strain-hardening is very large at the separating side(the maximum value of Vickers mirohardness is 190), decreases gradually toward the back side, and reaches the constant value of 142. It is concluded from this fact that metal receives uniform strain-hardening with the primary plastic flow and further strain-hardening is added only near the separating side of the chip due to the secondary plastic flow.

d. Deformation in the Layer of the Primary Plastic Flow

Generally the direction of arrangement of metal structure due to the primary plastic flow is straight as shown in Fig. 28 except the case which is associated with extreme chip curl. This direction, or ϵ, the angle between perpendicular line to the tool face and straight flow line in the chip, is related to cutting conditions, and the relation is shown in solid lines in Fig. 30.

This orientation angle ϵ decreases with an increase in rake angle and increases with increases in depth of cut and cutting speed. The large difference between the values for carbide and high-speed steel tools is considered to be due mainly to the different cutting

Fig. 30 Relationship between cutting conditions and orientation angle of metal structure due to the primary plastic flow [Work material, 0.43% carbon steel, tool material, high-speed steel SKH 2(18-4-1) and carbide S1(WC-TiC-Co); clearance angle, 6 deg; width of cut, 3.0 mm; dry]; (a) Effect of rake angle [depth of cut, 0.10 mm; cutting speed, 10 m/min for high-speed steel tool and 70 m/min for carbide tool]; (b) Effect of depth of cut [rake angle, 20 deg; cutting speed, 10 m/min for high-speed steel tool and 70 m/min for carbide tool]; (c) Effect of cutting speed [rake angle, 0 deg; depth of cut, 0.10 mm]

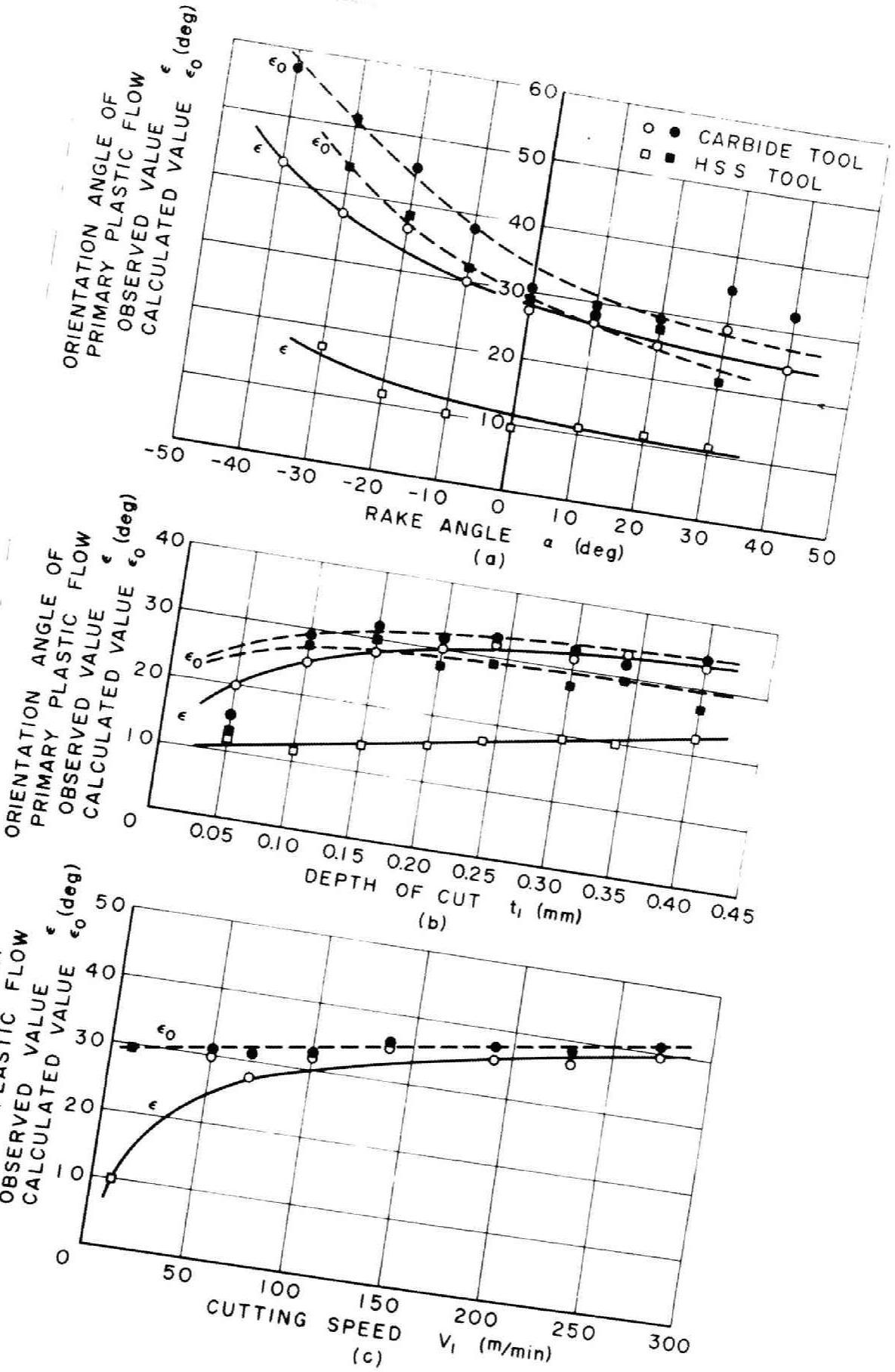
ORIENTATION ANGLE OF PRIMARY PLASTIC FLOW
OBSERVED VALUE ε (deg)
CALCULATED VALUE ε0 (deg)
CARBIDE TOOL
HSS TOOL
RAKE ANGLE α (deg)
(a)
DEPTH OF CUT t1 (mm)
(b)
CUTTING SPEED V1 (m/min)
(c)

Fig. 30

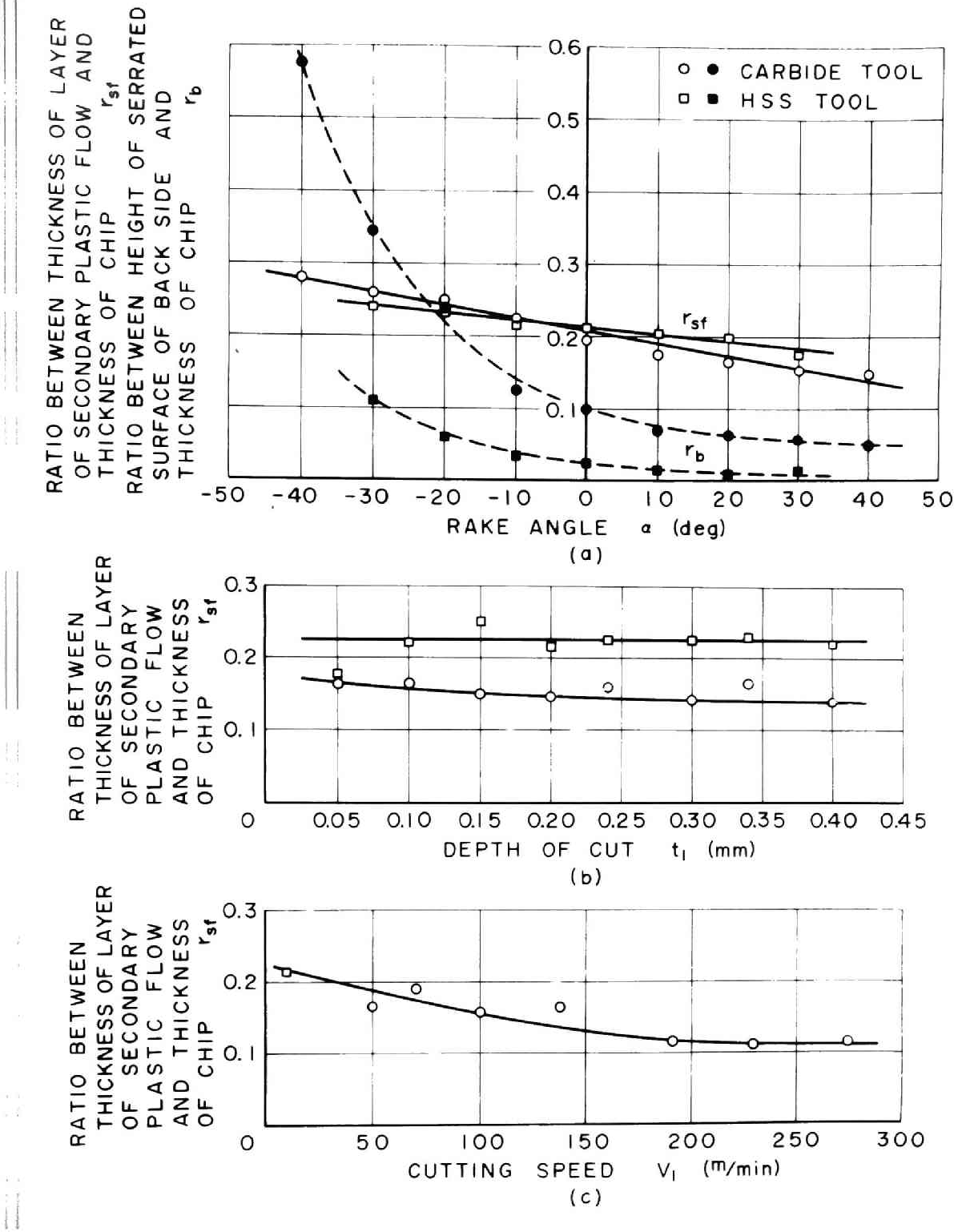

Fig. 31 Relationships between cutting conditions and thickness of the layer of the secondary plastic flow and between cutting conditions and height of the serrated back surface of chip [Work material, 0.43% carbon steel; tool material, high-speed steel SKH 2(18-4-1) and carbide S1(WC-TiC-Co); clearance angle, 6 deg; width of cut, 3.0 mm; dry]; (a) Effect of rake angle [depth of cut, 0.10 mm; cutting speed, 10 m/min for high-speed steel tool and 70 m/min for carbide tool]; (b) Effect of depth of cut [rake angle, 20 deg; cutting speed, 10 m/min for high-speed steel tool and 70 m/min for carbide tool]; (c) Effect of cutting speed [rake angle, 0 deg; depth of cut, 0.10 mm]

speeds at which both tools were tested; namely, a low speed of 10 m/min for high-speed steel tool and high speeds over 50 m/min for carbide tool.

e. Thickness of the Layer of the Secondary Plastic Flow

The dimensionless quantity r_{sf} is defined for a discussion of the layer of the secondary plastic flow in order to eliminate a factor of chip thickness. This is a ratio between thickness of the layer of the secondary plastic flow t_{sf} and chip thickness t_2.

$$r_{sf} = \frac{t_{sf}}{t_2} \qquad [38]$$

The effects of cutting conditions on this dimensionless ratio are shown in Fig. 31. The ratio decreases with increases in rake angle and cutting speed. The effect of depth of cut is small.

f. Serrated Surface of the Back Side of Chip

The separating surface of chip is very smooth due to contact with the tool face. On the other hand, the back side of chip usually has a serrated appearance. This is significant in some cases. An exaggerated example is shown in Fig. 32. This chip was obtained when carbon steel was cut with a depth of cut of 0.10 mm at a cutting speed of 70 m/min by a carbide tool with rake angle of -40 deg.

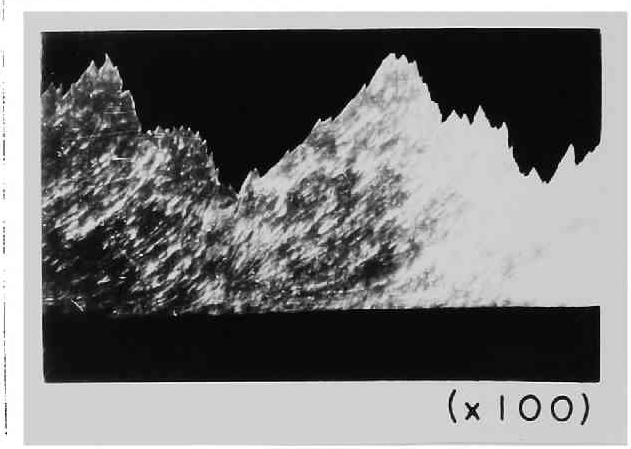

Fig. 32 Photograph of a chip with serrated appearance at the back side [Work material, 0.43% carbon steel; tool material, carbide S1(WC-TiC-Co); rake angle, -40 deg; clearance angle, 6 deg; width of cut, 3.0 mm; depth of cut, 0.10 mm; cutting speed, 70 m/min; dry]

The serrated condition of the back side of the chip appears to be directly related to chatter of the cutting tool. Chatter marks with a pitch of about 2 mm were observed on the machined surface in this example.

A dimensionless quantity r_b is defined as a ratio between height of serrated surface of the back side t_{ss} and chip thickness t_2.

$$r_b = \frac{t_{ss}}{t_2} \qquad [39]$$

The variation of this dimensionless quantity in relation to rake angle is shown in dashed lines in Fig. 31(a). The serrated appearance is extremely large for negative rake angle and it decreases with an increase in rake angle. This means that smooth machining is performed when a large rake angle tool is used.

g. Continuous Chip with Built-Up Edge

In the cutting associated with the formation of built-up edge, a part of the sloughed-off built-up edge is welded to the chip and flows out along the tool face. This built-up edge is observed in the longitudinal section of chip as shown in Fig. 33. It is evident from this microphotograph that the secondary plastic flow is extremely accelerated at the portion

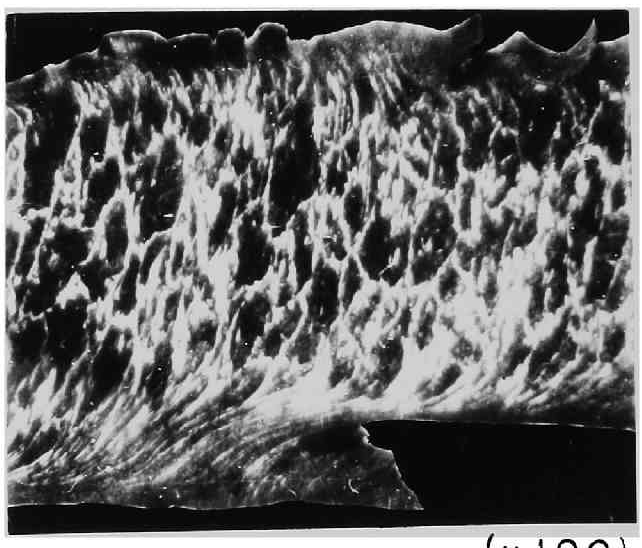

(x 100)

Fig. 33 Photograph of a chip with a part of the sloughed-off built-up edge [Work material, 0.43% carbon steel; tool material, high-speed steel SKH 2(18-4-1); rake angle, 20 deg; clearance angle, 6 deg; width of cut, 3.0 mm; depth of cut, 0.34 mm; cutting speed, 10 m/min; dry]

Table 3 Period of formation of built-up edge [Work material, 0.43% carbon steel; tool material, high-speed steel SKH 2(18-4-1) and carbide S1(WC-TiC-Co); rake angle, 20 deg; clearance angle, 6 deg; width of cut, 3.0 mm; dry]

TOOL MATERIAL	DEPTH OF CUT (mm)	CUTTING SPEED (m/min)	PERIOD OF FORMATION OF BUILT-UP EDGE (sec) MAX.	MIN.	AVE.
CARBIDE	0.05	70	0.186	0.065	0.10
H S S	0.24	10	0.253	0.033	0.13

where a sloughed-off built-up edge has been welded. It appears that the built-up edge is not independent, but is a part of chip and is related to the secondary plastic flow.

The period of formation and sloughing-off of built-up edge was determined by observing the longitudinal section of the chip. It varies even under the same cutting conditions. Examples are listed in Table 3. Moreover, a large built-up edge is not always associated with a long period, and the formation of a small built-up edge sometimes takes a long period. It is also concluded from a wide range of experiments that the period is not affected by cutting speed.

XI. VERIFICATION OF THE EXISTENCE OF THE FLOW REGION BY A STUDY OF THE PLASTIC FLOW IN A CHIP

As was mentioned in the previous sections, it is concluded from theoretical and experimental results that in metal cutting there exists a transitional deformation zone, i.e., the flow region between the rigid region of the work and the plastic region of the steady chip. The existence of the flow region can also be proven by a study of the plastic flow in a chip as follows.

Referring to Fig. 26, if the primary plastic flow occurs along a single shear plane OC, the direction of arrangement of metal structure, or ϵ_0, the angle between the perpendicular line to the tool face and the straight grid line in the chip in the case of the single shear plane concept, is expressed as Equation [22].

The direction of arrangement of metal structure ϵ in the case of chip formation associated with the flow region is expressed as Equation [20].

It is evident from geometrical consideration that ϵ is less than ϵ_0. The difference between two angles ϵ_0 and ϵ is related to the area of the flow region. The area ACB shown in Fig. 26 is expressed as

$$S = \frac{1}{2} t_2^2 (\tan \epsilon_0 - \tan \epsilon). \qquad [40]$$

Therefore, the existence of the flow region can be verified by comparing the observed value ϵ and the calculated value ϵ_0; that is, if both angles are equal, the primary plastic flow occurs along a single plane, while if the calculated value ϵ_0 is greater than the observed value ϵ, the area S has a positive value and hence the flow region does exist.

Experimental procedure is the same as mentioned in Section X-b.

Conducting a wide range of experiments, the cutting ratio r was obtained from Equation [17], and then the conventional shear angle ϕ_0 was calculated from Equation [18]. Both are shown in Fig. 34. As is usually mentioned, the cutting ratio and the conventional shear angle increase with increases in rake angle, depth of cut, and cutting speed.

From these data, the angle for direction of arrangement of metal structure in the chip ϵ_0 was calculated from Equation [22] and is shown in dashed lines in Fig. 30.

Fig. 34 Relationship between cutting conditions and conventional shear angle and cutting ratio [Work material, 0.43% carbon steel; tool material, high-speed steel SKH 2(18-4-1) and carbide S1(WC-TiC-Co); clearance angle, 6 deg; width of cut, 3.0 mm; dry]; (a) Effect of rake angle [depth of cut, 0.10 mm; cutting speed, 10 m/min for high-speed steel tool and 70 m/min for carbide tool]; (b) Effect of depth of cut [rake angle, 20 deg; cutting speed, 10 m/min for high-speed steel tool and 70 m/min for carbide tool]; (c) Effect of cutting speed [rake angle, 0 deg; depth of cut, 0.10 mm]

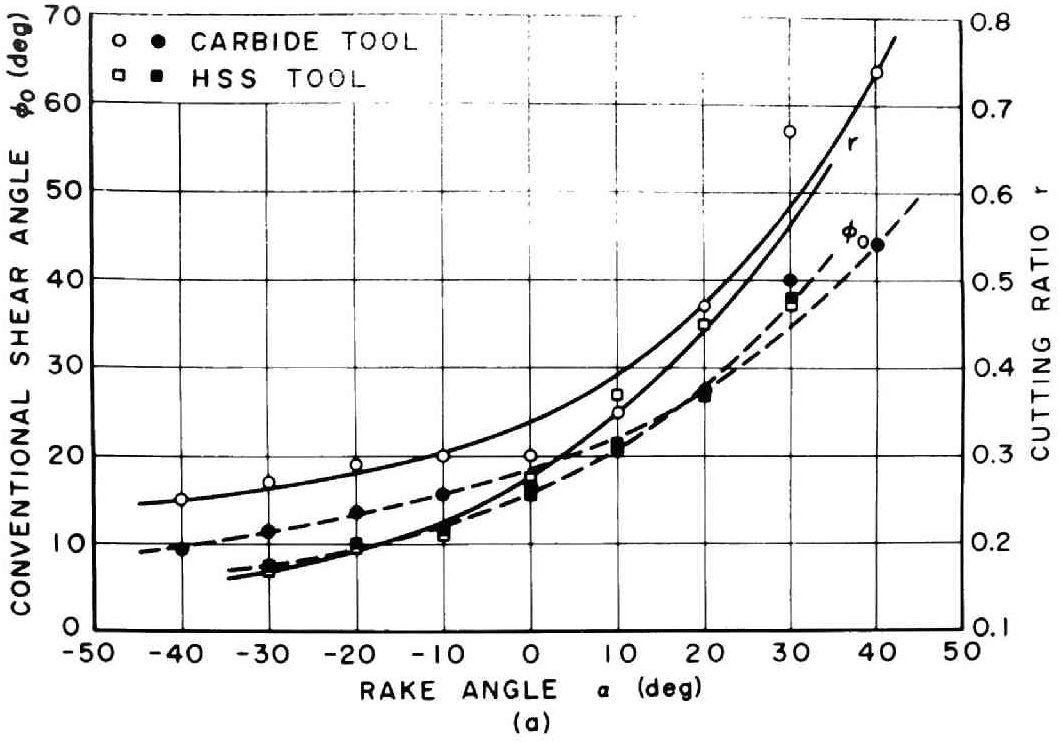
CARBIDE TOOL
HSS TOOL
CONVENTIONAL SHEAR ANGLE ϕ_0 (deg)
CUTTING RATIO r
RAKE ANGLE α (deg)
r
ϕ_0

(a)

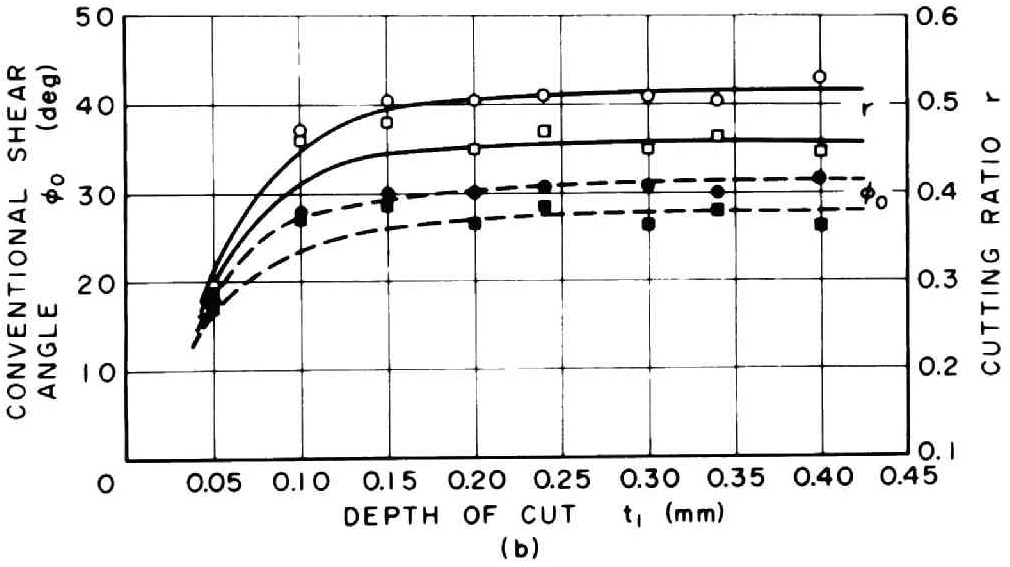
CONVENTIONAL SHEAR ANGLE ϕ_0 (deg)
CUTTING RATIO r
DEPTH OF CUT t_1 (mm)
r
ϕ_0

(b)

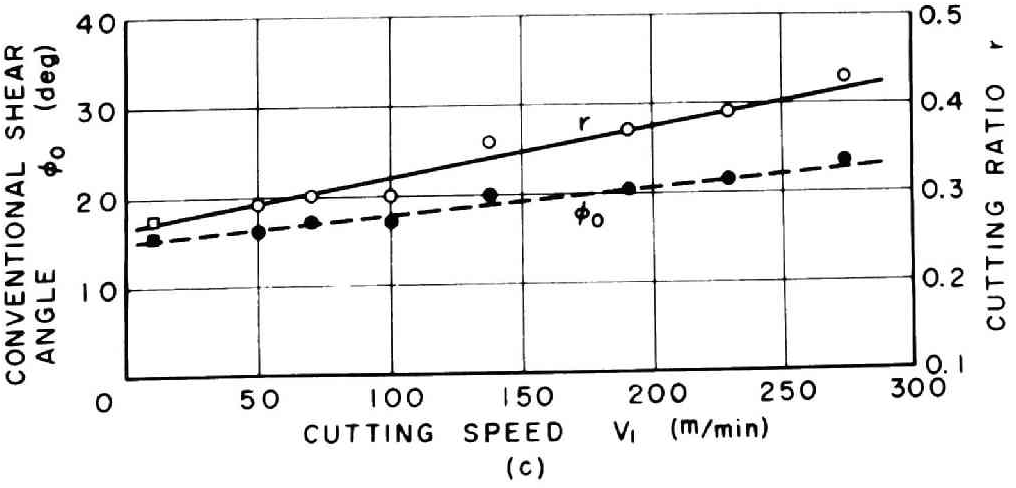
CONVENTIONAL SHEAR ANGLE ϕ_0 (deg)
CUTTING RATIO r
CUTTING SPEED V_1 (m/min)
r
ϕ_0

(c)

Fig. 34

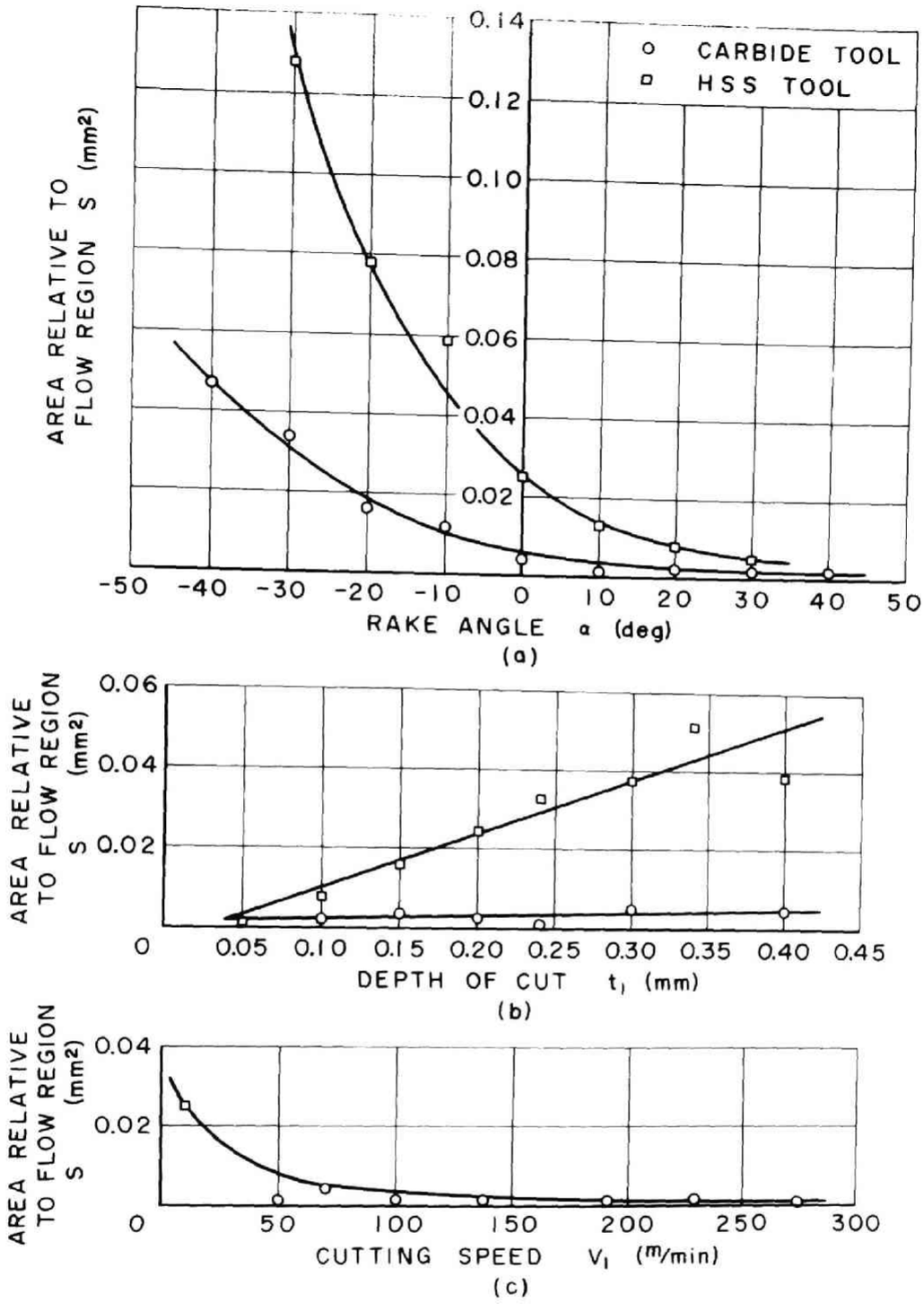

Fig. 35 Relationship between cutting conditions and area relative to the size of the flow region [Work material, 0.43% carbon steel; tool material, high-speed steel SKH 2(18-4-1) and carbide S1(WC-TiC-Co); clearance angle, 6 deg; width of cut, 3.0 mm; dry] (a) Effect of rake angle [depth of cut, 0.10 mm; cutting speed, 10 m/min for high-speed steel tool and 70 m/min for carbide tool]; (b) Effect of depth of cut [rake angle, 20 deg; cutting speed, 10 m/min for high-speed steel tool and 70 m/min for carbide tool]; (c) Effect of cutting speed [rake angle, 0 deg; depth of cut, 0.10 mm]

Referring to both angles ϵ_0 and ϵ in Fig. 30, the area ACB, which is related to the size of the flow region, was calculated from Equation [40]. Fig. 35 shows the relationship between this area and cutting conditions. It is concluded that the flow region always exists in spite of its various sizes for various cutting conditions. The effects of cutting conditions on the size of the flow region are as follows.

The size of the flow region increases with a decrease in rake angle, and it is extremely small for rake angles over 30 deg. These are the opposite of the experimental results for lead[see Section V-c]. The size of the flow region is affected greatly by cutting speed, and is extremely large for low cutting speed below 50 m/min. It also increases in direct proportion to depth of cut at low speeds, but is little affected by depth of cut at high speeds.

The decrease in the size of the flow region with an increase in cutting speed indicates that speed has an effect on the plastic flow; that is, the higher the rate of shear, the narrower the region in which the plastic flow occurs. This localization of the plastic flow in the flow region with an increase in cutting speed is consistent with a study of speed effect in static material tests made by Zener and Hollomon(30).

XII. THE MECHANISM OF CHIP CURL IN ORTHOGONAL CUTTING*

Several theories have been presented regarding the chip-curl phenomenon in orthogonal cutting; they include the bending moment theory

---

* For a detailed discussion on this and the next sections, see Reference(31).

by Henriksen(32), the temperature theory by Hahn(33), and the shearing-strain conductivity theory by Takeyama(34). These theories have explained the chip-curl phenomenon in some respects.

In this and the next sections, the phenomenon of chip curl in orthogonal cutting will be investigated from the standpoint of the flow region concept, the mechanism of chip curl will be analyzed, and the experimental results on lead and carbon steel will be discussed.

In previous sections, the boundary lines of the flow region have been assumed straight lines, extending from the tip of the cutting tool to the starting and ending points of flow on the free surface. In reality, however, the starting and ending boundary lines are convex downward and upward, respectively[the reason for this was explained in Section VII-b], as shown in Fig. 36. This is one reason for chip curl and will be discussed later. Moreover, it has been assumed that the shearing stresses on the boundary lines of the flow region are uniformly distributed along the lines. However, if the shearing stress on the ending boundary line of the flow region is not distributed uniformly, but decreases from the tip of the cutting tool to the free surface along the line as shown in Fig. 36, this is an another cause of chip curl.

a. Chip Curl due to Ununiformly Distributed Shearing Stress on the Ending Boundary Line of the Flow Region

If the stress distribution on the ending boundary line of the flow region is assumed as shown in Fig. 36, and the shearing stress-strain relationship in the plastic range is straight as shown in Fig. 37, taking the strain-hardening property of the work material into consideration, the shearing strain is maximum at the tip of the cutting tool, and minimum at the back side of chip. Therefore, metal

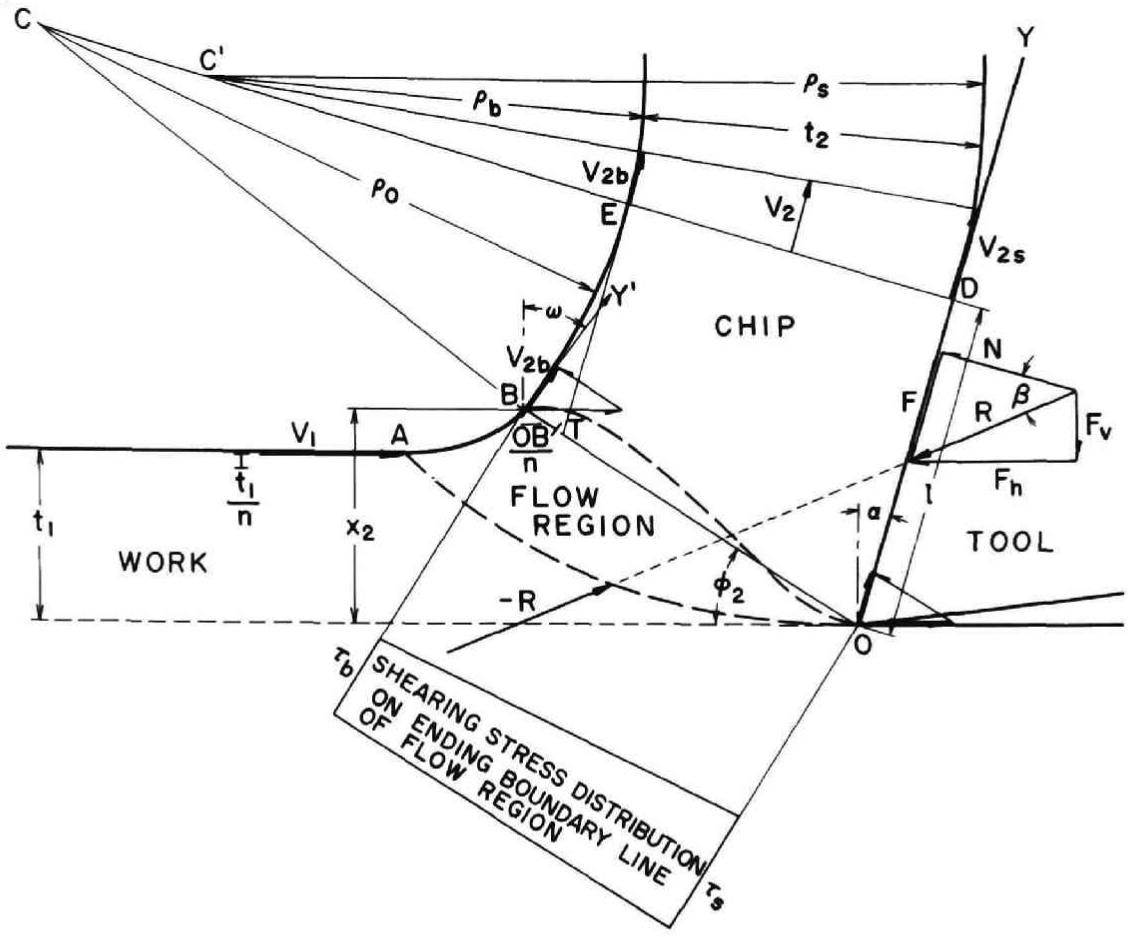

Fig. 36 Mechanism of chip curl in orthogonal cutting; [1] Chip curl due to ununiformly distributed shearing stress on the ending boundary line of the flow region

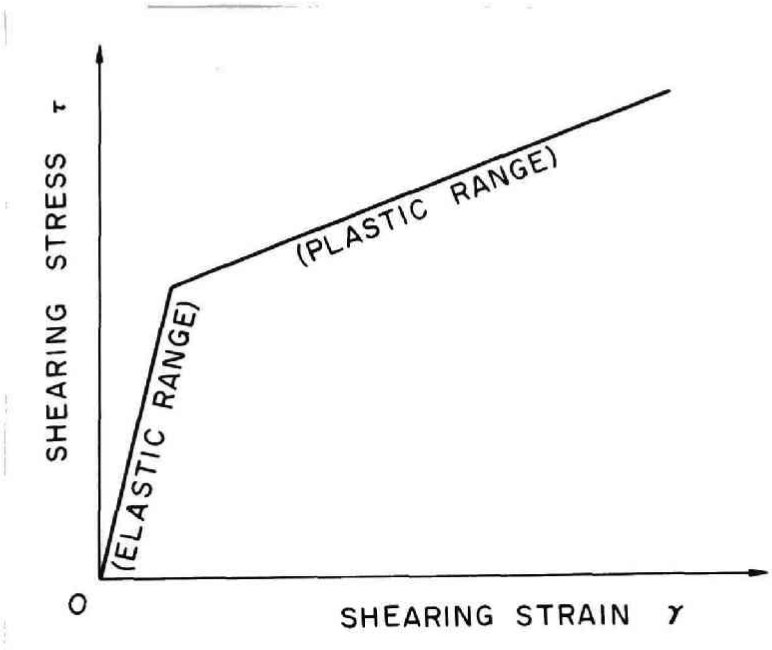

Fig. 37 Shearing stress-strain diagram for the strain-hardening material with linear relationship in the plastic range

particles have motion components toward OY along the tool face(which makes a lip angle $\delta = \frac{\pi}{2} - \alpha$ with the machined surface, where α is rake angle) at the tip of the cutting tool and toward a direction BY'(which makes an angle $\psi_2 = \frac{\pi}{2} - \omega$, where ω is the angle between the perpendicular line to the cutting direction and the direction of movement of a metal particle at the ending point of the flow region, $\omega > \alpha$) at the back side of chip. Thus a metal particle, which has reached the plastic region of the steady chip after plastic deformation in the flow region, begins to curl gradually; for example, a metal particle on the free surface curls along an arc with radius of curvature ρ_0 and reaches a point E which is an intersection between the back side of chip and a straight line connecting the center of curvature C and the chip separating point D on the tool face. In this case, a straight line CD is perpendicular to the tool face. On the other hand, a metal particle, which has passed through the tip of the cutting tool, moves straightly along the tool face OD and reaches the separating point D, accompanying an acceleration of flowing-out speed due to the heat generated and the compression action on the tool face. Comparing speeds of movement of metal particles at the separating and back sides of chip on the line CD, it is evident that a metal particle at the back side of chip is forced to move along a contour of curl radius ρ_b, which is different from ρ_0, and a metal particle at the separating side of chip along a contour of curl radius $\rho_s (= \rho_b + t_2$, where t_2 is chip thickness), as explained in the following.

A radius of curl, along which a metal particle on the back side of chip moves after passing through the ending boundary line until it reaches the steady state, is given by

$$\rho_0 = \frac{l \sin\phi_2 - x_2 \sin(\phi_2 - \alpha)}{\sin\phi_2 \cos(\omega - \alpha)}, \qquad [41]$$

where l is chip contact length on the tool face OD, x_2 is length of a

perpendicular from the ending point B of the flow region to the horizontal line through the cutting edge, and ϕ_2 is angle between the cutting direction and a straight line OB.

A flowing-out speed V_{2b} of a metal particle on the free surface just after passing through the flow region is obtained from the continuity condition of metal flow.

$$V_{2b} = \frac{t_1}{x_2} \frac{\sin\phi_2}{\cos(\phi_2-\omega)} V_1, \qquad [42]$$

where t_1 is depth of cut and V_1 is cutting speed. This velocity is transferred to the point E. On the other hand, the flowing-out velocity at the separating side of chip is accelerated as explained above and becomes V_{2s} at the separating point D. Assuming the velocity distribution on DE is linear, the average chip velocity is

$$V_2 = \frac{V_{2b} + V_{2s}}{2}. \qquad [43]$$

From the continuity condition,

$$t_1V_1 = t_2V_2. \qquad [44]$$

The flowing-out velocity at the separating side of chip is obtained from Equations [42] to [44].

$$V_{2s} = \frac{2x_2\cos(\phi_2-\omega) - t_2\sin\phi_2}{t_2x_2\cos(\phi_2-\omega)} t_1V_1 \qquad [45]$$

The steady chip after passing through DE is obliged to curl owing to the velocity difference at the back and separating sides of chip. The inner and outer radii are expressed as follows:

$$\rho_b = \frac{t_2}{2} \frac{t_2\sin\phi_2}{x_2\cos(\phi_2-\omega) - t_2\sin\phi_2} \qquad [46]$$

$$\rho_s = \rho_b + t_2$$
$$= \frac{t_2}{2} \frac{2x_2\cos(\phi_2-\omega) - t_2\sin\phi_2}{x_2\cos(\phi_2-\omega) - t_2\sin\phi_2}. \qquad [47]$$

Both are positive values, because

$$\rho_b \approx \frac{t_2}{2} \frac{\overline{OT}}{\overline{BT}} > 0,$$

where T is an intersection between the straight line OB and the parallel line through the point E to the tool face.

It is evident from Equations [41] and [46] that a metal particle on the back side of chip starts to curl with a radius ρ_0 in the transitional stage, and then with a radius ρ_b in the steady stage.

Although rake angle α and depth of cut t_1 do not appear explicitly in Equations [46] and [47], radius of chip curl is affected by them, since quantities such as t_2, x_2, ϕ_2, and ω are related to α and t_1.

b. Chip Curl due to the Upwardly Convex Ending Boundary Line of the Flow Region

Since it is rather difficult to deduce the radius of chip curl when the flow region with an upwardly convex ending boundary line is

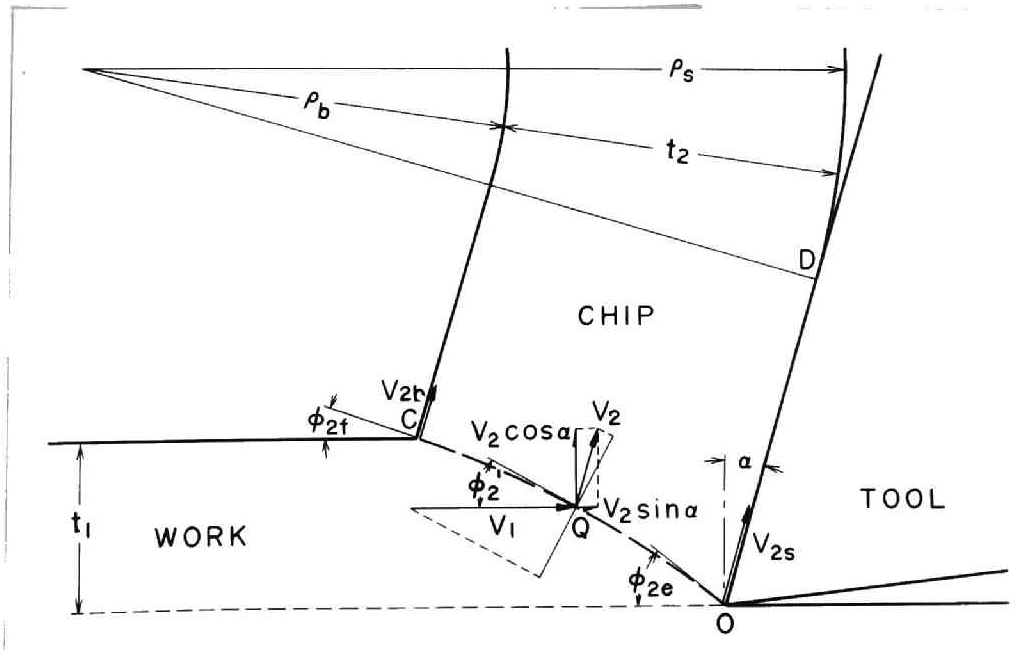

Fig. 38 Mechanism of chip curl in orthogonal cutting; [2] Chip curl due to the upwardly convex ending boundary line of the flow region

taken into consideration, in the following analysis, the flow region is exchanged with the conventional shear plane OC which is convex upward. The inclination angle of this plane is denoted by ϕ_{2e} at the tip of the cutting tool and ϕ_{2f} at the free surface as shown in Fig. 38.

The flowing-out velocity of a metal particle which has reached an arbitrary point Q on the plane OC is obtained from the continuity condition of velocity in normal direction to the plane.

$$V_2 = \frac{\sin\phi_2'}{\cos(\phi_2' - \alpha)} V_1, \qquad [48]$$

where ϕ_2' is the inclination angle of the tangent to the plane OC at an arbitrary point Q. In a particular case, the flowing-out velocities at the separating and back sides of chip are expressed

$$V_{2s} = \frac{\sin\phi_{2e}}{\cos(\phi_{2e} - \alpha)} V_1 \qquad [49]$$

and

$$V_{2b} = \frac{\sin\phi_{2f}}{\cos(\phi_{2f} - \alpha)} V_1, \qquad [50]$$

respectively. Inner and outer radii of chip curl are obtained as follows:

$$\rho_b = \frac{t_2 \sin\phi_{2f} \cos(\phi_{2e} - \alpha)}{\sin(\phi_{2e} - \phi_{2f}) \cos\alpha} \qquad [51]$$

$$\rho_s = \frac{t_2 \sin\phi_{2e} \cos(\phi_{2f} - \alpha)}{\sin(\phi_{2e} - \phi_{2f}) \cos\alpha} \qquad [52]$$

Since both are positive values, it is concluded that chip has a tendency to curl if the shear plane or the ending boundary line of the flow region is convex upward. However, this is not the only reason for chip curl, because, if it were, the chip might start to curl directly after passing the cutting edge, but in reality the chip begins

to curl after a short length of contact with the tool face.

Equations [46], [47], [51], and [52] do not completely explain the chip-curl phenomenon, since the heat generated, which is one of the important factors in the chip-curl phenomenon, is not taken into consideration and the analysis is made under some assumptions.

XIII. EXPERIMENTAL RESULTS ON CHIP CURL

a. Experimental Procedure

Orthogonal cutting was performed dry by feeding an orthogonal cutting tool into a tubular specimen of carbon steel[0.43% C; hardness, Rockwell B 92] in the longitudinal direction on a lathe[Niigata Iron Works Co., type 45SD; swing, 500 mm; center distance, 1100 mm; power, 15 HP] with the same experimental procedure as mentioned in Section X-b. Similar cutting test was made dry by feeding an orthogonal cutting tool into an annular specimen of lead[Pb 98.94%, Sn 1.03%, and Sb 0.03%; Brinell hardness number, 12 at a load of 500 kg; diameter, 125 mm; width of cut, 6.0 mm] in the transverse direction on the same lathe.

Two components of tool force were measured with a strain-gage type tool dynamometer(20).

After the cut the chip contact length on the tool face, chip thickness, and radius of chip curl were measured.

b. Cutting Tests on Lead

An example of chips obtained by orthogonal cutting of an annular specimen of lead with high-speed steel tools SKH 2(18-4-1) at a low cutting speed of 9 ^{m}/min is shown in Figs. 39 and 40, which show the

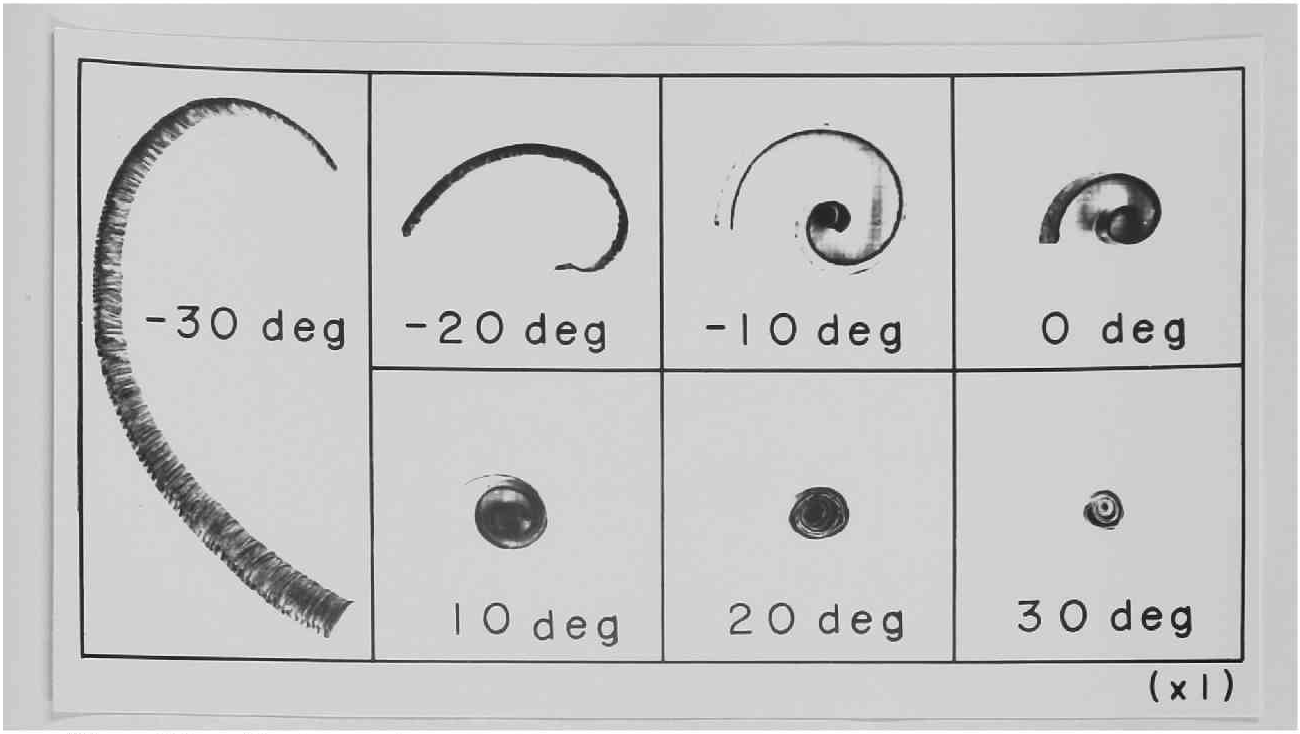

Fig. 39 Photographs of chips obtained by orthogonal cutting of lead in relation to rake angle [Tool material, high-speed steel SKH 2(18-4-1); clearance angle, 6 deg; width of cut, 6.0 mm; depth of cut, 0.10 mm; cutting speed, 9 m/min; dry]

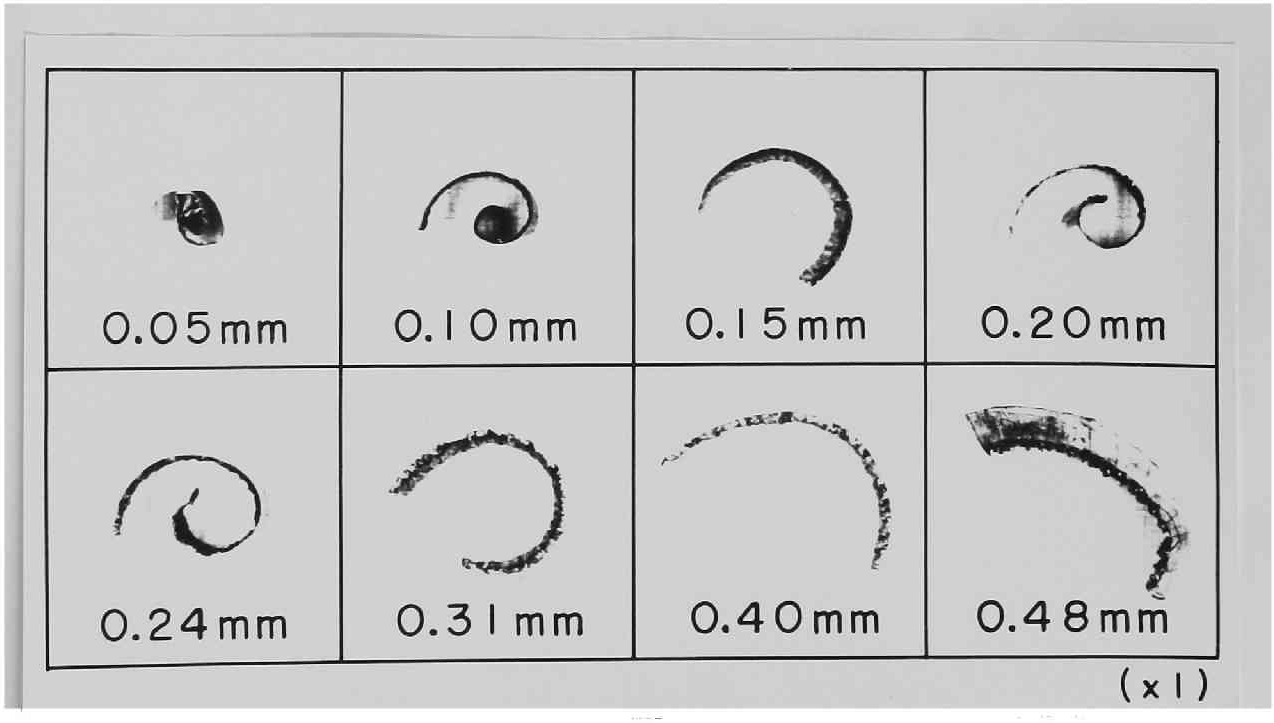

Fig. 40 Photographs of chips obtained by orthogonal cutting of lead in relation to depth of cut [Tool material, high-speed steel SKH 2(18-4-1); rake angle, 0 deg; clearance angle, 6 deg; width of cut, 6.0 mm; cutting speed, 9 m/min; dry]

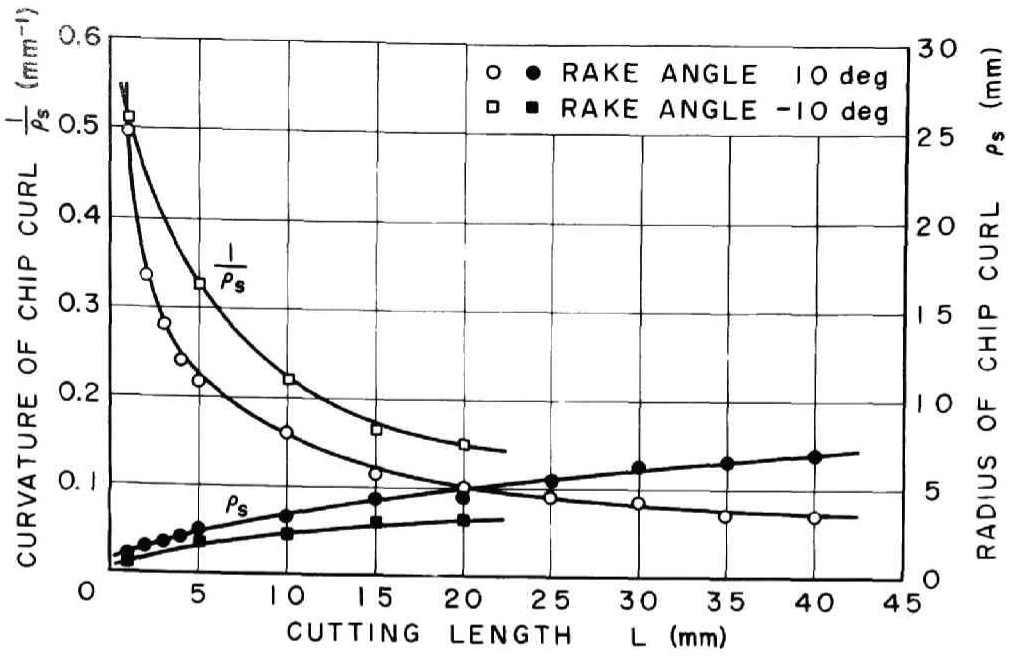

Fig. 41 Relationship between cutting length and curvature and radius of chip curl at the separating side [Work material, lead; tool material, high-speed steel SKH 2(18-4-1); rake angle, -10 and 10 deg; clearance angle, 6 deg; width of cut, 6.0 mm; depth of cut, 0.10 mm; cutting speed, 9 m/min; dry]

effects of rake angle and depth of cut, respectively. Most chips were spiral. Fig. 41 shows the relationship between the cutting length and the curvature and radius of chip curl at the separating side of chip for two typical chips which were obtained with depth of cut of 0.10 mm by cutting tools of -10 and 10 deg rake angles. It is evident from Fig. 41 that, as the cutting proceeds, the curvature of chip curl decreases, and the radius of chip curl increases, but the rate of change for both curvature and radius of chip curl decreases. Therefore, the radius of chip curl approaches a constant value as cutting proceeds. Regarding this transitional phenomenon on chip curl, Hahn(33) explained that it is caused by a change of temperature distribution in shear zone as cutting progresses. The radius of chip curl which appears in the following means a constant value at the separating side of chip which was reached after some cutting.

The effects of rake angle and depth of cut on radius of chip curl,

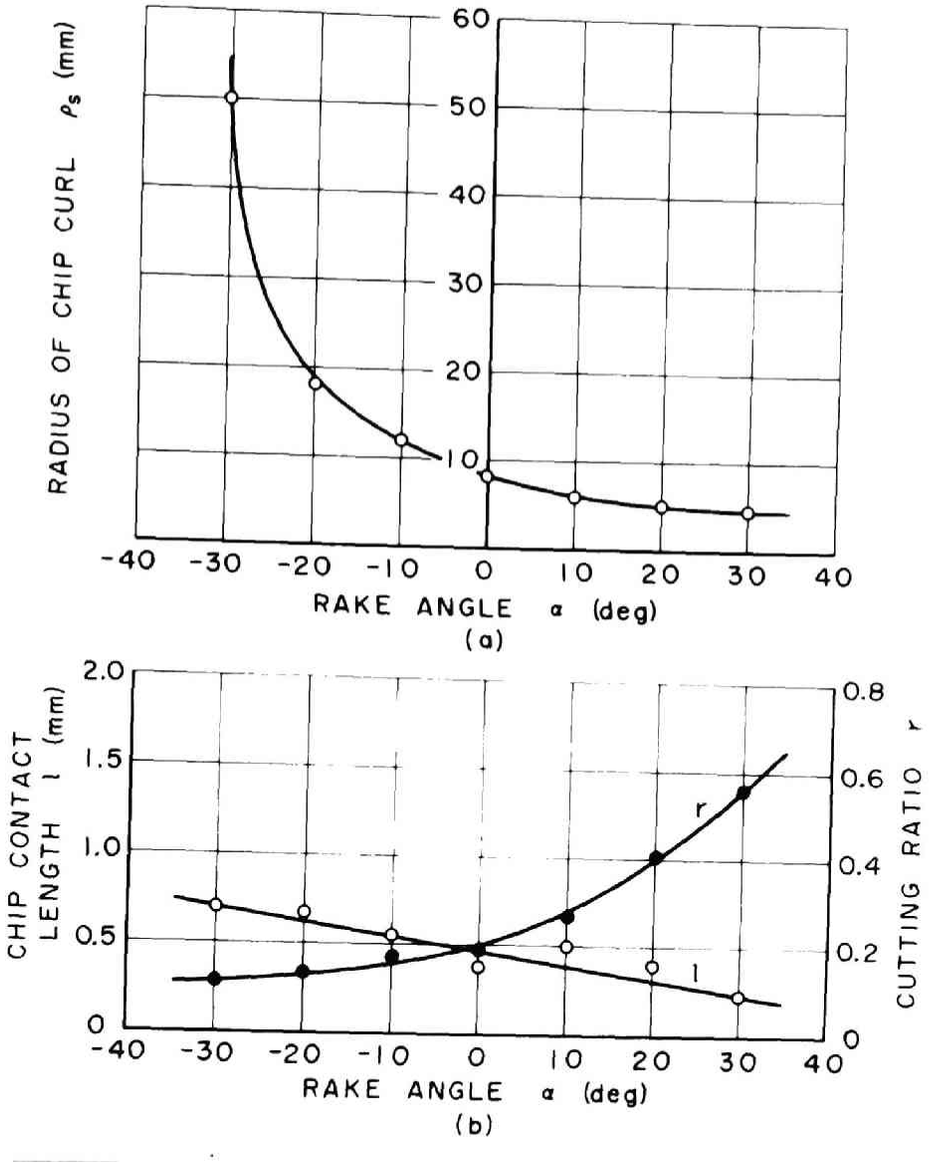

Fig. 42 Experimental results for lead in relation to rake angle; (a) Radius of chip curl; (b) Chip contact length on tool face and cutting ratio [Tool material, high-speed steel SKH 2(18-4-1); clearance angle, 6 deg; width of cut, 6.0 mm; depth of cut, 0.10 mm; cutting speed, 9 m/min; dry]

chip contact length on tool face, and cutting ratio are shown in Figs. 42 and 43, respectively. Referring to these figures, it is concluded that the radius of chip curl decreases with an increase in rake angle, and increases in almost direct proportion with an increase in depth of cut. Regarding cutting ratio and chip contact length, as is usually mentioned, cutting ratio increases with increases in rake angle and

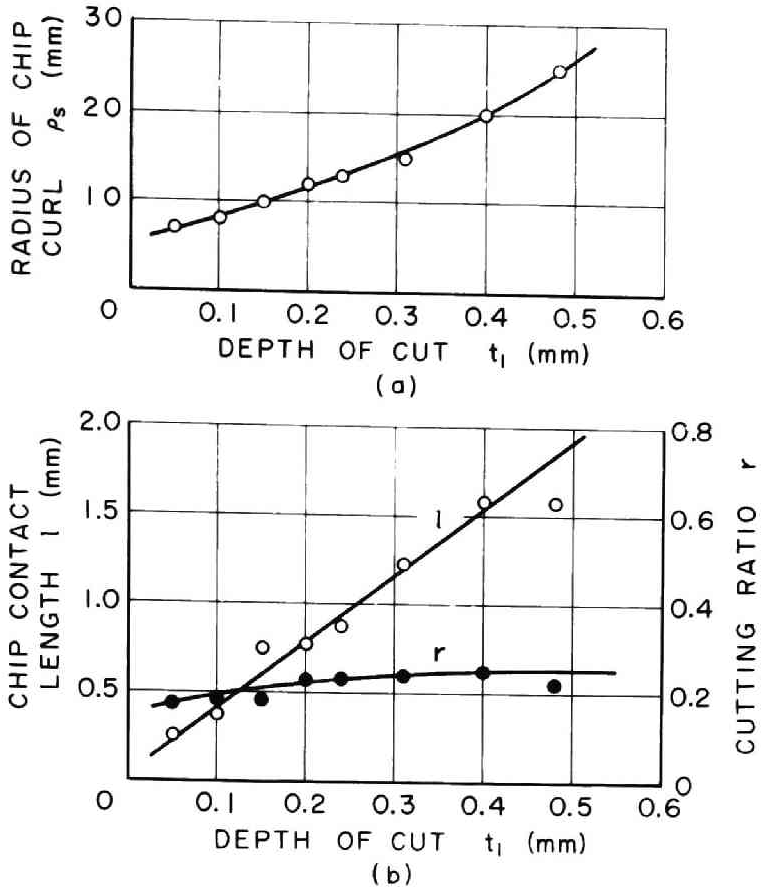

Fig. 43 Experimental results for lead in relation to depth of cut; (a) Radius of chip curl; (b) Chip contact length on tool face and cutting ratio [Tool material, high-speed steel SKH 2(18-4-1); rake angle, 0 deg; clearance angle, 6 deg; width of cut, 6.0 mm; cutting speed, 9 m/min; dry]

depth of cut, and chip contact length decreases with an increase in rake angle and increases with an increase in depth of cut.

c. Cutting Tests on Carbon Steel

Figs. 44 to 46 show experimental results on chip curl and other cutting data such as chip contact length, cutting ratio, mean friction angle on the tool face, normal and tangential forces on the tool face in relation to rake angle, depth of cut, and cutting speed, respectively, when 0.43% carbon steel was cut. Normal and tangential forces on the tool face N and F are calculated from the following equations:

Fig. 44 Experimental results for 0.43% carbon steel in relation to rake angle; (a) Radius of chip curl; (b) Chip contact length on the tool face and cutting ratio; (c) Mean friction angle on the tool face; (d) Normal and tangential forces on the tool face [Tool material, high-speed steel SKH 2(18-4-1) and carbide S1(WC-TiC-Co); clearance angle, 6 deg; width of cut, 3.0 mm; depth of cut, 0.10 mm; cutting speed, 10 m/min for high-speed steel tool and 70 m/min for carbide tool; dry]

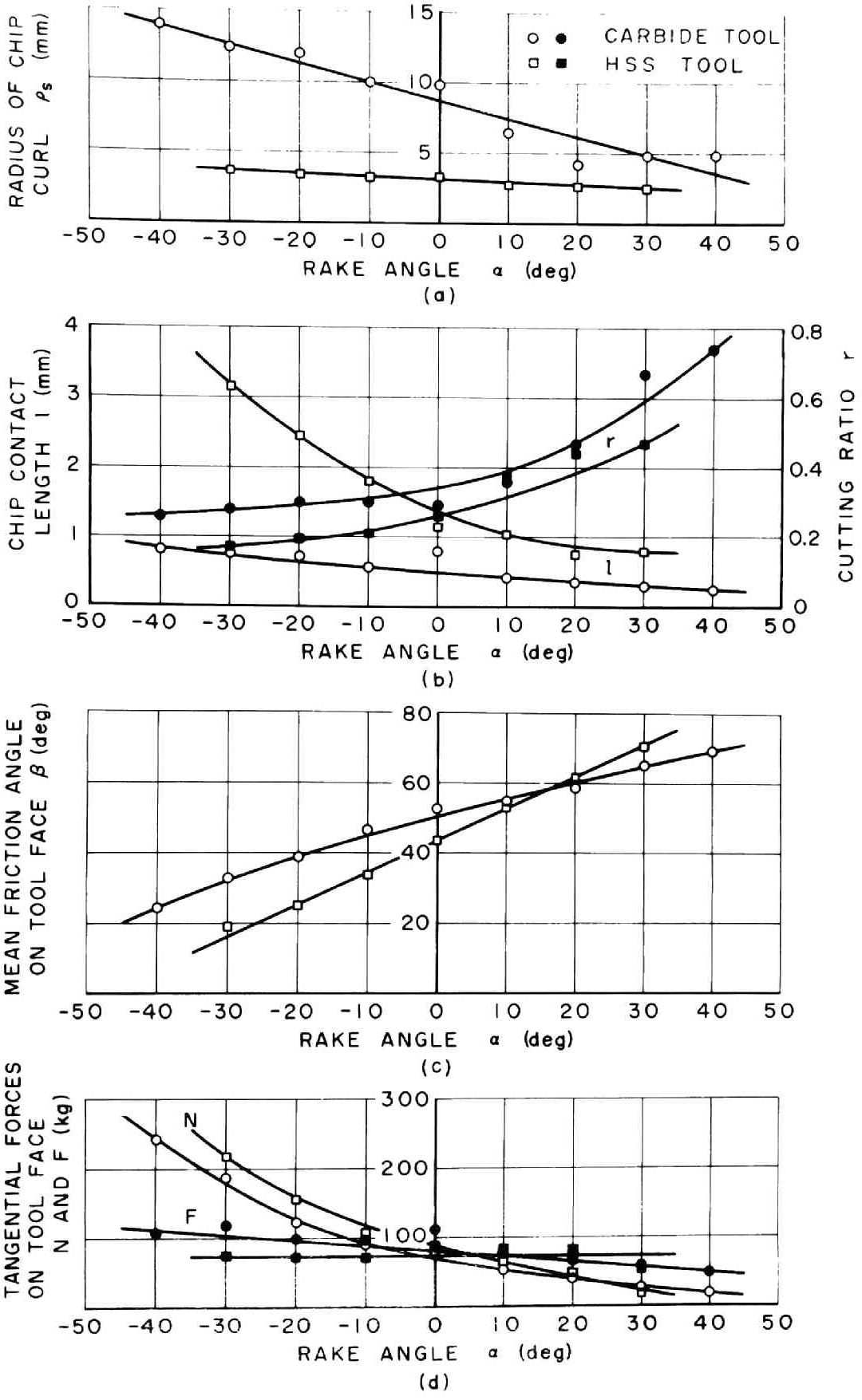
RADIUS OF CHIP CURL ρ_s (mm)
15
10
5
CARBIDE TOOL
HSS TOOL
-50 -40 -30 -20 -10 0 10 20 30 40 50
RAKE ANGLE α (deg)
(a)
CHIP CONTACT LENGTH l (mm)
4
3
2
1
0
0.8
0.6
0.4
0.2
0
CUTTING RATIO r
r
l
-50 -40 -30 -20 -10 0 10 20 30 40 50
RAKE ANGLE α (deg)
(b)
MEAN FRICTION ANGLE ON TOOL FACE β (deg)
80
60
40
20
-50 -40 -30 -20 -10 0 10 20 30 40 50
RAKE ANGLE α (deg)
(c)
NORMAL AND TANGENTIAL FORCES ON TOOL FACE N AND F (kg)
300
200
100
N
F
-50 -40 -30 -20 -10 0 10 20 30 40 50
RAKE ANGLE α (deg)
(d)

Fig. 44

Fig. 45 Experimental results for 0.43% carbon steel in relation to depth of cut; (a) Radius of chip curl; (b) Chip contact length on the tool face and cutting ratio; (c) Mean friction angle on the tool face; (d) Normal and tangential forces on the tool face [Tool material, high-speed steel SKH 2(18-4-1) and carbide S1(WC-TiC-Co); rake angle, 20 deg; clearance angle, 6 deg; width of cut, 3.0 mm; cutting speed, 10 m/min for high-speed steel tool and 70 m/min for carbide tool; dry]

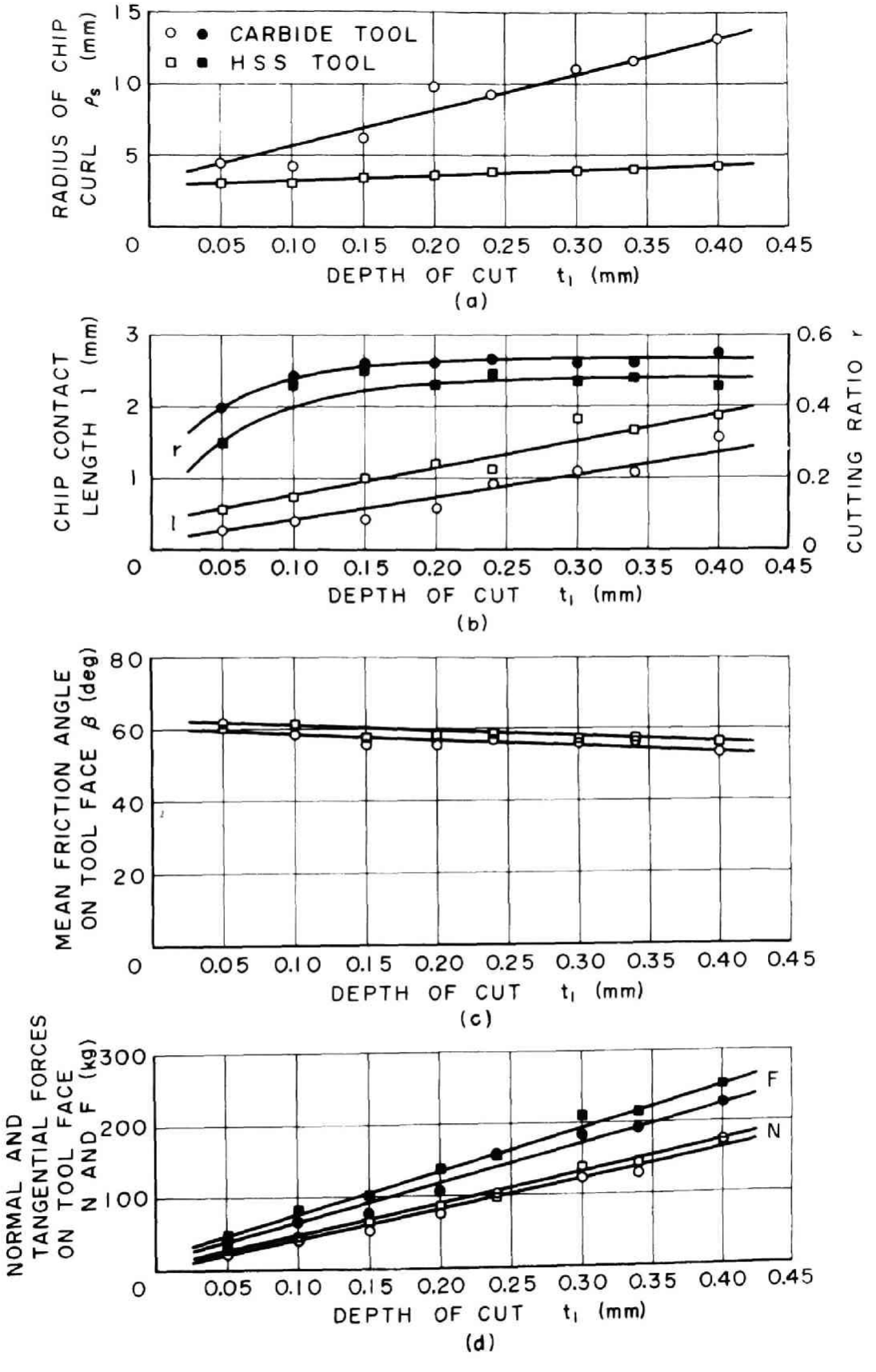
RADIUS OF CHIP CURL ρ_s (mm)
CARBIDE TOOL
HSS TOOL
DEPTH OF CUT t_1 (mm)
(a)
CHIP CONTACT LENGTH l (mm)
CUTTING RATIO r
r
l
DEPTH OF CUT t_1 (mm)
(b)
MEAN FRICTION ANGLE ON TOOL FACE β (deg)
DEPTH OF CUT t_1 (mm)
(c)
NORMAL AND TANGENTIAL FORCES ON TOOL FACE N AND F (kg)
F
N
DEPTH OF CUT t_1 (mm)
(d)

Fig. 45

Fig. 46 Experimental results for 0.43% carbon steel in relation to cutting speed; (a) Radius of chip curl; (b) Chip contact length on the tool face and cutting ratio; (c) Mean friction angle on the tool face; (d) Normal and tangential forces on the tool face [Tool material, high-speed steel SKH 2(18-4-1) and carbide S1(WC-TiC-Co); rake angle, -30, 0, and 30 deg; clearance angle, 6 deg; width of cut, 3.0 mm; depth of cut, 0.10 mm; dry]

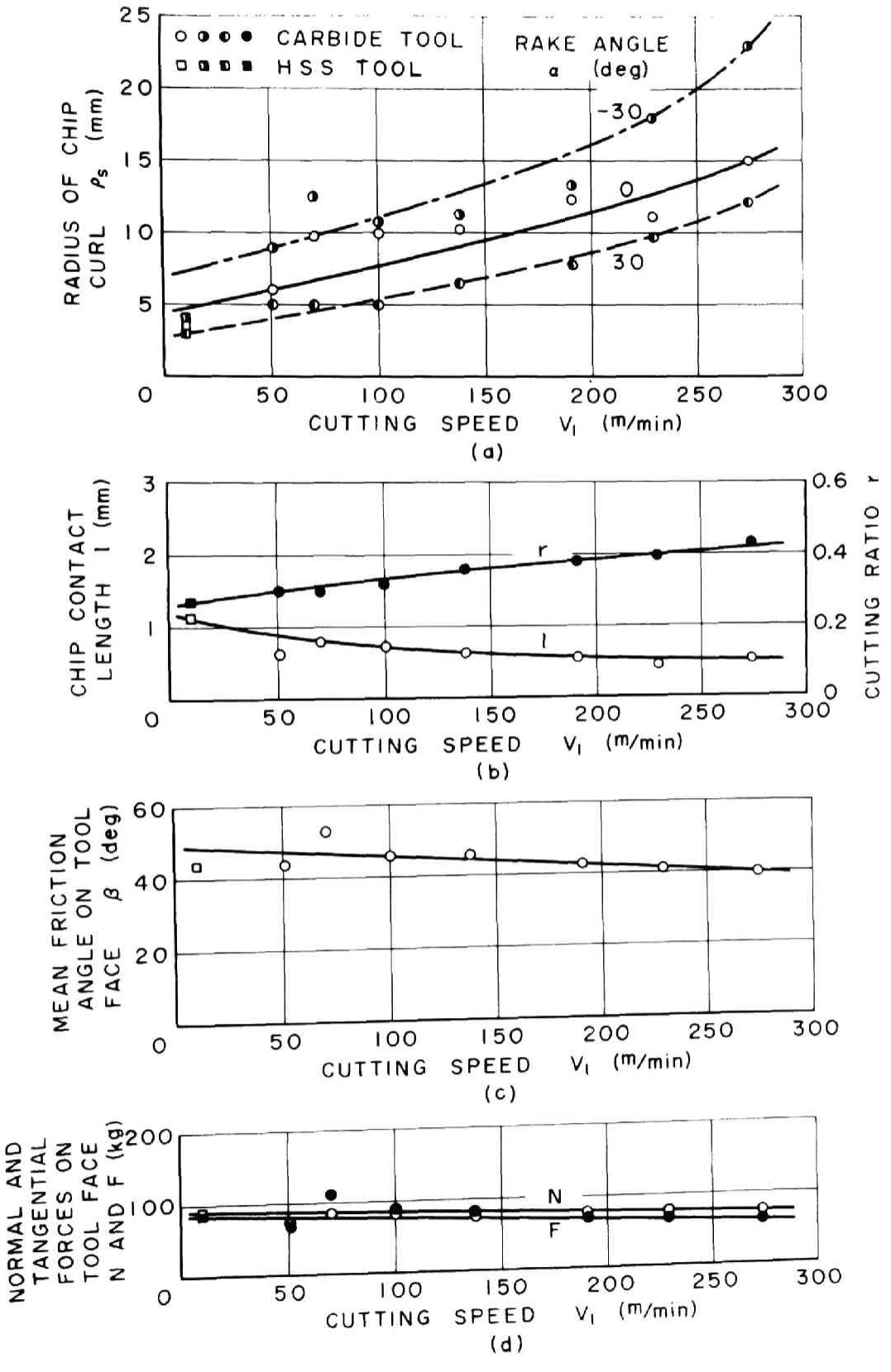
CARBIDE TOOL
HSS TOOL
RAKE ANGLE
α (deg)
-30
0
30
RADIUS OF CHIP CURL ρs (mm)
CUTTING SPEED V1 (m/min)
(a)
CHIP CONTACT LENGTH l (mm)
CUTTING RATIO r
r
l
CUTTING SPEED V1 (m/min)
(b)
MEAN FRICTION ANGLE ON TOOL FACE β (deg)
CUTTING SPEED V1 (m/min)
(c)
NORMAL AND TANGENTIAL FORCES ON TOOL FACE N AND F (kg)
N
F
CUTTING SPEED V1 (m/min)
(d)

Fig. 46

$$N = F_h \sin\alpha + F_v \cos\alpha \qquad [53]$$

$$F = F_h \cos\alpha - F_v \sin\alpha, \qquad [54]$$

where F_h is horizontal or principal cutting force and F_v is vertical or thrust cutting force.

In this experiment, a tubular specimen of carbon steel was cut by feeding an orthogonal cutting tool in the longitudinal direction on a lathe. Chips obtained were helical, and as a result it was relatively easy to measure the radius of the chip curl.

Referring to Fig. 44, with an increase in rake angle, chip contact length decreased, cutting ratio and mean friction angle on the tool face increased, normal force on the tool face decreased, and tangential force decreased or did not change. The radius of chip curl decreased with an increase in rake angle as in cutting tests on lead. Takeyama(34) reported the opposite result. The rate of decrease in curl radius with an increase in rake angle is larger in high speed cutting by carbide tool S1(WC-TiC-Co) than in low speed cutting by high-speed steel tool SKH 2(18-4-1).

Referring to Fig. 45, with an increase in depth of cut, chip contact length, cutting ratio, and normal and tangential forces on the tool face increased, and mean friction angle on the tool face decreased. The radius of chip curl increased in almost direct proportion with an increase in depth of cut as was observed when cutting lead. Similar results have been reported by other investigators. The rate of increase in curl radius with depth of cut is larger in high speed cutting by carbide tool than in low speed cutting by high-speed steel tool.

From Figs. 43 and 45 the relation between radius of chip curl ρ_s and depth of cut t_1 is expressed as follows:

$$\rho_s = a t_1 + c, \qquad [55]$$

where a and c are constants.

Assuming that the cutting model is homologous when the depth of cut is changed, the radius of chip curl should be proportional to chip thickness as expressed in the equations for curl radius, i.e., Equations [46] and [47] or Equations [51] and [52] deduced in the previous section. Since there is a linear relationship between depth of cut and chip thickness in this case, the curl radius is also related to depth of cut in direct proportion. This tendency is consistent with Equation [55].

Referring to Fig. 46, the radius of chip curl increases with an increase in cutting speed, and the larger the rake angle, the smaller the curl radius. Variations of chip contact length, cutting ratio, mean friction angle on the tool face, and normal and tangential forces on the tool face in relation to cutting speed for rake angle of 0 deg are also shown in Fig. 46. With an increase in cutting speed, the cutting ratio increases and other quantities decrease slightly.

Henriksen(32) considered that the chip is a cantilever which is supported at the shear plane and it curls due to the action of a bending moment based on uniformly distributed normal stress on the tool-chip interface, and deduced the equation for the radius of chip curl as follows:

$$\frac{\rho_m}{E} = \frac{\rho_b + \rho_s}{2E} = \frac{t_2^3}{6l^2\sigma_f} \qquad [56]$$

$$\sigma_f = \frac{N}{b\,l}, \qquad [57]$$

where b is width of chip(nearly equal to width of cut), E is modulus of elasticity for chip, and σ_f is uniformly distributed load per unit length on the tool face. The following is a discussion on this bending moment theory for chip curl, using the data obtained in Figs. 44 to 46.

It is assumed for the sake of simplicity that the modulus of elasticity for chip is constant, though it depends upon cutting conditions, especially upon cutting temperature. Using the data in Figs.

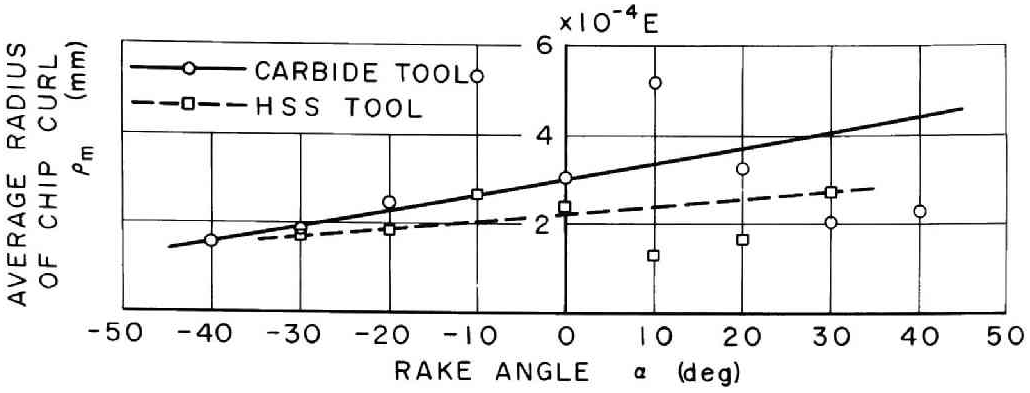

Fig. 47 Calculated values for the average radius of chip curl in relation to rake angle [Work material, 0.43% carbon steel, tool material, high-speed steel SKH 2(18-4-1) and carbide S1 (WC-TiC-Co); clearance angle, 6 deg; width of cut, 3.0 mm; depth of cut, 0.10 mm; cutting speed, 10 m/min for high-speed steel tool and 70 m/min for carbide tool; dry]

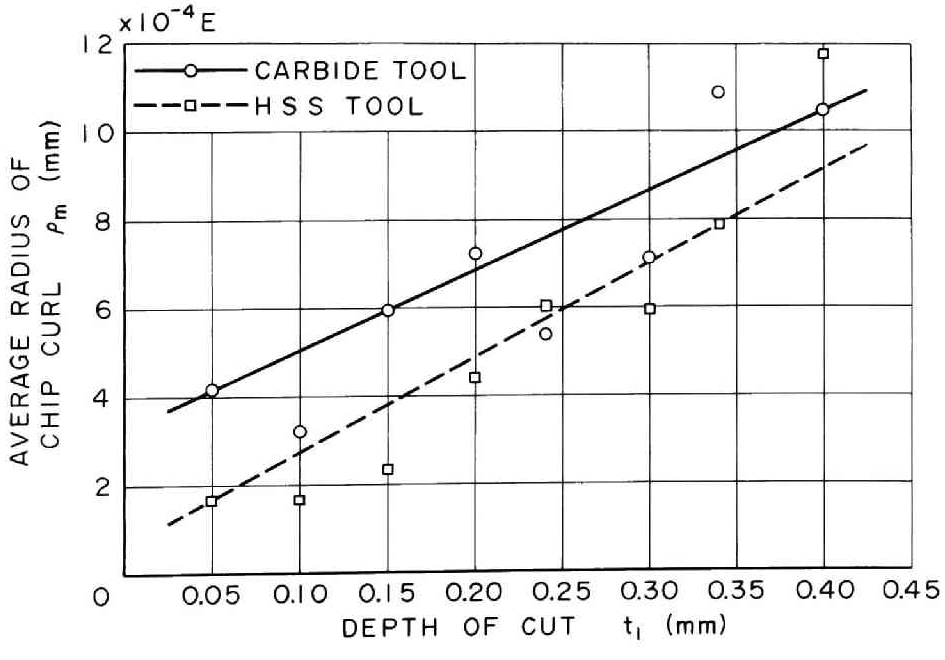

Fig. 48 Calculated values for the average radius of chip curl in relation to depth of cut [Work material, 0.43% carbon steel, tool material, high-speed steel SKH 2(18-4-1) and carbide S1 (WC-TiC-Co); rake angle, 20 deg; clearance angle, 6 deg; width of cut, 3.0 mm; cutting speed, 10 m/min for high-speed steel tool and 70 m/min for carbide tool; dry]

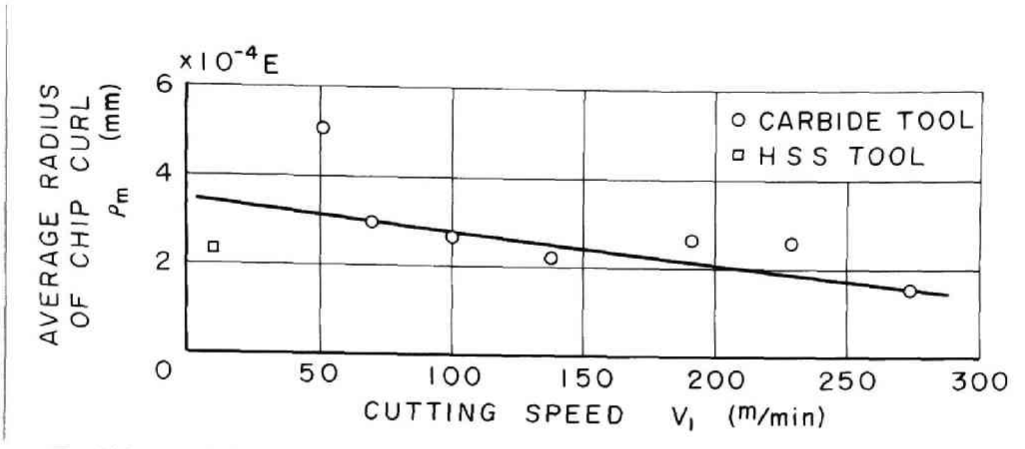

Fig. 49 Calculated values for the average radius of chip curl in relation to cutting speed [Work material, 0.43% carbon steel; tool material, high-speed steel SKH 2(18-4-1) and carbide S1(WC-TiC-Co); rake angle, 0 deg; clearance angle, 6 deg; width of cut, 3.0 mm; depth of cut, 0.10 mm; dry]

44 to 46, the average radius of chip curl was calculated from Equations [56] and [57], and plotted in relation to rake angle, depth of cut, and cutting speed in Figs. 47 to 49. Comparing these results with experimental results shown in Figs. 44(a), 45(a), and 46(a), the trends of change of chip curl in relation to cutting conditions are in agreement only when changing depth of cut, and not when changing rake angle and cutting speed.

In the above discussion a concentrated load at the separating point of chip on the tool face as Henriksen(32) considered in his analysis and the tangential force on the tool face are not taken into consideration. However, it is concluded from the above discussion that the bending moment or the normal force acting on the tool-chip interface is not necessarily a main factor producing the chip-curl phenomenon.

XIV. CONCLUSIONS

Instead of the conventional theory of the mechanism of orthogonal cutting based on the single shear plane concept, the concept of the flow region, the transitional deformation zone which exists between the rigid region of the work and the plastic region of the steady chip, was developed.

The mechanism of chip formation in orthogonal cutting was analyzed in the case of a simple continuous chip, and the concept was also applied to discontinuous chip formation.

The secondary plastic flow in the chip on the tool-chip interface was investigated as well as the primary plastic flow in the flow region.

The flow region concept was also applied to explain the chip-curl phenomenon in orthogonal cutting.

The above analyses and cutting tests lead to the following conclusions.

(1) The transitional deformation zone, i.e., the flow region exists between the rigid region of the work and the plastic region of the steady chip for both mechanisms of continuous and discontinuous chip formations in metal cutting.

(2) Conflicts in the cutting mechanism based on the single shear plane concept, such as an abrupt change of movement of a metal particle, an infinite acceleration which a metal particle receives, extremely large strain and strain rate, etc., can be removed by the flow region concept.

(3) The expressions for inclination angles of the boundary lines of the flow region were deduced theoretically in the case of a simple continuous chip under the assumption of a perfectly plastic solid, and confirmed in cutting tests with lead.

(4) The flow region concept was applied to discontinuous chip formation. The behavior of the cutting process of discontinuous chip formation is almost the same as that of continuous chip formation except that fracture occurs when the shearing stress or strain on the ending boundary line of the flow region reaches the breaking limit as the cut proceeds. Considering the strain-hardening property of metal, equations expressing angles of the starting boundary line and the ending boundary line(i.e., fracture line) of the flow region were deduced theoretically, and determined to be in agreement with the experimental results for carbon steel.

(5) Metal receives large shearing strain and work-hardening especially at the separating side of chip according to the secondary plastic flow along the tool-chip interface as well as the primary plastic flow in the flow region.

(6) The direction of the arrangement of metal structure in the chip due to the primary plastic flow in the flow region was investigated over a wide range of cutting conditions, and the existence of the flow region was proven indirectly from this investigation.

(7) The size of the flow region depends upon cutting conditions. One of the important factors is the cutting speed. The higher the cutting speed, the narrower the size of the flow region.

(8) The phenomenon of chip curl in orthogonal cutting is partly explained by the fact that the ending boundary line of the flow region is convex upward and the shearing stress distribution is not uniform along this line.

ACKNOWLEDGMENT

The author wishes to express his sincerest appreciation to Dr. K. Okushima, Professor of Precision Engineering, Kyoto University, Japan, for his valuable guidances and suggestions throughout this entire investigation.

All analyses and experiments were supported by research funds from the Ministry of Education of the Japanese Government, and done at the Machinability Laboratory in the Department of Mechanical Engineering, Kyoto University, Japan, as the author's postgraduate work in 1956 through 1958. The author would like to thank Messrs. C. Noda, M. Matsushita, and S. Okado, who were engineering students at that time, for their great help during the conduct of experiments.

This manuscript was written and completed in 1960 during the author's temporary stay in the Department of Industrial Engineering, The Pennsylvania State University, U. S. A., conducting machinability research. The final manuscript translated into English was reviewed by Mr. G. L. Thuering, Head of Department of Management Engineering and Professor of Industrial Engineering, The Pennsylvania State University, U. S. A., to whom the author owes great appreciation.

GLOSSARY OF SYMBOLS

a : constant expressing the relationship between radius of chip curl and depth of cut with symbol 'c'

b : width of cut or width of chip

c : constant expressing the relationship between radius of chip curl and depth of cut with symbol 'a'

E : modulus of elasticity for chip

f : ratio between size of the flow region and chip thickness ($= {}^{s}/t_2$)

F : tangential force on the tool-chip interface

F_h: horizontal or principal cutting force

F_v: vertical or thrust cutting force

k : constant expressing the degree of strain-hardening of material with symbol 'm'

k_1: ratio between chip contact length and depth of cut ($= {}^{l}/t_1$)

k_2: ratio between chip contact length and chip thickness ($= {}^{l}/t_2$)

K : angle relative to inclination angle of the starting boundary line of the flow region in discontinuous chip formation

K_1: angle relative to inclination angle of the starting boundary line of the flow region in continuous chip formation

K_2: angle relative to inclination angle of the ending boundary line of the flow region in continuous chip formation

l : chip contact length on the tool face

L : cutting length

m : constant expressing the degree of strain-hardening of material with symbol 'k'

N : normal force on the tool-chip interface

r : cutting ratio ($= {}^{t}1/t_2$)

r_b: ratio between height of serrated surface of the back side and thickness of chip ($= {}^{t}ss/t_2$)

r_{sf}: ratio between thickness of the layer of the secondary plastic flow and chip thickness ($= {}^{t}sf/t_2$)

R : resultant cutting force

s : size of the flow region

S : area in respect to the size of the flow region

t_1: depth of cut

t_2: thickness of continuous chip or maximum thickness of discontinuous chip

t_{sf}: thickness of the layer of the secondary plastic flow in the chip

t_{ss}: height of serrated surface of the back side of chip

V_1: cutting speed or cutting velocity

V_2: chip flowing-out speed or chip velocity

V_{2b}: flowing-out velocity of a metal particle at the back side of chip

V_{2s}: flowing-out velocity of a metal particle at the separating side of chip

x : distance from an arbitrary point on the free surface of the flow region to the horizontal line through the cutting edge

x_2: length of a perpendicular from the ending point of the flow region to the horizontal line through the cutting edge

z : distance from the tool face toward the back side of chip

α : rake angle

β : mean friction angle on the tool-chip interface

γ: shearing strain

γ_0: conventional shearing strain based on the cutting mechanism accompanying a single shear plane

γ_1: shearing strain on the starting boundary line of the flow region

γ_2: shearing strain on the ending boundary line of the flow region or strain in the chip

γ_{sf}: plastic shearing strain which metal receives due to the secondary plastic flow

δ : lip angle of a cutting tool

ϵ : angle between a perpendicular line to the tool face and a grid line in the steady chip which was formerly perpendicular to the cutting direction

ϵ_0: angle between a perpendicular line to the tool face and a grid line in the steady chip which was formerly perpendicular to the cutting direction in the case of the conventional cutting mechanism based on the single shear plane concept

θ: angle between a perpendicular line to the tool face and a tangent to a curved grid line caused by the secondary plastic flow on the tool-chip interface

ρ_0: transitional radius of chip curl at the back side of chip

ρ_b: inner radius of chip curl at the back side of chip

ρ_m: mean radius of chip curl at the center line of chip

ρ_s: outer radius of chip curl at the separating side of chip ($= \rho_b + t_2$)

σ_f: uniformly distributed load per unit length on the tool-chip interface or normal stress on the tool face

τ : shearing stress

τ_0: yield shearing stress or shear-flow stress

τ_2: shearing stress on the ending boundary line of the flow region

τ_b: shearing stress on the ending boundary line at the back side of chip

τ_s: shearing stress on the ending boundary line at the separating side of chip

τ_{OA}: shearing stress on the starting boundary line of the flow region

τ_{OB}: shearing stress on the ending boundary line of the flow region ($= \tau_2$)

τ_{OD}: shearing stress on the tool-chip interface

ϕ : inclination angle of an arbitrary radial plane in the flow region

ϕ_0: conventional shear angle based on the cutting mechanism accompanying a single shear plane

ϕ_1: inclination angle of the starting boundary line of the flow region

ϕ_2: inclination angle of the ending boundary line of the flow region

ϕ_2': inclination angle of the tangent to the upwardly convex ending boundary line of the flow region at an arbitrary point

ϕ_{2e}: inclination angle of the upwardly convex ending boundary line of the flow region at the tip of the cutting tool

ϕ_{2f}: inclination angle of the upwardly convex ending boundary line of the flow region at the free surface

Φ: sector angle of the flow region

ψ: angle of the tangent to the free surface of the flow region with the machined surface

ψ_2: angle of the tangent to the free surface at the ending point of the flow region with the machined surface

ω: angle between the perpendicular line to the cutting direction and the direction of movement of a metal particle at the ending point of the flow region on the free surface

REFERENCES

(1) V. Piispanen: Lastunmuodostumisen Theoriaa; Teknillinen Aikakauslehti, Vol. 27, 1937, pp. 315-322.

(2) V. Piispanen: Theory of Formation of Metal Chips; Journal of Applied Physics, Vol. 19, 1948, pp. 876-881.

(3) H. Ernst and M. E. Merchant: Chip Formation, Friction and High Quality Machined Surfaces; Surface Treatment of Metals, ASM, 1941, pp. 299-378.

(4) M. E. Merchant: Mechanics of the Metal Cutting Process --- I. Orthogonal Cutting and a Type 2 Chip, II. Plasticity Conditions in Orthogonal Cutting; Journal of Applied Physics, Vol. 16, 1945, pp. 267-275 and pp. 318-324.

(5) E. H. Lee and B. W. Shaffer: The Theory of Plasticity Applied to a Problem of Machining; Journal of Applied Mechanics, Vol. 18, Trans. ASME, Vol. 72, 1951, pp. 405-413.

(6) R. Hill: The Mechanics of Machining --- A New Approach; Journal of the Mechanics and Physics of Solids, Vol. 3, 1954, pp. 47-53.

(7) K. Okushima and K. Hitomi: On the Cutting Mechanism for Soft Metals; Memoirs of the Faculty of Engineering, Kyoto University, Japan, Vol. 19, 1957, pp. 135-166; Trans. Japan Society of Mechanical Engineers, Vol. 23, 1957, pp. 674-680.

(8) K. Nakayama: A Study on the Mechanism of Metal Cutting; Journal of the Society for Precision Mechanics of Japan, Vol. 23, 1957, pp. 528-532.

(9) D. Kececioglu: Shear-Strain Rate in Metal Cutting and Its Effects on Shear-Flow Stress; Trans. ASME, Vol. 80, 1958, pp. 158-168.

(10) D. Kececioglu: Shear-Zone Size, Compressive Stress, and Shear Strain in Metal-Cutting and Their Effects on Mean Shear-Flow Stress; Trans. ASME, Series B, Journal of Engineering for Industry, Vol. 82, 1960, pp. 79-86.

(11) D. G. Christopherson, P. L. B. Oxley, and W. B. Palmer: Orthogonal Cutting of a Work-Hardening Material --- Theoretical and Experimental Investigation; Engineering, Vol. 186, No. 4820, July 25, 1958, pp. 113-116.

(12) I. Finnie and M. C. Shaw: The Shear Stress in Metal Cutting; Trans. ASME, Vol. 77, 1955, pp. 115-123.

(13) K. Okushima and K. Hitomi: An Analysis of the Mechanism of Orthogonal Cutting; Memoirs of the Faculty of Engineering, Kyoto University, Japan, Vol. 20, 1958, pp. 95-116; Trans. Japan Society of Mechanical Engineers, Vol. 25, 1959, pp. 54-60.

(14) I. Finnie and M. C. Shaw: The Friction Process in Metal Cutting; Trans. ASME, Vol. 78, 1956, pp. 1649-1657.

(15) T. Sata and M. Mizuno: Friction Process on Cutting Tool and Cutting Mechanism; Journal of the Scientific Research Institute, Japan, Vol. 49, 1955, pp. 163-174; Trans. Japan Society of Mechanical Engineers, Vol. 21, 1955, pp. 416-423.

(16) A. W. Meyer and F. R. Archibald: Carbide Milling of Steel; Mechanical Engineering, Vol. 67, 1945, pp. 659-667.

(17) F. R. Archibald: Analysis of the Stresses in a Cutting Edge; Trans. ASME, Vol. 78, 1956, pp. 1149-1154.

(18) J. H. Creveling, T. F. Jordan, and E. G. Thomsen: Some Studies of Angle Relationships in Metal Cutting; Trans. ASME, Vol. 79, 1957, pp. 127-138.

(19) H. Takeyama: Cutting Speed Effect in Metal Machining --- Effect of Tool-Chip Contact Area; Journal of the Society for Precision Mechanics of Japan, Vol. 22, 1956, pp. 108-113.

(20) K. Okushima et al.: A Strain-Gage Type Three-Component Tool Dynamometer; Trans. Japan Society of Mechanical Engineers, Vol. 21, 1955, pp. 709-711.

(21) B. W. Shaffer: The Mechanics of the Simple Shearing Process during Orthogonal Machining; Trans. ASME, Vol. 77, 1955, pp. 331-336.

(22) K. Okushima and K. Hitomi: An Analysis of Discontinuous Chip Formation; Presented at the Japan Society of Mechanical Engineers, March, 1959, unpublished.

(23) R. Hill: On the Limits Set by Plastic Yielding to the Intensity of Singularities of Stress; Journal of the Mechanics and Physics of Solids, Vol. 2, 1954, pp. 278-285.

(24) M. Field and M. E. Merchant: Mechanics of Formation of the Discontinuous Chip in Metal Cutting; Trans. ASME, Vol. 71, 1949, pp. 421-430.

(25) N. H. Cook, I. Finnie, and M. C. Shaw: Discontinuous Chip Formation; Trans. ASME, Vol. 76, 1954, pp. 153-162.

(26) E. H. Lee: A Plastic-Flow Problem Arising in the Theory of Discontinuous Machining; Trans. ASME, Vol. 76, 1954, pp. 189-194.

(27) A. Nadai: Theory of Flow and Fracture of Solids; Engineering Societies Monographs, Vol. 1, McGraw-Hill Book Company, Inc., New York, N. Y., 1950, p. 349.

(28) K. Okushima and K. Hitomi: Plastic Flow in the Chip in Metal Cutting; Trans. Japan Society of Mechanical Engineers, Vol. 26, 1960, pp. 423-429; Bulletin of Japan Society of Mechanical Engineers, Vol. 3, 1960, pp. 556-560.

(29) A. B. Albrecht: Chip Studies Reveal What Happens during Turning; American Machinist, Vol. 97, May 25, 1953, pp. 121-125.

(30) C. Zener and J. H. Hollomon: Effect of Strain Rate upon Plastic Flow of Steel; Journal of Applied Physics, Vol. 15, 1944, pp. 22-32.

(31) K. Okushima and K. Hitomi: The Mechanism of Chip Curl in Orthogonal Cutting; Journal of the Society for Precision Mechanics of Japan, Vol. 25, 1959, pp. 320-327.

(32) E. K. Henriksen: Stress Distribution in the Continuous Chip --- A Solution of the Paradox of Chip Curl; Trans. ASME, Vol. 73, 1951, pp. 461-466.

(33) R. S. Hahn: Some Observations on Chip Curl in the Metal-Cutting Process under Orthogonal Cutting Conditions; Trans. ASME, Vol. 75, 1953, pp. 581-590.

(34) H. Takeyama: Study on High Speed Machining --- Analysis of Chip Curl in Orthogonal Cutting; Journal of the Society for Precision Mechanics of Japan, Vol. 23, 1957, pp. 140-144 and pp. 277-281.

August 31, 1961

Kasundo Hitomi